UNIVERSITY OF OKLAHOMA

GRADUATE COLLEGE

PETROGRAPHIC QUARTZITE SOURCE DISCRIMINATION IN THE UPPER GUNNISON BASIN, COLORADO: IMPLICATIONS FOR THE ARCHAEOLOGICAL STUDY OF PREHISTORIC HUNTER-GATHERS

A THESIS

SUBMITTED TO THE GRADUATE FACULTY

in partial fulfillment of the requirements for the

Degree of

MASTER OF ARTS

By

CODY L. DALPRA
Norman, Oklahoma
2016

PETROGRAPHIC QUARTZITE SOURCE DICRIMINATION IN THE UPPER GUNNISON BASIN, COLORADO: IMPLICATIONS FOR THE STUDY OF PREHISTORIC HUNTER-GATHERS

A THESIS APPROVED FOR THE
DEPARTMENT OF ANTHROPOLOGY

BY

_____
Dr. Bonnie L. Pitblado, Chair

_____
Dr. Patrick Livingood

_____
Dr. Asa R. Randall

© Copyright by CODY L. DALPRA 2016
All Rights Reserved.

For my parents Charles and Cindy, who have supported me no matter what mistake or hardship occurred. Without them I would not be here or never have discovered the absolute joy of the mountains, adventure, and discovery.

Acknowledgements

Several people have helped me with this thesis who I am eternally grateful for. First, I acknowledge my undergrad advisor Robert Brunswig who pushed me to go to graduate school and to pursue archaeology. His continued support over the years is invaluable. I would like to thank my fellow graduate students who I have studied with and discussed/debated issues with in class at both Utah State University and the University of Oklahoma. Janessa Doucette-Frederickson gave me valuable assistance with figures. My family and friends have given me gracious support over the years, without which I am not sure I would have completed this thesis. I appreciate the University of Oklahoma Anthropology Department that took a chance on my transfer and have been more than supportive during my time here. Anytime I had a question the faculty and staff were more than happy to assist me no matter how stressed I was. Carol Dehler and Molly Boeka Cannon at Utah State University assisted with my petrographic analysis training and statistics respectively. The National Science Foundation (BCS-0728664 and BCS-0960077) and the Bureau of Land Management (Gunnison Field Office) provided funding for the research under the supervision of Bonnie Pitblado. Accordingly, I could not have completed this research without the 2009 Utah State University archaeological field school, staff, students, and volunteers that collected the UGB quartzite samples. I also would like to acknowledge Elizabeth Francisco and Dan Haas (BLM Gunnison and Colorado, respectively); Forest Frost, Bill Commins, and Ken Stahlnecker (National Park Service, Black Canyon of the Gunnison, and Curecanti National Recreations Areas, respectively); and Justin Lawrence (Gunnison National Forest) that facilitated sample collection. I gratefully acknowledge my committee members for the comments and edits that helped make this a solid document. Patrick Livingood in particular gave valuable statistical input. Lastly, my chair Bonnie Pitblado supported me during times when I was not sure I could be an archaeologist. Without her, I would not only have never finished this thesis, but would not be in archaeology at all.

Cody L. Dalpra

Table of Contents

List of Tables

List of Figures

Abstract

Recently (Pitblado et al. 2008, 2013), an interdisciplinary team of archaeologists and geologists collaborated to develop a protocol for sourcing quartzite in the Upper Gunnison Basin, Colorado where archaeological assemblages are commonly over 90 percent quartzite (Dalpra and Pitblado 2016). Investigations from this research program have concluded that two techniques, when used in tandem, offer the best discriminatory results: geochemical characterization via laser ablation inductively coupled plasma mass spectrometry (LA-ICP-MS) and petrography (Pitblado et al. 2008). The following study briefly reviews the results of geochemical fingerprinting of Gunnison Basin quartzite, but focuses primarily on the results of petrographic analysis. The results demonstrate the discriminatory power of petrography on quartzite through a Basin-wide study functioning as a proof of concept. This Basin-wide analysis is followed by a more in depth look at two prehistorically used quarry locations analyzing both cobbles and outcrops. It is important to not just demonstrate differences between the sources, but also the variability within each source. The petrographic research is one step toward the ultimate goal, to develop a quartzite-sourcing protocol for the Gunnison Basin to enable "matching" cultural chipped stone assemblages to the likeliest raw material sources. This will allow researchers to reconstruct prehistoric land-use strategies in the Gunnison Basin with more precision than has been possible before.

Chapter 1: Introduction

Prehistoric research has long used the geologic origin of stone tools and debitage to evaluate prehistoric behaviors associated with mobility and exchange patterns. North American archaeologists began using geochemical analysis in the 1960's (Beck and Jones 2011; Eerkens and Rosenthal 2004; Frison et al. 1968; Hamilton et al 2013; Healy et al. 1984; Hoard et al. 1992; Glascock and Neff 2003; Jones et al. 2003, 2012; Luedtke 1978, 1979; Metcalf and McDonald 2012; Odell 2000; Stross et al. 1976; Roll 2005; Weigand et al. 1977), establishing sizable databases of geochemical information that allow for relatively accurate determination of geologic source locations (Hughes 1998, 2011; Shackley 1995, 1998, 2005). To date, these techniques have only used obsidian or fine-grain volcanics (Eerkens and Rosenthal 2004; Hamilton et al 2013; Hughes 2011), and to a lesser extent cryptocrystalline chert (Cracker et al. 1999; Roll 2005; Speer 2014a, 2014b). Archaeologists have largely ignored quartzite in provenance studies, yet it is one of the most prevalent stone materials in the world. Quartzite has been viewed as a challenge for provenance analysis because of the few existing tests of geochemical methods (Ebright 1987). The purpose of this research is to aid in the creation of a robust database containing quartzite petrographic information to apply to issues of mobility and exchange in the Upper Gunnison Basin (UGB) in southwestern Colorado (Figures 1 and 2).

The Southern Rocky Mountains, especially the UGB, have a long history of human occupation extending to at least year round Folsom occupation, 10,500 radiocarbon years before present (^{14}C yr BP) (Benedict 1992a; Black 2000; Kornfeld et al. 2010; Metcalf and McDonald 2012; Pitblado 2016; Stiger 2001). This region contains great environmental diversity in a vertically oriented landscape unique to the

Rocky Mountain region. Based on models of hunter-gatherer lifeways (Kelly 1992, 1995), it is logical to assume that a highly variable and productive environment enabled a relatively longer-term occupation than previously proposed, particularly when applied to the traditional theories of Paleoamerican mobility covering expansive territories (Beck and Jones 2011; Kelly and Todd 1988; Goodyear 1989; Pitblado et al. 2013; Shackley 1998, 2005). Further, the relative availability of raw lithic material affects the design and use of local tool assemblages (Andrefsky 1994; Bamforth 1986). This traditional image has been tested in the Great Basin and American Southwest, areas of dispersed resources (e.g. Jones et al. 2003, 2012; Shackly 1998), but not in the UGB, a diverse environment with abundant lithic resources.

Figure 1. View of the Upper Gunnison Basin from the basin floor looking north toward Crested Butte. Photo courtesy of Bonnie Pitblado.

Figure 2. Location map of the project area with sampled outcrop and cobble sources in the Upper Gunnison Basin.

Research Program Background

Chipped stone assemblages in the UGB are dominated by quartzite, which has a weak sourcing track record discussed in the next chapter. This lack of an ability to source tools and debitage from chipped stone assemblages frustrates archaeologists in the UGB by the imposing interpretive limitations (Pitblado et al. 2008). Motivated by this limitation affecting the research of the Basin's prehistoric hunter-gathers, Pitblado et al. (2006, 2008, and 2013) began a research program designed to understand the occurrences and distributions of quartzite throughout the UGB. Pitblado et al. (2008) reported the results of a pilot study using six different sourcing techniques on 20 samples. The pilot study results indicated that laser ablation inductively coupled plasma mass spectrometry (LA-ICP-MS) and petrography best discriminated quartzite in the UGB. This prompted a Basin-wide research program referred to here as the total quartzite sourcing research program.

Including the work detailed in this thesis, the total quartzite sourcing research program consist of three phases: first, collect quartzite from around the UGB including known quarries and geologically mapped quartzite outcrops and cobbles; second, analyze the samples using LA-ICP-MS; and third, analyze the samples with petrography (microscopic characterization). Bonnie Pitblado, Carol Dehler, and Hector Neff completed the first two steps between 2007 and 2013 (Pitblado et al. 2013). This document focuses on the petrographic analysis of a subset of the UGB quartzite samples. Examining samples at the microscopic level results in a quantitative mineral composition profile that complements geochemical analysis, recording the relationships between mineral grains and cement types that can influence chemical characterization.

Pitblado et al. (2013) reported LA-ICP-MS results of 402 samples from 48 discrete UGB quartzite sources in an effort to discriminate among quartzite sources. LA-ICP-MS was selected over other geochemical techniques because it is minimally destructive (Neff 2010; Speakman and Neff 2005). Sampled sources in the UGB include known prehistoric quarry sites, outcrops, and secondarily deposited cobbles. Three separate Principal Component Analyses (PCA) were run on the 28 cobble and 20 outcrop sources (n=48 total).

A PCA on exclusively cobbles demonstrated that eight components account for 99 percent of the variability, with the first two components accounting for 31 and 24 percent respectively. Samples from southeast of the town of Gunnison (and close to the Chance Gulch site, that is discussed later) and in the center of the project area of the UGB have a signature that is distinct from cobbles occurring elsewhere, although these samples do exhibit a high amount of internal variability not seen in the outcrop sources.

PCA on the outcrop sources revealed six components that together account for 100 percent of the variability. The first two components account for the majority of samples at 46 and 21 percent. A dendrogram based on this data demonstrates a general grouping by geologic age, with the exception of Cretaceous Parlin Flats samples CD09-3 and CD09-5, which grouped with Jurassic aged sources (Figure 3). Of special note here is that the three Jurassic aged groups clustered together. Pitblado et al. (2013) suggested that further analysis could differentiate among these sources or possibly the local forms of these occurrences.

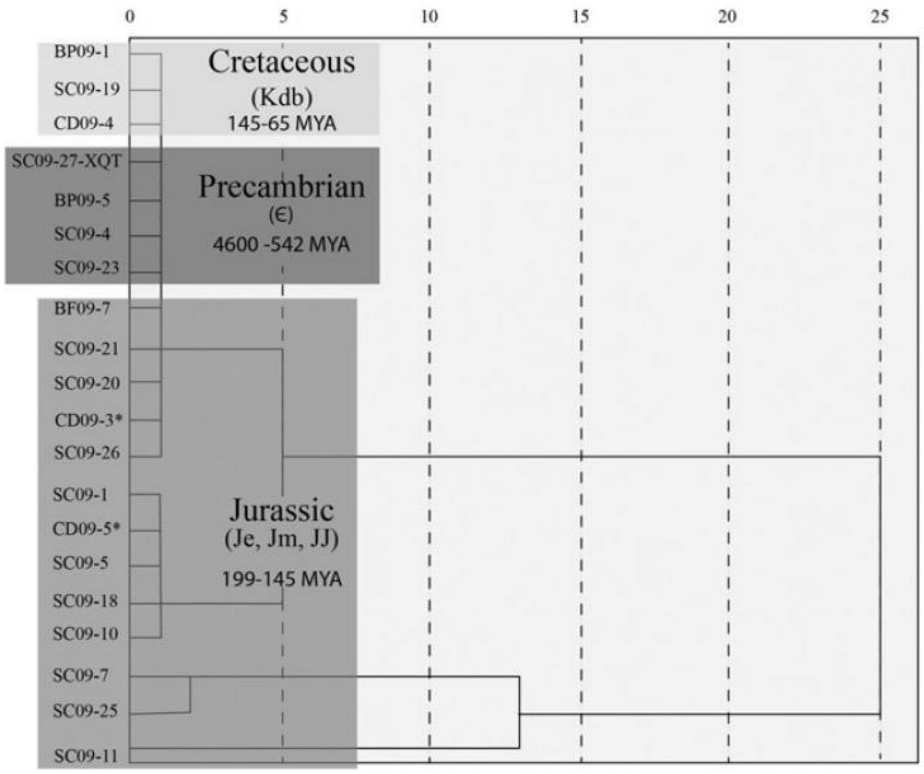

Figure 3. UGB outcrop samples dendrogram of the compete-linkage cluster analysis of averaged trace element signatures (Pitblado et al. 2013).

The PCA on all 48 sources outcrop and cobble sources demonstrated ten components accounting for 92 percent of the variability, with the first two components responsible for 42 and 12 percent, respectively (Figure 4). Generally, this discriminated between outcrop and cobble sources, although 7 outcrop sources grouped with 28 cobble sources. Geographically, the PCA indicates that principal component 1 (PC1) has higher scores in the central and northern areas, while the east and west-central areas record lower scores. PC1 correlates with the enrichment of many trace elements and is a powerful metric. Overall, cobble sources show more variability than outcrop sources. Outcrop sources in general have depleted trace element signatures due to their more homogenous nature compared with the more heterogeneous cobble sources. Outcrop

sources usually come from single geological formations, whereas cobble sources usually represent a mixing of numerous formations (Neff 2010; Pitblado et al. 2013).

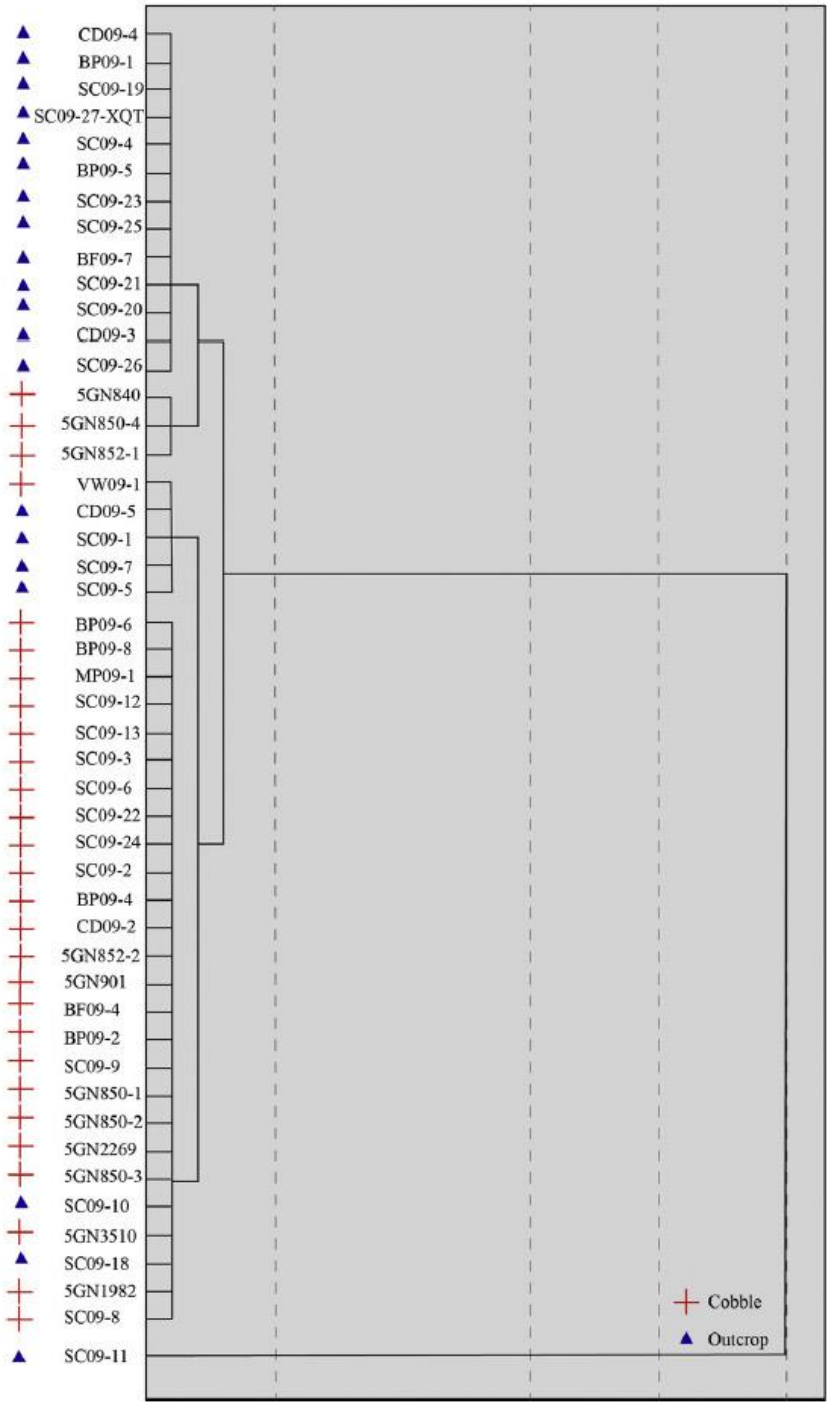

Figure 4. UGB outcrop and cobble dendrogram of complete-linkage cluster analysis of averaged trace-element signatures for all 48 sampled localities (Pitblado et al. 2013).

Problem Statement

The petrographic analysis of UGB quartzite is an independent analysis of the previously completed geochemical study (Pitblado et al. 2013). A direct comparison of the previous geochemical results to the petrographic results is not within the scope of this project because that would require the analysis of all 402 samples. Time and space limitations of a master's thesis do not allow for the analysis of all 402 samples. As an independent supplemental analysis, petrography allows for a more detailed understanding of mineral constituents not possible with geochemical analysis such as LA-ICP-MS alone because it describes individual grain relationships with mineralogical composition instead of strictly elemental composition. I first will look at the petrographic variability of quartzite Basin-wide followed by a detailed look at two prehistoric quarry sites including the intensively used 5GN1 and a locality called Parlin Flats. Site 5GN1 is a Jurassic outcrop and cobble source, while Parlin Flats is a Cretaceous outcrop source. The preceding geochemical analysis (Pitblado 2013) focused on a coarse grain or first pass at the data and was not aimed at fine grain source discrimination. Accordingly, the coarse grain analysis initially grouped both 5GN1 and Parlin Flats together, although the geochemistry also suggested at areas of differentiation. The close similarities between 5GN1 and Parlin Flats provides an ideal test of petrography's descriptive power that may provide the potential for stone artifact sourcing. This additional detailed analysis will demonstrate the homogeneity or heterogeneity of these individual sources and whether they change across space, facilitating a fine-grained understanding necessary for any subsequent artifact sourcing. The four main research questions of this study are:

1. What mineralogical and textual characteristics of UGB quartzite are identifiable at the microscopic level?
2. What is the petrographic variability at the very well-known and widely used prehistoric outcrop and cobble quarry 5GN1?
3. Can petrographic results refine our understanding of the Jurassic to Cretaceous bedrock transition at Parlin Flats, where that lithological contact is represented?
4. Is there a perceptible difference between the 5GN1 and Parlin Flats sources?

I address question 1 through the Basin-wide study consisting of petrographic analysis of 50 randomly selected quartzite samples collected from 48 discrete UGB source locations throughout the Basin. This represents 12% of 402 total samples. This Basin-wide study represents a proof of concept for the discriminatory power of quartzite petrography in the UGB. Questions 2, 3, and 4 focus on the well-known quartzite source of 5GN1 and Parlin Flats in the southern and southeastern areas of the UGB. Three samples from 5GN1 and four samples from Parlin Flats are included in the Basin-wide study in Chapter 4 because of the random sampling in addition to each individual source examination. An additional 16 samples are analyzed for the detailed 5GN1 analysis in Chapter 5, and an additional 11 samples are analyzed for the Parlin Flats analysis in Chapter 6. This amounts to 27 samples added for the detailed analysis presented in Chapters 5 and 6. In total, 77 quartzite samples are included in the analysis, which represents 19% of the 402 total samples.

Chapter 2: Archaeological and Geological Background

Upper Gunnison Basin Archaeology

Nearly 3,000 recorded archaeological sites from Folsom (10,500-10,000 ^{14}C yr BP) to historic times cover the 11,000 km^2 area of the UGB (Andrews 2013; Andrews et al. 2008; Cassels 1983; Pitblado 2003; Pitblado et al. 2013; Stiger 2001). The UGB is one of the high altitude intermountain basins in the Southern Rocky Mountains and one of five in Colorado, with elevations ranging between 2200-4300 m asl (Figure 2) (Benedict 1991; Mutel and Emerick 1992). The UGB contains five unique vertically oriented ecozones containing different flora and fauna that are seasonally variable (Benedict 1991; Pitblado 2003; Vale 1995; Wyckoff and Dilsaver 1995). Within this distinctive environment, chipped stone artifacts dominate archaeological assemblages. Interestingly, archaeological chipped stone assemblages in the UGB often contain more than 90% quartzite tools and debitage for the entire archaeological time span (Black 1991, 2000; Dalpra and Pitblado 2016; Pitblado 2002; Pitblado et al. 2013; Stiger 2001). Throughout the Southern Rocky Mountains chert and quartzite dominate assemblages with obsidian rarely found in the region. Obsidian is usually transported from northern New Mexico, but also occasionally from southern Idaho sources such as Valles Caldera and Malad (Black 2000; Metcalf and McDonald 2012). One small obsidian source is present near Cochetopa Pass on the southern edge of the UGB, although the cobbles derived are very small, allowing for small artifact manufacture only.

Early Paleoamerican

The early Paleoamerican period can be divided into early and late periods (Buchanan and Collard 2007; Cannon and Meltzer 2008; Frison 1993; Pitblado 2003;

Pitblado and Brunswig 2007). In the UGB 69 Paleoamerican sites have been reported with 82 components as several are multicomponent (Pitblado 2016). In general the early Paleoamerican period includes Goshen-Plainview, and Folsom sites (13,500-10,200 ^{14}C yr BP), whereas the late Paleoamerican period includes Cody (Eden and Scottsbluff), Hell Gap, Angostura, Jimmy Allen/Frederick, Great Basin Stemmed, and Concave Base Stemmed (10,200-7,500 ^{14}C yr BP) (Bamforth 2002; Frison 1993; Holen and Holen 2013; Kornfeld et al. 2010; Meltzer 2006; Miller et al. 2013; Pitblado 2003; Pitblado and Brunswig 2007). Early Paleoamerican projectile points are large, often well manufactured lanceolate points with the characteristic the Folsom channel flake removed (Kornfeld et al. 2010; Pitblado 2003).

No Clovis sites have been recorded in the UGB, although some isolated finds are reported in private hands, but this has not been professionally confirmed (Pitblado 2016). One possible site was recorded (5GN149) with dense lithic scatter with large, thin bifaces and overshot flakes, but Clovis afflation could not be substantiated (Cooper 2006; Cooper and Meltzer 2009). In the UGB early Paleoamerican sites include projectile point surface finds, and the Mountaineer Folsom site, which consists of shallow deposits of Folsom projectile points and debitage from their manufacture with possible structure platforms (Andrews 2010, 2013; Andrews et al. 2008; Stiger 2001, 2006; Pitblado 2002, 2003, 2016). Other Folsom sites in the Basin include the much smaller Soderquist, Flat Top (Andrews 2010), and Lanning sites (Andrews 2010; Pitblado 2016). In neighboring regions several Folsom sites are documented including the Jerry Craig, Upper Twin Mountain, and Barger Gulch sites in Middle Park, Black Mountain near Creede and, Linger, Reddin, Stewards Cattle Guard, and Zapata in the

San Luis Valley (Jodry 1999; Jodry and Stanford 1996; Jodry et al. 1992, 1996; Kornfeld 2013; Kornfeld et al. 2010; Surovell and Waguespack 2007; Surovell et al. 2005).

Late Paleoamerican

The late Paleoamerican period is characterized by large lanceolate and stemmed projectile points in chipped stone assemblages. Two of the most commonly found late Paleoamerican projectile points in the Basin are the oblique flaked Angostura and the parallel oblique flaked Jimmy Allen/Frederick types, which both are frequently basally ground (Kornfeld et al. 2010; Pitblado 2003). The late Paleoamerican period is better represented in the UGB than the early Paleoamerican period with numerous surface finds and five excavated sites. The oldest radiocarbon date in the UGB of 9,800 ^{14}C yr BP came from an unlined fire pit at the Elk Creek site (Kornfeld et al. 2010; Stiger 2001; Pitblado 2002, 2003). Other notable late Paleoamerican sites in the UGB include Tenderfoot, Kezar Basin, Ponderosa/Soap Creek and Chance Gulch (Euler and Stiger 1981; Jones 1984; Stiger 2001; Pitblado 2003). Both Kezar Basin and Tenderfoot have yielded deer, antelope, bighorn sheep, and bison bone associated with possible structures. Chance Gulch is a multicomponent site with an excavated in-situ hearth that radiocarbon dated to 7990+/- 50 ^{14}C yr BP with 17 surface and 7 in-situ projectile points of primarily the Angostura type (Pitblado 2002, 2016).

Archaic

The Early Archaic (7500-5000 ^{14}C yr BP) and Middle Archaic (5000-3000 ^{14}C yr BP) periods demonstrate an increased occurrence of roasting pits, hearths, structures, windbreaks, and ground stone compared to the Paleoamerican periods (Stiger 2001).

The Early Archaic period is also characterized by a swift change to side-notched projectile points that exhibit more morphological variation when compared with Paleoamerican projectile points (Kornfeld et al. 2010). Projectile point technology changed from relatively large lanceolate to smaller stemmed and notched points with an increase in stylistic variability (Reed and Metcalf 1999). Generally, beginning in the Early Archaic and becoming even more pronounced during the Middle Archaic, the number of sites increases and suggest a broadening diet. This broadening diet is evidenced by an increased dependence on plant materials with increasing amounts of recorded groundstone and manos (Kornfeld et al. 2010; Reed and Metcalf 1999; Stiger 2001). Many Archaic sites in the UGB have been excavated contributing to their greater representation in the archaeological record (see Stiger 2001 for a lengthy list).

Middle Archaic projectile points are mostly McKean variants exhibiting lanceolate flaking with indented bases and convex blade edges narrower at the base than at the middle of the point (Kornfeld et al. 2010). Radiocarbon dates are more numerous during the Middle and even more during the Late Archaic as compared to earlier periods, suggesting a significant population increase (Kornfeld et al. 2010; Stiger 2001). It is important to be cautious of this interpretation because most of these radiocarbon dates come from CRM projects prompted by energy extraction. Energy extraction occurs in areas due to geologic factors that may create a sampling bias, because these areas do not represent all of prehistory or human mobility/settlement patterns. These areas receive a higher concentration of archaeological surveys and excavations when compared to the rest of the basin. Further, formation processes and different erosion processes may alter the preservation and presence of charcoal to date (Surovell et al.

2009). A majority of the archaeological work in the Gunnison Basin involves Archaic sites. The concentration of sites is higher during the Late Archaic (3000-1500 ^{14}C yr BP), with the Early and Middle periods being similarly well represented (Pitblado 2002, 2003). Pottery begins to appear during the Late Archaic in the Gunnison Basin as unadorned Brownware.

Late Prehistoric

The last culture period recognized in the UGB is the Late Prehistoric (1500-150 ^{14}C yr BP) period, which again is characterized by more radiocarbon dates that may indicate as population growth (Kornfeld et al. 2010; Stiger 2001). Environmental degradation is suggested to have caused a drastic shift in the use and occupation of the UGB (Black 1983; Stiger 2001). During the Late Prehistoric period small corner notch triangular points are most common with the ubiquitous Cottonwood Triangular present as well. Stiger (2001) argued that an increase in game drives and an increased frequency of non-quartzite toolstone signaled this abrupt change from the Archaic, although he overemphasized the increase in non-quartzite toolstone during the Late Prehistoric. While the use of chert/chalcedony and obsidian/fine grain volcanics did increase it was marginal as the total toolstone assemblage when compared basin wide did not dip below 70 percent quartzite (Dalpra 2015). Stiger (2001) further argued that the Late Prehistoric was characterized by logistically organized, highly mobile hunting parties instead of a more permanent hunter-gather in the UGB, although this is derived from a highly fragmentary and incomplete archaeological record largely based on undated surface sites. In fact, Peart (2013), refuted these assertions as contradicting of what many dated site assemblages actually show. Throughout prehistory, peoples in the UGB

lived a shifting yet intensive, mobile lifeway, leaving behind material culture consisting mainly of chipped stone tools and debitage with the occasional presence of pottery (Lipe and Pitblado 1999; Pitblado et al. 2013).

Quartzite Geology and Petrography

Geologic Setting

The UGB is one of five intermountain basins in the Colorado section of the Southern Rocky Mountains (Figure 2). The UGB lies east of the Uncompahgre Plateau, south of the Elk Mountains, west of the Sangre de Cristo Mountains, northwest of the San Luis Valley, and north of the San Juan Mountains. The only outlet in the UGB below 8,700 feet asl is the infamously narrow and deep Black Canyon of the Gunnison. Several different geological processes have contributed to the current landscape in the UGB including erosion, sedimentation, folding, faulting, peneplanation, volcanism, and intrusive igneous magmatism (Liestman 1985; Prather 1982).

Unlike the San Juan Mountains to the south, which are dominated by Tertiary volcanic rocks, the UGB shows a complex and diverse geologic history, with ages ranging from Precambrian to Quaternary (Liestman 1985; Streufert 1999). Precambrian rocks are the oldest in the world, and are relatively rare on Earth's surface. Precambrian rocks in the UGB are separated into two major formations: the younger metasedimentary Black Canyon Schist and the older metavolcanic Dubois Greenstone (Hedlund and Olson 1981; Tweto 1987). The Dubois Greenstone comprises three different sub-groups: metabasalt and meta-andesite flows, felsite porphyries and metatuffaceous rocks, and epiclastic rocks from older volcanic depositions (Hedlund

and Olson 1981). During the Late Paleozoic and Early Mesozoic eras, uplift and erosion caused the peneplanation of nearly all rocks to the Precambrian basement prior to the deposition of Upper Jurassic Junction Creek Sandstone (Hedlund and Olson 1981). This is especially true in the southern UGB where virtually no Paleozoic rocks are found, although a few remain in the northern portion. These deposits include the Pennsylvanian Maroon formation (Red shale, siltstone, arkosic sandstone and conglomerate with evaporites), Pennsylvanian Gothic shale, and Pennsylvanian Belden shale, which are the only remnants of the ancestral Rocky Mountains in the UGB (Cullers 2000; Larsen and Cross 1956; Prather 1982). The Maroon Formation is one of the best studied formations partly because of the imposing and famous Maroon Bells (14, 014 and 14,156 feet asl) near Aspen that formed as shallow inland marine deposits (Cullers 2000; Liestman 1985). Paleozoic and Mesozoic rocks are mainly sedimentary with small igneous intrusions (Gaskill 1977; Streufert 1999).

Mesozoic and Cenozoic rocks are common in the UGB. During the Upper Jurassic period much of Colorado and the entirety of the UGB was covered by an arid dune field (Cullers 1995; Golonka and Ford 2000) that later formed both the Jurassic Entrada sandstone and Navajo sandstone (Prather 1982). The Entrada sandstone is prevalent in the UGB, while the Navajo sandstone is concentrated in the Colorado Plateau to the southwest of the UGB. Mid-Jurassic climate change due to the breakup of the supercontinent Pangea contributed to the formation of Jurassic Junction Creek sandstone. The climate changed to a lush and moist tropical environment, silicifying Junction Creek sandstone in comparison to Entrada sandstone (Cullers 1995; Golonka and Ford 2000; Prather 1982). Both formations are very similar in composition,

essentially forming from similar dune fields, causing debate among geologists over where the contact zone lies (Prather 1982). The Entrada can reach up to 300 m in thickness, but in the UGB it only reaches a maximum thickness of 125 m, part of which is likely Junction Creek sandstone (Liestman 1985). Many rocks from the Mesozoic and older time periods were subjected to contact metamorphism during emplacement of late Cretaceous and younger intrusive igneous rocks (Gaskill 1977).

The Middle Jurassic period also saw the formation of rivers flowing north carrying cobbles, volcanic ash, and sand (Golonka and Ford 2000; Liestman 1985; Young 1973). The volcanic ash and sand formed the Morrison Formation (mudstone, sandstone, siltstone, and limestone), which by no coincidence runs north-south expansively with the uplifted area over much of the greater Rocky Mountain region. Dramatic climate change resulted in a vast epeiric sea (shallow inland sea) covering most of the region during the Cretaceous period, depositing the Dakota sandstone and Burro Canyon (sandstone, shale, limestone, chert, and conglomerate) Formations. The epeiric sea had a variable coastline, with the rise and fall of the sea level contributing to these formations (Cullers 1995; MacKenzie 1975). Dakota sandstone in particular formed from the fine-grain sand beaches. The ordered nature of the Cretaceous formations suggests consistent depositional processes over long periods of time.

During the late Cretaceous the Laramide Orogeny uplifted the Precambrian basement through faults, forming the modern Rocky Mountains (Liestman 1985; Livaccari 1991; Prather 1982). This dramatic uplift was caused by the Kula and Farallon plates impacting the North American plate at a low subduction angle (English and Johnston 2004; Livaccari 1991). The Laramide Orogeny is also the cause of

intermountain basin formation throughout the Rocky Mountains because these areas did not contain faults allowing the Precambrian basement to be uplifted (English and Johnston 2004; Livaccari 1991).

During the Cenozoic era multiple concurrent geological processes occurred including erosion, sedimentation, glaciation, volcanism, and intrusive igneous magmatism (Epis and Chapin 1975; Prather 1982). All processes except glaciation occurred simultaneously during the early Cenozoic era when the volcanic San Juan Mountains formed (English and Johnston 2004; Epis and Chapin 1975; Prather 1982). Oligocene volcanic events adjacent to the UGB that deposited tertiary volcanic rocks include the eruptions of the West Elk Volcano 30 million years ago and the La Garita caldera 27.8 million years ago (Lamphere 1988; Stamm et al. 2004). During the Quaternary period intense glaciation covered the whole Rocky Mountains terminating at the end of the Pleistocene when human populations began to rapidly expand (Bendedict 1992a, 1992b; Prather 1982). Many features of the modern landscape are the result of the long glacial periods contributing recognizable features including the horns, tarn lakes, and cirques common throughout the Rocky Mountains.

Within the project area, units containing quartzite include Precambrian metaquartzite, Paleozoic and Mesozoic orthoquartzite, Paleozoic and Mesozoic conglomerate, Paleozoic and Mesozoic contact-metamorphosed sandstone, and Tertiary and Quaternary gravels (DeWitt et al. 1985; Hedlund and Olson 1973, 1974; Streufert 1999; Tweto 1987; Zech 1988). Major formations sampled in the following research include Cambrian Saguache quartzite, Ordovician Harding sandstone, Ordovician Parting sandstone, Jurassic Junction Creek sandstone, Jurassic Morrison Formation,

Cretaceous Dakota sandstone, and Cretaceous Burro Canyon Formation (Pitblado et al. 2013).

Quartzite Definition

Quartzite is an exceptionally hard, quartz-rich rock that fractures irregularly through grains and cement, forming an irregular or conchoidal fracture surface (Howard 2005; Liestman 1985). Geologically, quartzite is classified as sandstone, where mineralogical composition and texture are the two major classification criteria created during deposition (Tucker 2001). Carozzi (1993) describes quartzite as a tight mosaic of interlocking crystals and grain overgrowths resulting in a quartzitic texture, while Howard (2005) describes quartzite as having a composition of 95% quartz or greater. On average, sandstones contain between 60 and 70 percent quartz grains (Blatt and Christie 1964; Pettijohn 1957). Clearly, geologists do not just have different definitions, but are classify the material in different ways. Mineralogical composition relates to source rock composition, tectonism, weathering, and subsequent diagenetic processes after initial deposition.

Three major grain types are generally used to describe mineralogical composition of quartzite: quartz, feldspar, and lithics (here meaning a sand-sized rock fragment commonly of sedimentary or igneous origin, including accessory minerals) (Dott 1964). Composition is commonly displayed in ternary diagrams called QFL plots where quartz, feldspar, and lithics are charted as end members (Figure 5). Texture is the expression of the grain size, sorting, and shape in combination with the amount of interstitial pore material known as matrix. Matrix is the main classification for the differences between arenite, wacke (<15% matrix), and mudstone (<75% matrix) (Dott

1964; Pettijohn et al. 1987).

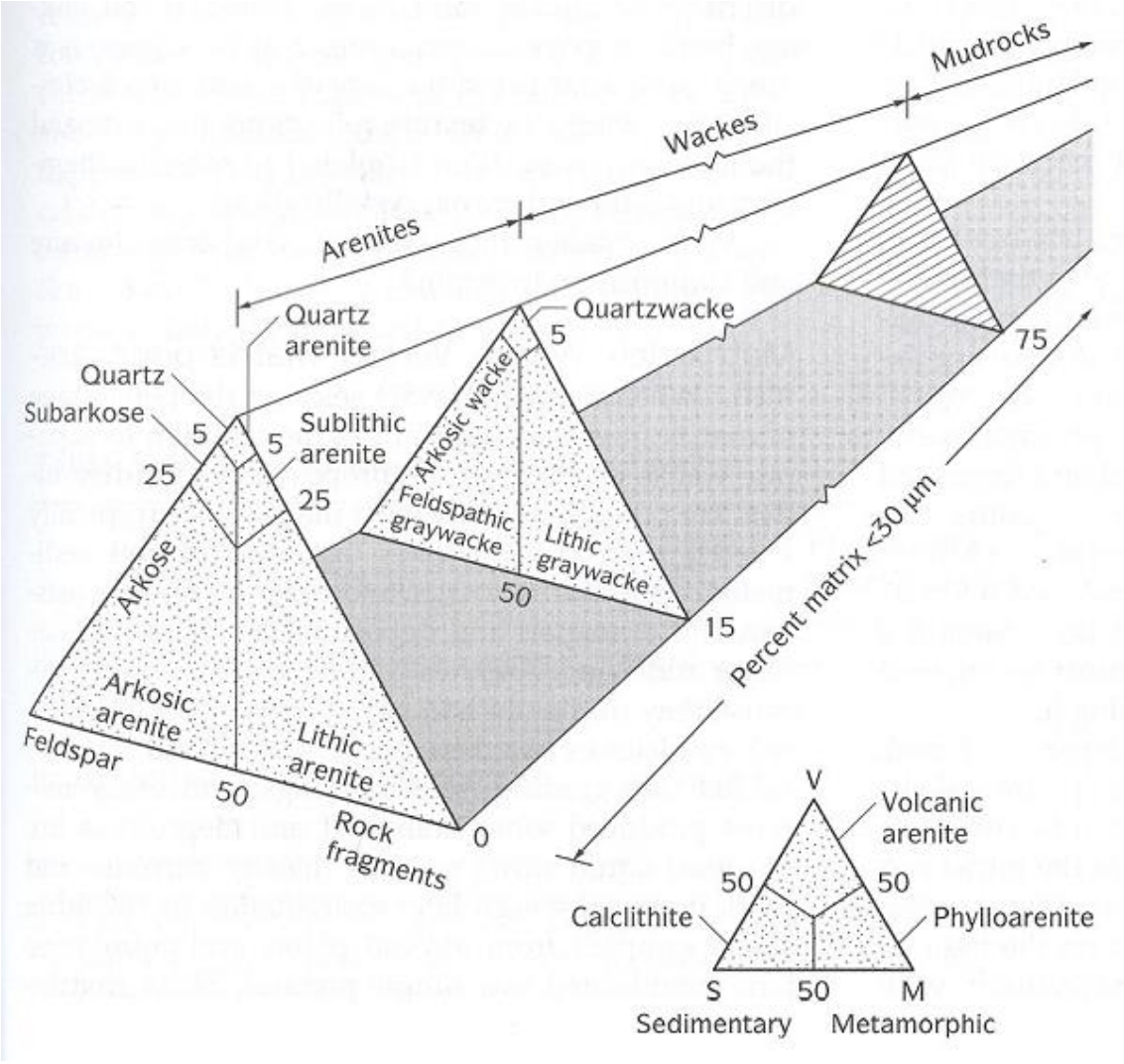

Figure 5. Dott (1964) ternary diagram classification for sandstone and quartzite classifaction.

Quartzite is almost always classified geologically as a quartz arenite, meaning it contains 95% or more quartz grains. Quartz arenites are divided into subfeldspathic and sublithic arenites depending on the higher quantity of either feldspar or lithic grains maintaining 75% or more quartz grains. Lower quantities of quartz are classified as either a feldspathic arenite or a lithic arenite. Wackes are also subdivided, and whereas all arenites are grain supported, wackes range from grain supported to matrix. Matrix

referring to a cement of a different minerology, rather than grain attributes such as quartz overgrowths. Geologists use other terms to further differentiate sandstone. Arkose sandstone is more than 25% feldspar and is synonymous with feldspathic arenite (Howard 2005). Although different quartzite definitions do exist beyond these two examples, I define quartzite in this research as all quartz arenites that contain 90% or more quartz grains. This includes some subfeldspathic and sublithic arenites.

At a macroscopic level there are two major quartzite classes formed by subsequent diagenic processes: orthoquartzite and metaquartzite. Orthoquartzite refers to a sedimentary rock, while metaquartzite is metamorphic. The major difference is the degree of heat and pressure applied during formation (Carozzi 1993; Ebright 1987). Metaquartzite experiences higher heat and pressure, causing fusion of individual grains and resulting in extremely hard rock that fractures irregularly instead of conchoidally. Under the microscope, metaquartzite shows little cement and demonstrates sutured boundaries between connecting grains (Figure 6) (Carozzi 1993; Tucker 2001), whereas orthoquartzite contains quartz overgrowths and cement that visibly separates individual grains (Figure 7) (Ebright 1987). In the pilot study on UGB quartzite (Pitblado et al. 2008), many samples consisted of elements other than silica separating them from microcrystalline silicates (i.e., chert, flint, and chalcedony) commonly used as prehistoric toolstone (Cackler et al. 1999; Luedtke 1978, 1979; Roll et al. 2005). This variable mineralogy not only allows for chemical discrimination, but also the greater petrographic detail further distinguishing the quartzite within and beyond the UGB.

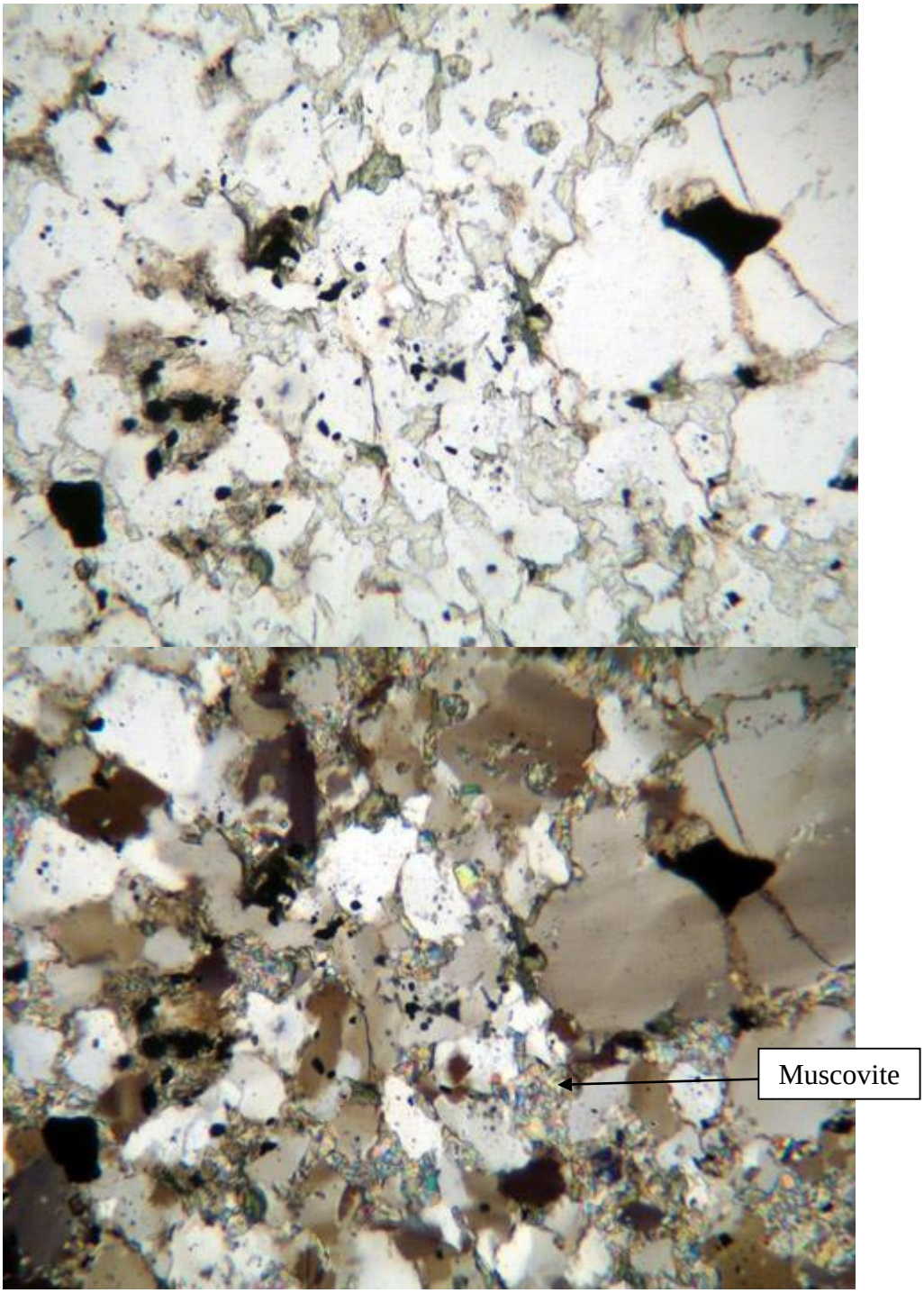

Figure 6. Sample CD09-2D with muscovite birefringent material (center) with sutured grain boundaries evident, and the poorly sorted quartz grains. The sutured grains are a key characteristic of metaquartzite. Top photomicrograph is in plane light with the bottom in cross-polarized light under 10X magnification.

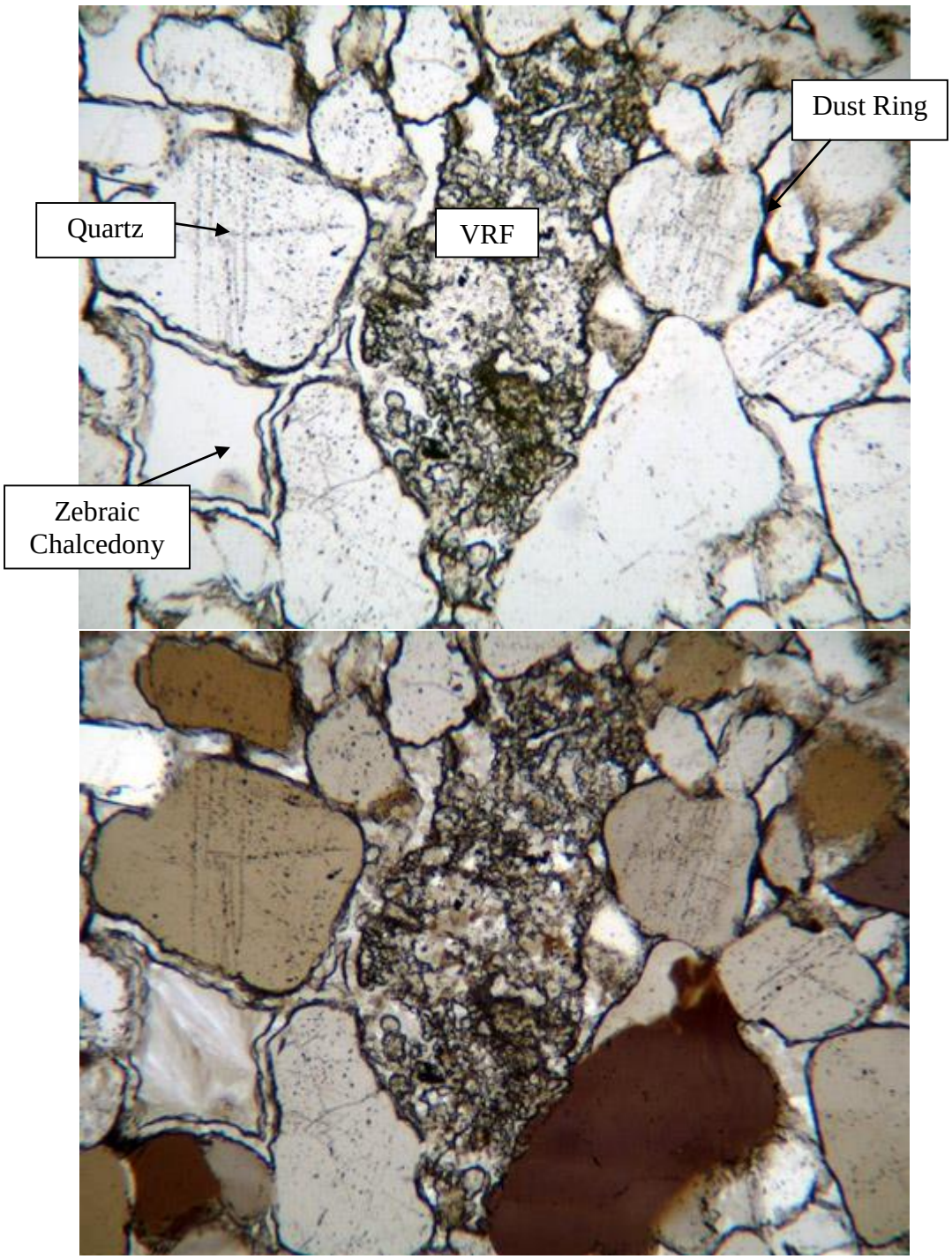

Figure 7. Sample SC09-18B with a Volcanic Rock Fragment (VRF), surrounded by quartz grains exhibiting thick dust rings and zebraic chalcedony cement. Notice the black dots and lines on the quartz grains indicating increased during formation. Top photomicrograph is in plane light with the bottom in cross-polarized light under 10X magnification.

Petrographic Characteristics and Classification of Quartzite

Several different characteristics are used to petrographically characterize quartzite in the UGB. These not only allow for the differentiation between different the types of quartzite, but also a detailed analysis of quartzite at a much finer level.

Microscopic evaluation begins with qualitative data recording. Lithifaction and diagenesis are described through qualitative sediment texture attributes of grain size and morphology. Grain size is measured through conversion from an internal grid in the Olympus BH2 microscope to millimeters and assigned size on the Udden-Wentworth grain-size scale (Table 1, Wentworth 1922). On the Zeiss Axio AX10 Imager Z1 used with the 5GN1 and Parlin Flats samples grain size is averaged from minimally 30 grain measurements from an image through software tied to the microscope. Grain morphology consists of two main categories: roundness and sorting. Roundness includes six categories from very angular to well rounded (Powers 1953; Pettijohn et al. 1987). Grain sorting is determined by comparing the degree of similarity in grain size (Carozzi 1993; Scholle 1979; Tucker 2001). Five categories ranging from very well to poorly sorted describe grain sorting.

Table 1. Udden-Wentworth (Wentworth 1922) grain size scale. This is the standard size description of grain size within petrography and is used in this research.

Millimeters (mm)		Micrometers (μm)	Phi (ϕ)	Wentworth size class		Rock type
	4096		-12.0	Boulder		
	256		-8.0	Cobble	Gravel	Conglomerate/ Breccia
	64		-6.0	Pebble		
	4		-2.0	Granule		
	2.00		-1.0	Very coarse sand		
	1.00		0.0	Coarse sand		
1/2	0.50	500	1.0	Medium sand	Sand	Sandstone
1/4	0.25	250	2.0	Fine sand		
1/8	0.125	125	3.0	Very fine sand		
1/16	0.0625	63	4.0	Coarse silt		
1/32	0.031	31	5.0	Medium silt		
1/64	0.0156	15.6	6.0	Fine silt	Silt	Siltstone
1/128	0.0078	7.8	7.0	Very fine silt		
1/256	0.0039	3.9	8.0			
	0.00006	0.06	14.0	Clay	Mud	Claystone

Mineral composition is assigned from point counting individual grains. Point counting is the systematic quantitative description of a sample by counting every grain present under the microscope crosshairs. This is completed with the use of a point count mechanism attached to the microscope stage that allows for precise horizontal transecting through a sample. The point count mechanism creates an artificial grid with equally spaced intervals. The size of the grid varies by sample because each grid point must be wider than the largest grain, yet account for as much of the sample as possible (Tucker 2001). This technique is standardized in geology as the Gazzi-Dickinson method (Dickinson 1970, 1985; Dickenson and Suczek 1979; Graham et al 1975; Ingersoll et al. 1984). Qualitative assessment is additionally assigned as stated above to

describe the diagenic processes involved with the formation of the sample (e.g., grain roundness, sorting, and texture).

Individual grain identification is determined through visual characteristics under plane and cross-polarized light. The sample is rotated so that polarized light vibrates at different angles within the crystal (Raith et al. 2011; Scholle 1979; Tucker 2001). An upper polarizer set at a right angle to the lower polarizer is inserted and withdrawn from the microscope. When the upper polarizer is inserted, the mineral sample is viewed between crossed polarizers. With no sample or an isotropic sample present, no light will be visible because the polars are crossed. However, if a randomly oriented anisotropic mineral is inserted, the crystal will appear and will go extinct (dark) every 90° of stage rotation (Raith et al. 2011; Tucker 2001). Plane and cross-polarized light allow for the identification of minerals through this extinction, because the individual grain texture and color are not otherwise visible. Other optical properties including relief, birefringence, and twinning are diagnostic of certain minerals and are discussed below.

Quartzite is dominated by quartz grains, with feldspar (mainly microcline and orthoclase), muscovite, and accessory minerals like tourmaline and zircon (Carozzi 1993). Some rounded grains of chert and volcanic rock fragments occur, although infrequently.

Monocrystalline quartz grains are derived from plutonic igneous and metamorphic rocks, older reworked sandstone, or phenocrysts of volcanic and pyroclastic rocks (Carozzi 1993; Raith et al. 2011; Tucker 2001). Monocrystalline quartz grains are split into two different types based on how they demonstrate undulatory extinction (turn dark) when the microscope platform is rotated (Tucker

2001). Quartz monocrystalline undulatory (QMU) grains display a wavy or rolling extinction where the grain gradually turns dark when rotated on the platform (Table 2). Quartz moncrystalline nonundulatory (QMN) grains display a straight extinction where the entire grain turns dark when simple based on grain shape. Grains of volcanic origin contain a bipyrimidal phenocryst shape and are strain-free, displaying a straight nonundulate extinction. Grains from older reworked sandstones show remnants of abraded overgrowths and a generally rounded to subrounded shape, which typically have undergone increased stress, contributing to a rolling undulate extinction. These are the most common grains in UGB silicified sandstones and quartzite. Grains derived from phenocrysts in rhyolites show overgrowths and intervening inclusions generated during the different accretion phases, which are usually noundulatory (Carozzi 1993; Scholle 1979; Tucker 2001). Quartz polycrystalline grains are derived either from plutonic igneous rock bodies (tabular and/or massive plutons), metamorphic origins, or vein filling, identified by subparallel or intersecting quartz crystals with different extinctions within a single grain. These are formed through high strain and heat. Quartz polycrystalline grains are split into two separate categories for petrography: quartz polycrystalline simple (QPS) and quartz polycrystalline complex (QPC). The difference between these categories is that QPS contains three or fewer crystals in a single grain while QPC contains more than three crystals in a grain. All quartz grains can display Bohme lamallae, which are parallel, irregular planar trails on a quartz grain that indicate high stress or a low grade metamorphic origin (Raith et al. 2011). Other grains and minerals that occur in UGB quartzites include micas (specifically muscovite and biotite), feldspars, rock fragments, and heavy minerals.

Feldspar grains are the most frequently occurring grain besides quartz (Tucker 2001). Feldspars are softer and some such as plagioclase have distinct twinning, a unique attribute shared by few other minerals where crystal-structure intergrowths of two or more crystals mirror or rotate against each other's orientation (Raith et al. 2011). Twinning is easily identifiable under cross-polarized light with the individual parts demonstrating different birefringence and extinction. Birefringence is a mathematical range from largest to smallest refractive index, where those with high birefringence demonstrate bright colors and those with low birefringence show dull colors or black and white (Raith et al. 2011). Without a stain, it is difficult to tell the difference between feldspars and quartz in plane and polarized light, especially when the feldspar grains are weathered, as most are in UGB quartzites. To account for this difficulty, a potassium-feldspar (K-spar) hydrofluoric stain that turns feldspars a distinct yellow is commonly used in analysis, and is used in this study.

Rock fragments are the coarsest grains in quartz and sandstones and are referred to as “lithics” in geology (Scholle 1979; Tucker 2001). Lithics are groups of fine-grain igneous and sedimentary rocks picked up from surrounding bedrock deposits (Carozzi 1993; Tucker 2001). Rock fragments can be confused with heavy minerals such as iron because they appear black under cross-polarized light, but heavy minerals stay black and do not display extinction unlike rock fragments. Because of this unique attribute heavy minerals are also referred to as "dark" minerals. Rock fragments are usually made of many different small grains aggregated together instead of a single grain as in heavy minerals.

Table 2. Petrographic classification explanation for this study. All different categories are unique grains documented in the UGB quartzite and will be discussed further.

Petrographic Classification	Description
QMU	Quartz Monocrystalline Undulatory-Grain displays a wavy or rolling extinction
QMN	Quartz Moncrystalline Nonundulatory-Grain displays a straight extinction
QPS	Quartz Polycrystalline-Three or less crystals in a single grain
QPC	Quartz Polycrystalline-More than three crystals in a grain
Matrix	A dominate cement that envelops all grains
Silca Cement	Quartz overgrowths or commonly chalcedony
Wx Feldspar	Weathered Feldspar
VRF	Volcanic Rock Fragment
Calcite	Carbonate
Chalcedony	Silcia, mainly zebraic in the samples
SRF	Dentrical Chert fragment
Biotite	High Birefringence, displays pleochroism and parallel extinctions
Iron	Dark or opaque minerals
Sericite	Highly degraded feldspar degrading into clay when subjected to hydrothermal alteration
Chlorite	A sheet silicate mineral similar to mica but is less birefringent appearing green in plane light and brown in cross polarized light

Micas commonly occur as sheet silicates in the matrix of quartzite and sandstones. Muscovite and biotite are easy to identify under cross polarized light because both are highly birefringent and exhibit parallel extinction (Scholle 1979; Tucker 2001). Biotite displays a brown to green pleochroism from plane to cross-polarized light. Pleochroism is a property where different colors are exhibited as a function of variable light vibrations when the microscope platform is rotated (Raith et al. 2011). Muscovite is almost colorless in plane light, but has bright second order colors under cross-polarized light (Carozzi 1993; Scholle 1979; Tucker 2001). Clay minerals also commonly occur with micas. Common clay minerals in the UGB quartzite samples are kaolinite and chlorite. Both minerals form through chemical weathering processes leaching ions (ions are removed by dissolution into water). Kaolinite is chemically weathered feldspar, and chlorite is chemically weathered rock fragments (Kroll et al. 1986). Both are identified by a slightly different pleochroism, transitioning from brown to a dull green with less birefringence than biotite.

In a rock, the pore-filling material consists of cement that precipitates normally with groundwater between grains to bind them together, thus making sand, sandstone. This occurs during the lithification and/or diagenic sediment process. Quartzite cement can begin as a pressure solution, but most commonly it is precipitated silica overgrowths on quartz grains formed in an aqueous solution or well-ordered, low temperature quartz (Carozzi 1993). On monocrystalline grains overgrowths have the same optical extinction orientation, but for polycrystalline grains the overgrowth matches the orientation with the individual crystals in direct contact. This trend also extends to chert grains. The area between a grain and overgrowth is a capillary pore that

forms dust rings containing minute mineral grains, clay mineral coatings, iron oxides, and organic matter, all of which contribute to the overall shape of the grain, but stop at the boundary with overgrowths (Carozzi 1993). Silica-base overgrowths and chalcedony cements are common in UGB quartzite. Pressure solution cements, normally carbonates such as calcite, contain independent extinctions to crystal structure and grain contact. Calcite can appear in different colors, but is mainly white and occasionally black, appearing dull and without grain shape or boundaries common with other structures in quartzite and sandstones. Chalcedony in UGB quartzite is almost exclusively zebraic with a combination of brown/black and white stripes, which alternate when rotating the microscope platform. Less common cements in quartz arenites include gypsum, barite, celestite, and opal. Chlorite occurs frequently in clay cements, although these do not appear in the samples examined with one exception.

Previous Quartzite Provenance Research

Archaeological efforts to source quartzite have been mostly successful when attempted, yet the aggregate nature of sedimentary quartzite is difficult to understand (when compared to obsidian and fine grain volcanics) contributing to little peer-reviewed literature (Ebright 1987; Church 1994, 1996; Howard 2005; Liestman 1985). Since quartzite is one of the most common rocks in the world and often fracture concordially, it was frequently used by prehistoric peoples for stone tool manufacture, grinders (for maize, nuts, and grains), and sculptures. Stross et al. (1988) provided the first successful archaeological example utilizing quartzite provenance analysis by combining Instrumental Neutron Activation Analysis (INAA) and petrography to differentiate two quarries 900 km apart as the source for the Egyptian Colossi of

Memmon. Liestman (1985) completed extensive research in the Curecanti National Recreation Area in the UGB, describing quartzite-bearing units and which quartzite materials are commonly found at archaeological sites there. Liestman also used limited petrography to describe quartzite. Similarly, Church (1994, 1996) used a combination of petrography and XRF to gain an understanding of quartzite and chert in the Bearlodge Mountains in Wyoming and Ogallala Orthoquartzite in Nebraska along the northern Missouri River with some promising results.

Chapter 3: Methods

Field Collection

Under the direction of Bonnie Pitblado and Carol Dehler Utah State University students completed field collection of quartzite samples during an archaeology field school in 2009. The collection sampled 48 discrete geological localities across the 11,000 km^2 of the UGB (Figure 2). Outcrop (primary) and cobble (secondary) quartzite exposures were targeted because prehistoric peoples had equal access to both (Pitblado et al. 2013). Sample sites included recorded archaeological sites and geological exposures visited after locating them on geological maps (Gaskill 1977; Gaskill et al. 1986, 1987; Streufert 1999). Samples came from all potential UGB quartzite sources including Precambrian metaquartzite and quartz veins, Paleozoic and Mesozoic orthoquartzite, Paleozoic and Mesozoic quartzite-bearing conglomerate, Paleozoic and Mesozoic contact-metamorphosed sandstone, and Tertiary and Quaternary quartzite-rich cobbles (Pitblado et al. 2013). The sampling focus was on the known quarries around the Chance Gulch site (cobble quarries), above the Gunnison River and modern Blue Mesa Reservoir, and other known bedrock and cobble quarries (Figure 2).

Both outcrops and cobbles were sampled, although in slightly different ways (Pitblado et al. 2013). A Jacob's staff assisted in measuring vertical increments on outcrops, with fist size samples taken at each meter increment. Lateral sampling occurred at one meter increments.

A separate protocol was necessary for cobble deposits. After identifying Tertiary and Quaternary cobbles in alluvial fans, a 30 m tape was laid in either north-south or east-west. Samples were recorded at one meter intervals, with ten centimeters on either side if necessary. If 10 samples were not found, the tape was re-laid on the same

cardinal axis with collection continuing until 10 quartzite samples (or quartzite-like material in the field) intersected on the transect. Students and supervising professors recorded all locations, photographed, and sketched the location of outcrop samples. All locations were recorded using GPS units in UTM coordinates, zone 13S (Pitblado et al. 2013).

Laboratory Methods

Two research assistants made the 402 samples made into billets (12-X-24-X-46 mm) under Dr. Dehler's supervision in the Geology Department at Utah State University (Pitblado et al. 2008; Pitblado et al. 2013). Quality Thin Section of Tucson, Arizona manufactured the billets into thin sections, hand polished to 30 microns and stained feldspar yellow for easy identification. My research begins with the microscopic analysis. All Basin-wide study point counts are completed with an Olympus BH2 microscope with a Cannon Powershot G6 camera (for photos), while 5GN1 and Parlin Flats samples were analyzed on a Zeiss Axio AX10 Imager Z1. Two different research locations in two states required the use of two different microscopes. The Olympus BH2 is at the Utah State University geology department, while the Zeiss Axio AX10 Imager Z1 is at the University of Oklahoma geology department. Both are optical microscopes with a polarized filter under the stage, a circular rotating stage, and a second removable polarized filter with light traveling in two perpendicular polarized light planes (the Zeiss is set up in the opposite configuration). Each slide is placed in the same orientation with the label to the right and point counts beginning at the same location on the point count mechanism.

Random sample selection is important for the proof of concept to prevent bias on. This way I could not place my knowledge of how the samples should differentiate, and instead focus on the accurate analysis. I thoroughly describe each sample in terms of texture, composition, bedding or foliation, and crosscutting relationships. One-hundred grain point counts were completed instead of the standard three hundred (Dickinson 1970, 1985; Ingersoll et al. 1984) after a test study conducted by Dr. Dehler and students concluded that a 100 point count statistically differentiates UGB composition as accurately as a 300 point count (Dehler 2012; Lister and Hobbs 1980; Tucker 2001). Dr. Dehler's test is verified by previous studies centered on orthoquartzite petrography in relation to provenance studies (Blatt and Christie 1963).

Analytical Methods

I recorded all data from the point counts in Excel spreadsheets and described them in a Word document. I imported the Excel data into IBM Statistics Package for the Social Science version 10.2 (SPSS ®) to perform statistical analysis. Ternary diagrams of row standardized or normalized petrographic data (Figure 5) are created in the Grapher 10 ® program putting data into one of three end members (quartz, feldspar, or lithics referred to as QFL) to display sample mineral composition. Ternary diagrams are commonly used with petrographic data graphically displaying three variables (in this case the QFL categories) row standardized for each individual category. The ternary diagrams are a powerful representation of sample composition and are the main graphic representation responsible for research questions 2-4 to describe sample variability. Petrographic categories for statistical analysis consist of between three and fifteen categories. Three categories are the QFL groupings while the fifteen categories refers to

the raw petrographic descriptive categories previously described in the Petrographic Characteristics and Classification of Quartzite section, and detailed in Table 2. Statistical analyses is run on both row standardized QFL categories and raw petrographic descriptive categories to fully understand statistical relationships. Ellipses are placed around the groups to demonstrate where each sample/group is located. These are not statistically calculated ellipses, but merely hand drawn lines to highlight the groupings achieved with the multivariate analyses detailed below. Multivariate analysis capable of working with the nominal and interval-ratio scale data is necessary given the multiple petrographic categories. Two similar analyses were utilized to group the data into meaningful clusters, K-means cluster analysis and discriminant analysis.

K-means cluster analysis is a form of cluster analysis that splits the dataset by utilizing an algorithm to partition each case into K clusters or groups (Aldenderfer and Blashfield 1984). K-means analysis partitions the sample mean to classify raw data into groups in a nonhierarchical manner. Essentially, it determines how to place the cluster centroids farthest apart from each other without isolating any one data point from a cluster (Aldenderfer and Blashfield 1984). K-means cluster analysis is an ideal analysis for classification with the three QFL groups utilized in this study. The primary assumptions are: 1) there are always K clusters; 2) there is always minimally one item in each cluster; 3) the clusters are non-hierarchical and do not overlap; and 4) each point is closer to its own centroid than to another cluster's centroid (Aldenderfer and Blashfield 1984). This procedure is ideal for large datasets with multiple variables, although the algorithm does require a set number of clusters by myself before it can

work. Testing the accuracy of the K-means clusters discriminant analysis is an appropriate follow up procedure.

Additional discrimination of the petrographic groupings is completed through discriminant analysis, which analyzes relationships between individual elements (Heidke and Miksa 2000; Klecka 1980; Miksa and Heidke 2001). Discriminant analysis functions in a different way than the K-means cluster analysis, yet delivers similar results. While it is not necessary to run both, I did this to check the accuracy of K-means groupings. An advantage of using discriminant analysis after K-means cluster analysis is that it yields an accuracy percentage to evaluate the groups. This is necessary because discriminant analysis uses categorical variables to find a linear combination separating categories into two or more classes.

Discriminant analysis allows for the study of two or more object groups while considering multiple variables (Heidke and Miksa 2000; Klecka 1980). This is useful when several different variables contribute to an outcome, in this case for quartzite petrographic group classification. Quartzite samples are the objects and the 15 (Table 2) petrographic descriptive categories are the variables. The QFL categories are additionally run through discriminate analysis as with K-means cluster analysis. While these groups differ in size, the final group size is set from the discriminant analysis results, as each individual point count category is used to predict further group membership.

Seven assumptions underlie discriminant analysis (Klecka 1980): 1) two or more groups; 2) minimum of two cases per group; 3) any number of discriminating variables, given that it is less than the total number of cases; 4) discriminating variables are

measured at the interval level; 5) no discriminating variable may be a linear combination of other discriminating variables; 6) the covariance matrices for each group must be (approximately) equal; and 7) each group has been drawn from a population with a multivariate normal distribution on the discriminating variables. Discriminant analysis additionally allows for the evaluation of the degree of petrographic groups variability within the UGB.

The grouping of data with K-means and discriminant analyses allows for the understanding of the many data points by reducing the dimensions to understandable variables or creating groups rather than individual data points. By using these analyses to group the samples it allows for the understanding of sample variability and differences intra and inter-source. For comparison value, especially between 5GN1 and Parlin Flats samples, the grouping of samples are essential.

The paired K-means and discriminant analysis is used with cobble, outcrop, and both cobble and outcrop data together in a three-tiered approach to understand if these source differences contribute to different compositions between cobble and outcrop sources. This approach is repeated with each quarry site. Since 5GN1 is both a quarry and outcrop sources, the three-tiered approach is completed. Parlin Flats is an outcrop, and requires one paired analysis. Last, all of the samples are compared together to understand the full composition of analyzed samples. The main focus is on the comparison of the two quarry sites 5GN1 and Parlin Flats to understand whether and to what degree source differentiation is possible using this petrographic and analytical approach.

Chapter 4: Basin-Wide Analysis-Characterizing the Variability of UGB Quartzite

Through the detailed petrographic analysis of 50 thin section samples from the UGB many basic trends appear. First, many of the thin sections do not meet the geologic definition of quartzite (95 percent quartz or more) (Appendix A: Table 1). Most samples are between 80 to 90 percent quartz composition with the mean being 86.5 percent, yet 26 percent (n=13) of the samples contain fewer quartz grains. Preliminary data analysis is shown with a ternary diagram illustrating initial data clustering within the QFL categories. This is an important first step, functioning as the basis for the following analysis, because it best displays compositional differences graphically.

To further interpret the dataset, multivariate techniques are used to detail the petrographic group characteristics and differences. This approach allows for discrete groupings necessary for the analysis and the conclusions this study intends. It is important to classify and interpret each petrographic category such as chalcedony or quartz monocrystalline ungulatory (QMU) to illustrate more than just categorical differences.

K-Means Cluster Analysis

In order to understand petrographic group differences, K-means cluster analysis is selected as the next step because its parameters fit the nominal multivariable dataset. This is run on both row standardized QFL categories and raw data. The QFL categories demonstrate the most powerful groupings. The following discussion reports the results from the QFL categories for petrographic groups.

Since I set the number of clusters in a K-means cluster analysis, multiple K-means analyses are run on the quartzite dataset with a different number of clusters. Five clusters, or groups, is optimal to analyze the data set because it is the most statistically significant number of clusters in the K-means analysis. In total there is six groups since group #6 describes an outlier described below. Statistical significance for clusters is determined by the highest similarity within a cluster and the lowest similarity between clusters and is checked for accuracy with a subsequent discriminant analysis. The optimal number of clusters is based on the most accurate groups as determined by the paired discriminant analysis, which results in a predictive accuracy percentage (Table 3; Appendix Table 2). Discriminant analysis is used with the K-means clusters here to understand the clusters and dataset better by gaining insight into the relationship between cluster membership and the variables used to predict cluster membership through its predictive accuracy.

Table 3. K-means cluster centers based off Quartz, Feldspar, and Lithics categories. Clusters 1-5 stand for random petrographic groups with group six withheld as it is an outlier group (crystalline limestone).

	Petrographic Group				
	1	2	3	4	5
Quartz	69.11	52.00	85.61	96.32	85.13
Feldspar	4.83	1.50	2.36	1.84	12.56
Lithics	26.06	46.50	12.04	1.84	2.31

Discriminant Analysis

The goal of using discriminant analysis here after K-means is to understand the appropriate group size and to understand the predictive power of the groups as demonstrated with the accuracy percentage resulting from discriminant analysis. This is

completed on all different distributions of quartzite in the study including cobbles and outcrops. A three-tiered approach is run analyzing cobbles, then outcrops, and finally both cobbles and outcrops together. The first discriminant analysis includes all 29 cobble samples with the QFL categories. The entire group of selected cobble samples are classified correctly making the accuracy of this first discriminant analysis 100 percent (Figure 8; Appendix A: Table 3). The second discriminant analysis includes all 20 outcrop sources with each of the 15 individual elements. All outcrop samples selected are correctly classified resulting in an accuracy of 100 percent in the second discriminant analysis (Figure 9; Appendix A: Table 4).

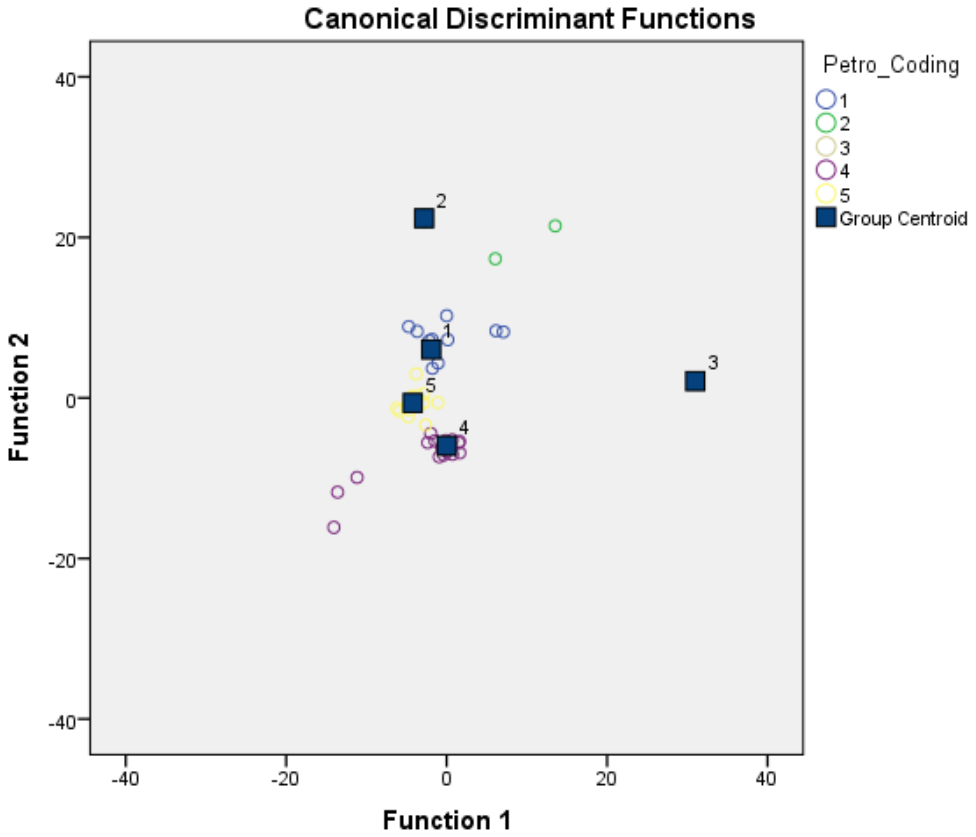

Figure 8. Cobble Discriminant Distribution Graph. Petro_Coding indicates the Petrographic groups.

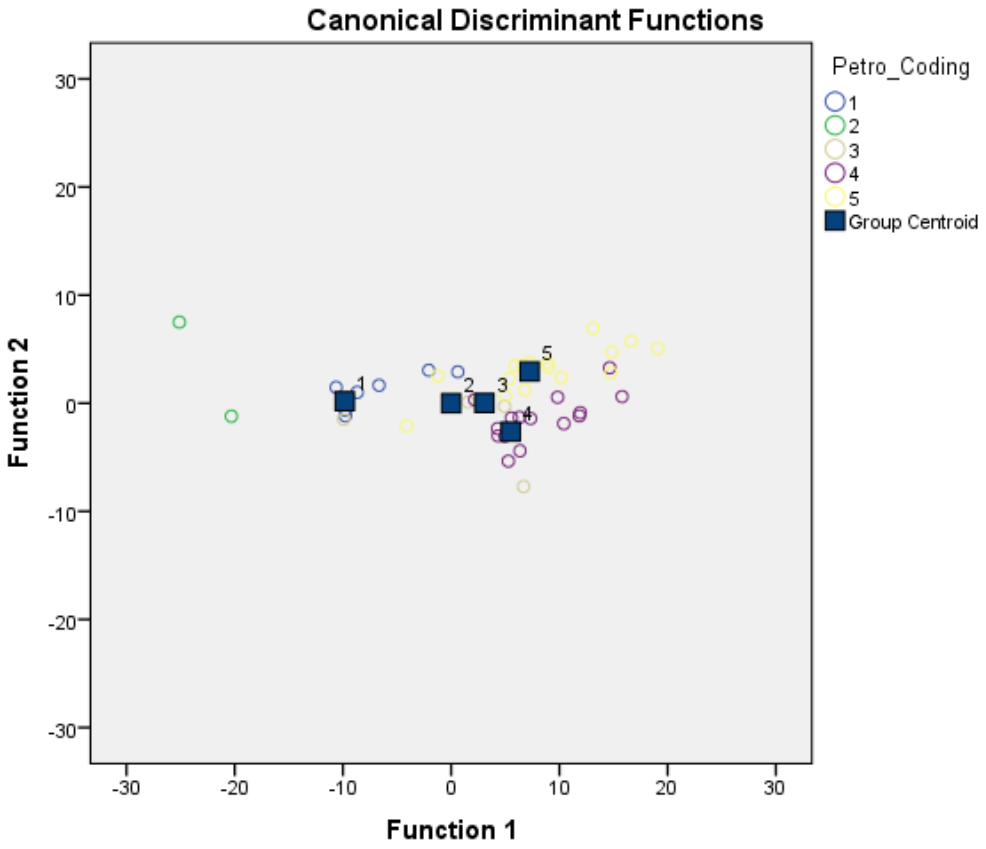

Figure 9. Outcrop Discriminant Graph. Petro_Coding indicates the Petrographic groups.

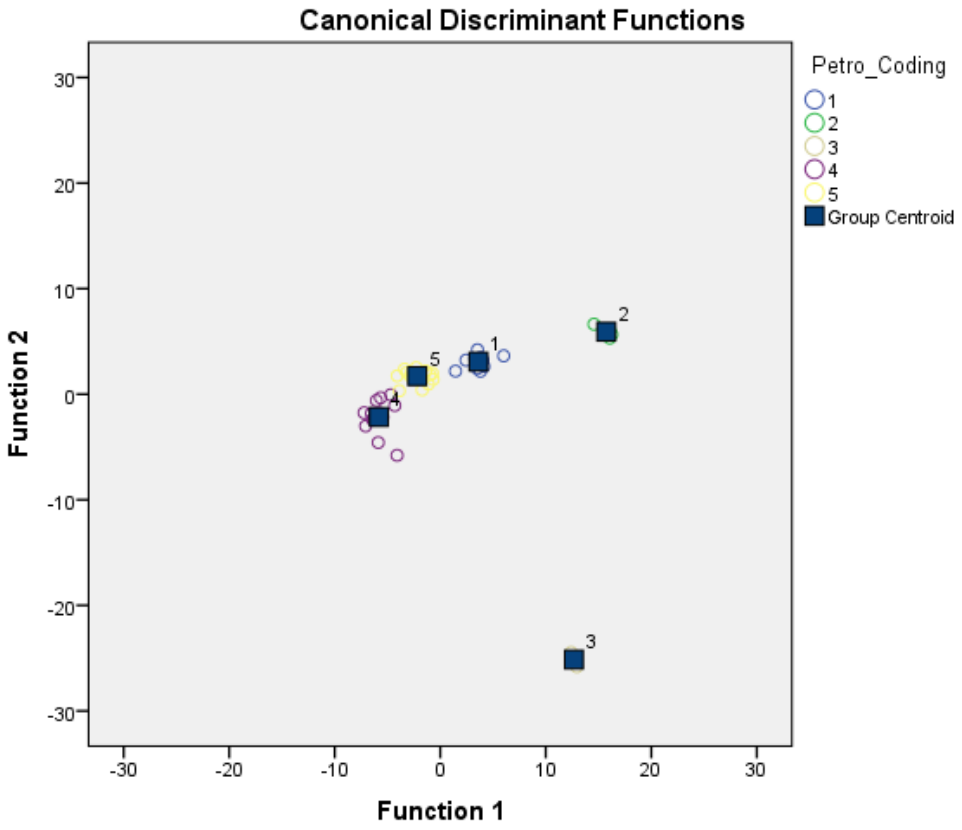

Figure 10. Cobbles and Outcrops Discriminant Graph. Petro_Coding indicates the Petrographic groups.

The third and final discriminant analysis on all 49 samples (without the one limestone outlier) resulted in one misclassification; sample CD09-4C (Figure 11; Appendix A: Table 5). This outlier is an outcrop source that was classified as Group #3 through K-means, but was placed into Group #5 with the third discriminant analysis. This is logical because when looking at the ternary diagram (Figure 12), the groups contain similar composition at the edges of each group where the ellipses are very close, facilitating an easy misclassification. With the one misclassification the accuracy of cobbles and outcrops is 98 percent in the third discriminant analysis.

Petrographic Groups

The following petrographic groups are derived by first viewing the graphic representation on a ternary diagram (Figure 11; Appendix A: Table 1), then through K-means cluster and discriminant analyses. The ellipses on the QFL ternary diagram are not calculated ellipses, but instead simply hand-drawn ellipses that encompass the groups derived from the paired K-means and discriminant analyses groups. The six petrographic groups reflect each group's unique mineral composition.

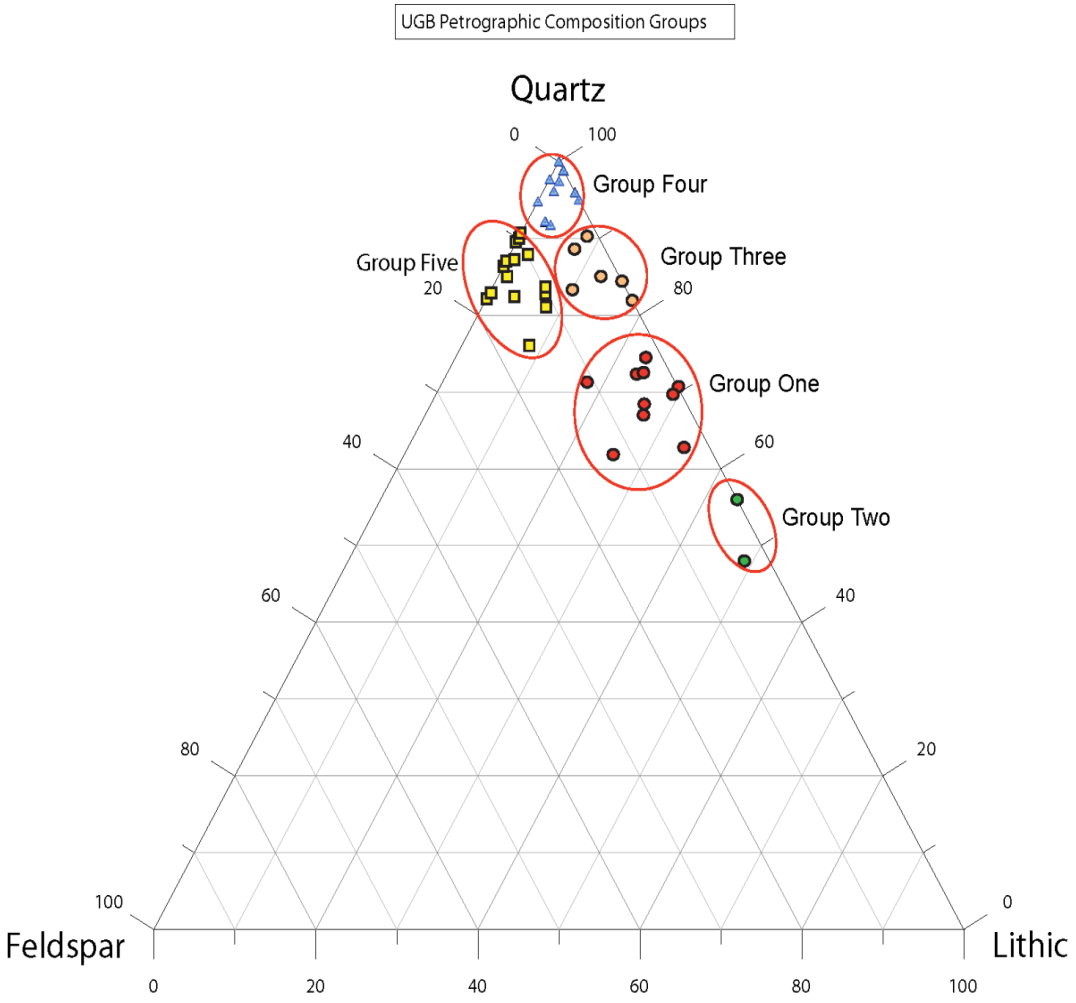

Figure 11. Random Sample Ternary Diagram showing concentrations of quartz, feldspar and lithics. The different symbols indicate the Petrographic group membership and not geologic formation. The top and right axis represents quartz, right and bottom axis represents lithic, and the left axis representing feldspar sample composition.

Group #1 (n=10) consists of moderate amounts of lithic material making it a litharenite or volcanic arenite, which does not fall within the traditional definition of quartzite as 90% quartz grains (Figure 7). The average slide in this group is similar to sample SC09-18B containing moderate sized quartz grains with thick dust rings that are surrounded by VRF's and a dark iron cement (Figure 7). QPC's are more visible than in most other samples. SC09-18B contains weathered feldspar and a significant amount of zebraic chalcedony, compromising the majority of the cement. Zebraic chalcedony is especially noticeable as a crystalline structure that alternates a pale white with a brown to near black, changing color as the mineral is turned on the stage in cross-polarized light. Moderate to well-sorted, sub-rounded to sub-angular grains range from silt to very fine sand in size (35 to 177 microns). The high amount (18 percent) of zebraic chalcedony in SC09-18B makes it typical of the group. Although VRF, biotite, and iron grains do add to the lithic total, these rarely make up more than 5 percent (as VRFs do in SC09-18B) of the total sample composition in Group #1. The mean composition in Group #1 is 80.61 percent quartz, 14.12 percent lithics, and 5.27 percent feldspar (Table 4). Important individual category means include 12.2 percent zebraic chalcedony, 4.7 percent VRF, 3.2 percent calcite, 3.1 percent biotite, and 1.5 percent iron.

Group #2 (n=2) contains the highest amount of lithics in all samples, yet is a small group overall. The high amount of lithics led the group to be classified as a lithic arenite, close to being a volcanic arenite (Figure 5). Sample SC09-13F contains fine quartz grains with a highly weathered feldspathic cement containing biotite (Figure 12).

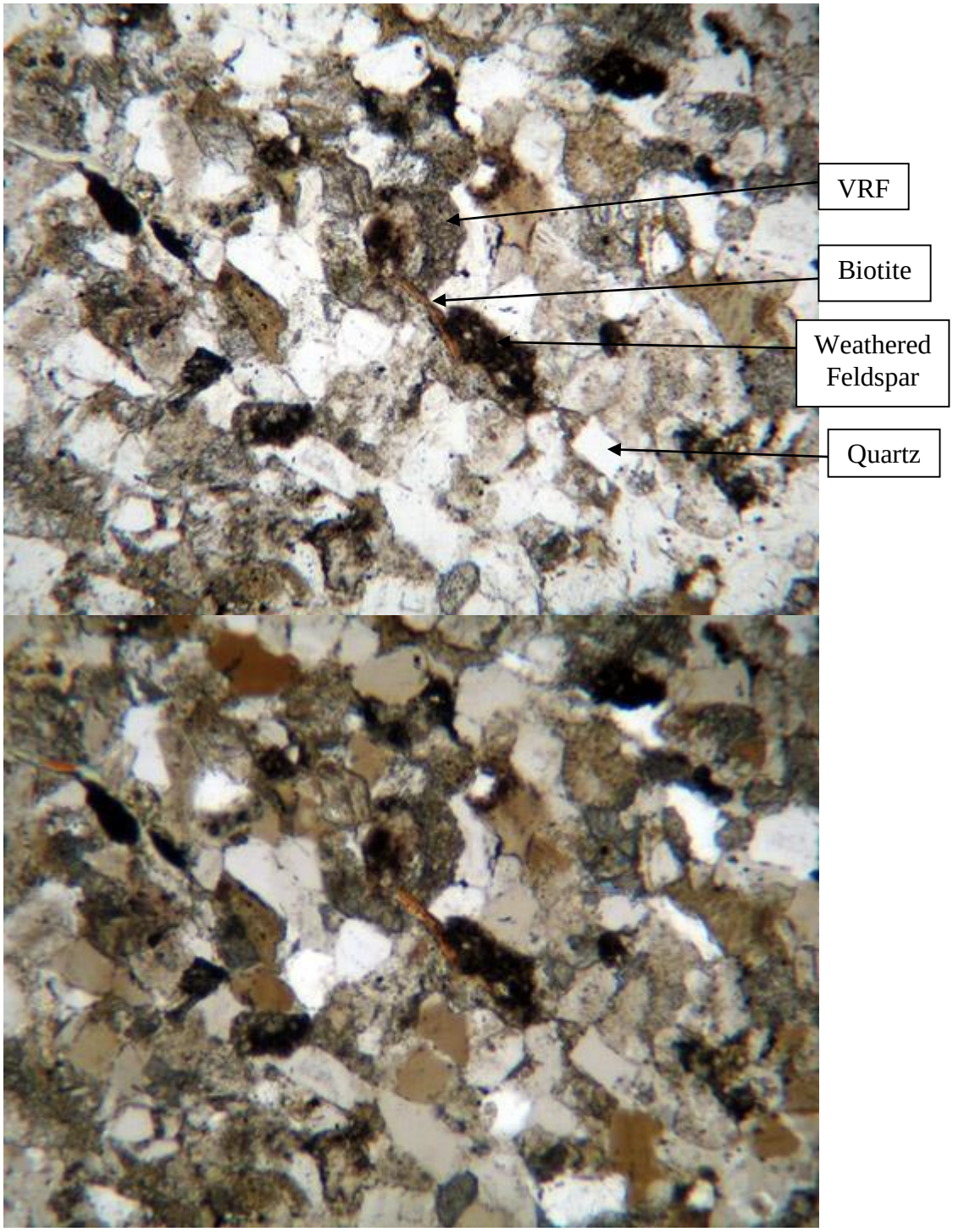

Figure 12. Sample SC09-13F with a ribbon of biotite (center) surrounded by volcanic rock fragments (VRF), weathered feldspar (dark grain) and quartz grains (QMU) with small overgrowths. Top photomicrograph is in plane light with the bottom in cross-polarized light under 10X magnification.

Biotite also occurs as a separate grain. Calcite occurs frequently with a high amount of volcanic inclusions on QMU's. SC09-13F is moderate to well-sorted, containing angular to sub-rounded grains, which range from fine silt to very fine sand (35 to 118 microns). Conversely, the other sample in this category is a metamorphic volcanic arenite (sample CD09-2D) (Figure 6). CD09-2D contains a few quartz grains surrounded by a high biorefringant clay or chert matrix with volcanic fragments very common. Quartz grains are sutured through either metamorphic processes or replacement. Large amounts of muscovite flakes commonly group together. Sample sorting is bimodal and variable with a relatively high percentage of QPC's (6 percent) for this project. CD09-2D is very poorly sorted, with angular to sub-angular grains ranging from fine silt to fine sand, bordering on medium sand grains (35 to 482 microns). Group #2 in general has a very high percentage of lithic material (46.5 percent between both samples), but is most likely an outlier as the different (sedimentary and metamorphic) compositions share a high amount of volcanic lithics. The mean composition in Group #2 is 52 percent quartz, 46.5 percent lithics, and 1.5 percent feldspar (Table 4). Important individual category means include 19 percent calcite, 0.5 percent biotite, 4 percent iron , 1 percent VRF, and 0 percent zebraic chalcedony.

Group #3 (n=6) contains the least amount of lithics for the high lithic groups placing the composition in the sublithic arenite category (Figure 5). Group #3 is similar to Group #1 in that it contains zebraic chalcedony as the main cement, yet with a lower amount (10 percent of the total composition instead of 18 percent). One exception to this is sample 5GN3510-E (Figure 13) in Group #3, which does not contain any

Table 4. Mean Percentage of Basin-Wide Study Petrographic Group Composition.

	QFL Categories				Important Individual Categories				
Petrographic Group	Quartz	Feldspar	Lithics	Total	VRF	Bioite	Iron	Zebraic Chalcedony	Calcite
1	80.61	5.27	14.12	100	4.7	3.1	1.5	12.2	3.2
2	52	1.5	46.5	100	1	0.5	4	0	19
3	86.6	2.4	10.96	100	3.83	1.33	1.33	3.17	3
4	96.4	1.8	1.8	100	0.8	0.13	0.2	0.27	0.13
5	85.19	12.57	2.24	100	0.75	1.81	0.31	0.69	0.44
6	Crystalline Limestone								

chalcedony, but instead contains detrital chert fragments (SRF). SC09-6G is an example of the average sample in this group (Figure 14). Mineral grains are moderately sorted quartz with a large amount of a zebraic chalcedony matrix, small pieces of biotite, and highly weathered and degraded feldspar. Many of SC09-6G's QMU's have a "dirty" appearance from volcanic inclusions lacking overgrowths. Some very small overgrowths are present through thick, well defined dust rings. VRF's consist of black volcanic cement, which differs in appearance from iron. This occasionally becomes a pseudo-matrix occupying much of the microscopic view. Biotite only occurs in very small broken pieces, suggesting that the sample had degraded through the chemical weathering processes.

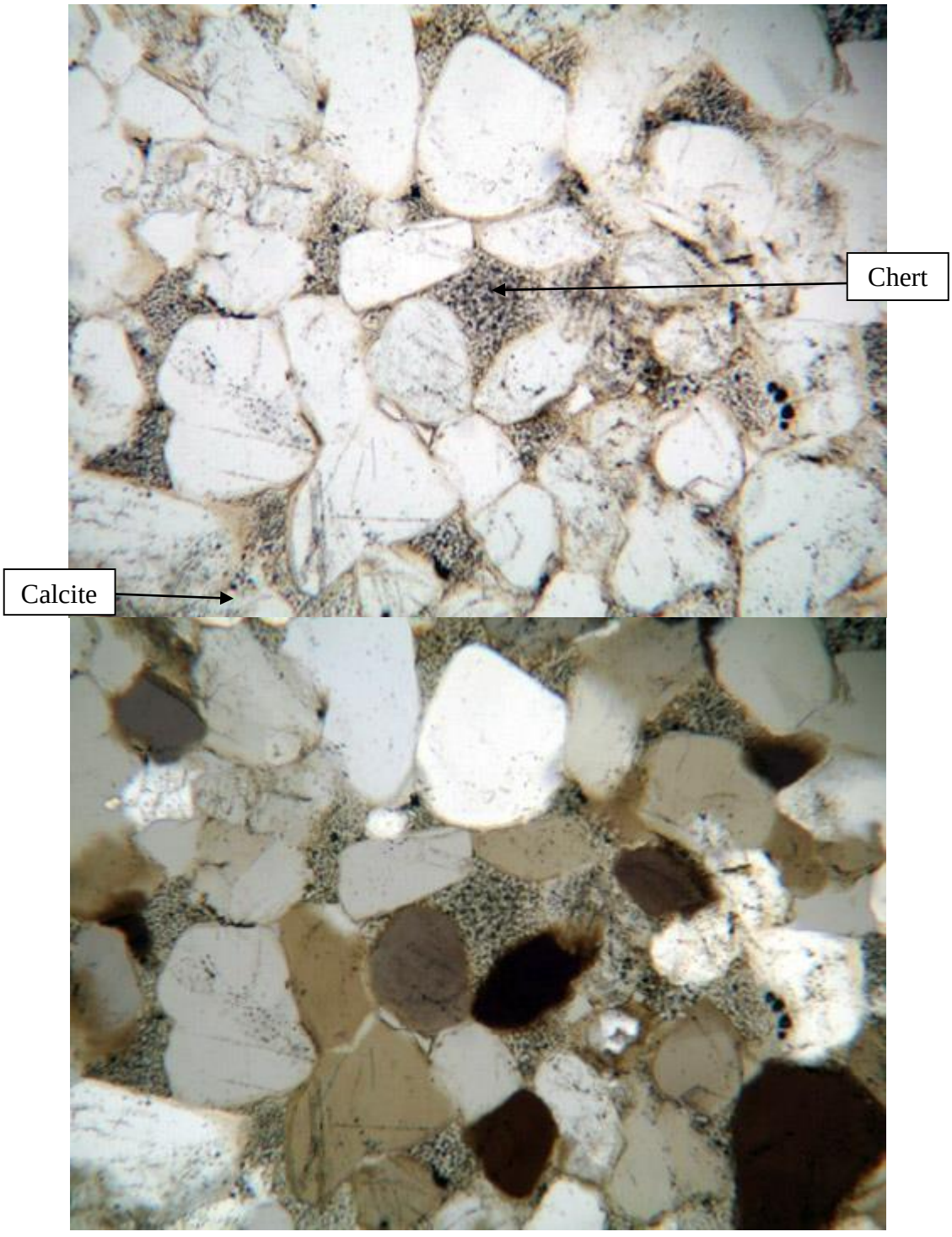

Figure 13. Sample 5GN3510-E demonstrating a dentrical chert fragment (SRF) at the center surrounded by quartz grains and some small amounts of calcite. Top photomicrograph is in plane light with the bottom in cross-polarized light under 10X magnification.

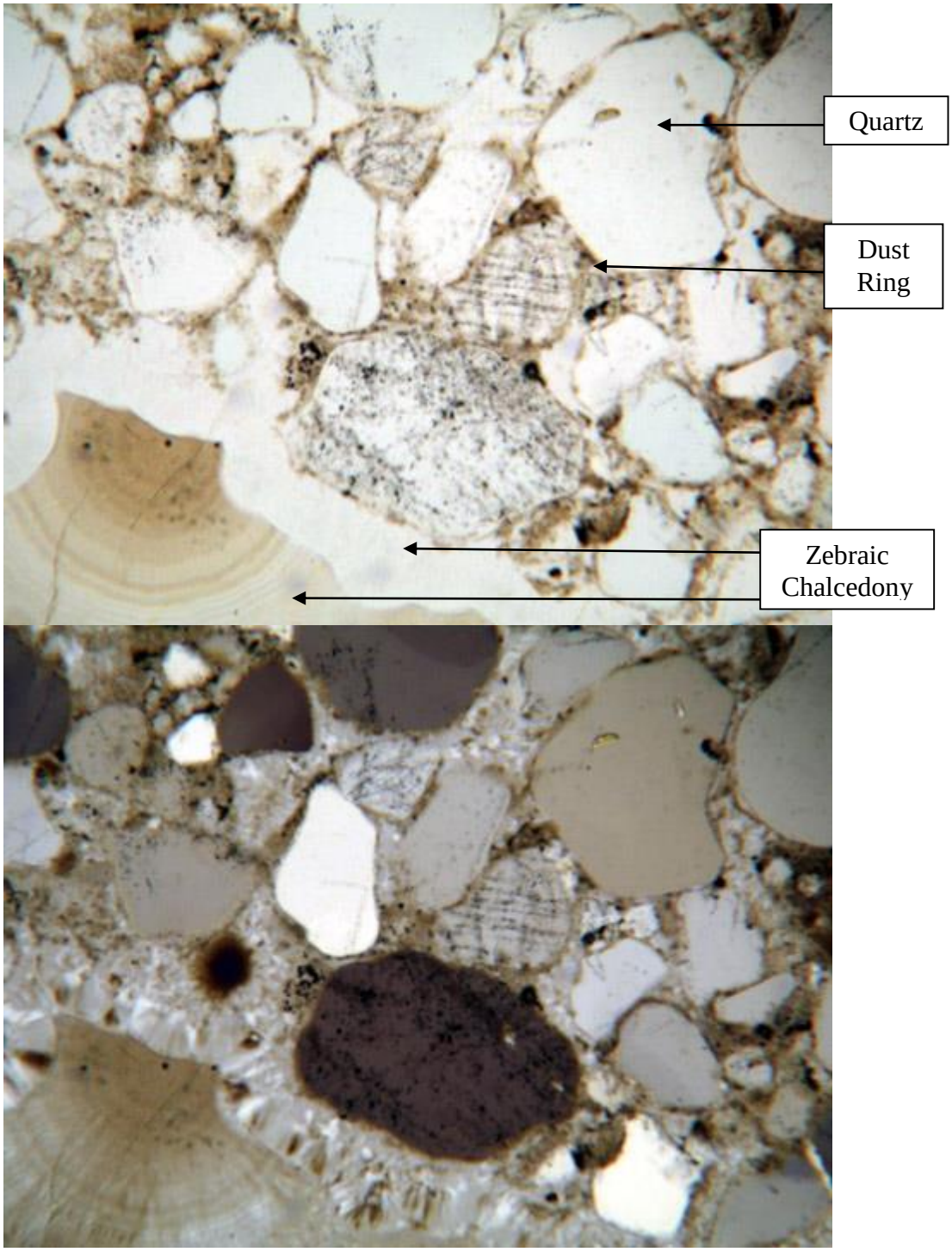

Figure 14. Sample SC09-6G showcasing the bimodal nature of this sample with quartz grains (QMU) with thick dust rings and volcanic inclusions next to a large amount of zebraic chalcedony and some small volcanic rock fragments (VRF) visible. Top photomicrograph is in plane light with the bottom in cross-polarized light under 10X magnification.

Some grains show high amounts of strain, while others appear to be a newer formation sequence with no evidence of straining, or in a bimodal depositional sequence. SC09-6G does have several plucked grains and varies from moderate to poorly-sorted. Grains are rounded to sub-angular range from silt to fine sand (35 to 295 microns), with no average grain size because of the samples' variable nature. Bohme lamellae (parallel, irregular planar trails on a quartz grain that indicate high stress or a low grade metamorphic origin) present on quartz grains, a chalcedony matrix, and zebraic chalcedony are the typical features of this sample and of Group #3 as a whole. The mean composition in Group #3 is 86.6 percent quartz, 10.964 percent lithics, and 2.4 percent feldspar (Table 4). Important individual category means include 3 percent calcite, 3.17 percent zebraic chalcedony, 3.83 percent VRF, 1.3 percent biotite, and 1.3 percent iron.

Group #4 (n=15) is the group with the most quartz grains fitting into the traditional category of quartzite (containing more than 90% quartz grains) (Carozzi 1993; Ebright 1987; Howard 2005). I hypothesize that this group represents the most often targeted form of quartzite for prehistoric knappers because of the high amount of silica. Sample SC09-26C is an example of this category because it contains 96.39 percent silica, and is classified as a quartz arenite (Figure 5 and Figure 15). Moderate sized quartz grains dominate this sample, although some VRF and calcite grains are present in very small amounts. Small to moderate overgrowths are common on quartz grains, as are QPC's, and silica cement. Biotite is not recorded in the point count due to the very small compositional amount. SC09-26C is almost all quartz grains with only 4 percent chert lithic grains. The sample is very well-sorted with sub-rounded to sub-

angular grains ranging between silt and very fine sand (29 to 236 microns), with an average grain of very fine sand (118 microns). This is the most homogenous category facilitating the fracture through grains and cement (the concordial fracture) that make an ideal tool raw material. The mean composition in Group #4 is 96.4 percent quartz, 1.8 percent feldspar, and 1.8 percent lithics (Table 4). Important individual category means include 0.8 percent VRF, 0.27 percent zebraic chalcedony, 0.2 percent iron, 0.13 percent biotite, and 0.13 percent calcite.

Group #5 (n=16) is similar to Group #3 containing primarily quartz grains, but instead of a small amount of lithic material it contains feldspar, making it subarkose and arkose arenite (Figure 5). Feldspar in this study is extremely degraded with very few exceptions where twinning is rarely observed. Sample 5GN850-3B is representative of this group (Figure 16). 5GN850-3B contains predominately moderately sorted QMU's with a small amount of degraded feldspar. The sample is characterized by very thick overgrowths that lack defined dust rings, with the weathered feldspar being highly degraded and barely visible (10 percent of composition). Some very small amounts of VRF's are visible within a matrix of calcite. 5GN850-3B is moderate sorted with rounded to sub-rounded grains containing grain sizes ranging between silt to very fine sand (83 to 236 microns). The mean composition in Group #5 is 85.19 percent quartz, 12.57 percent feldspar, and 2.24 percent lithics (Table 4). Important individual category means include 1.81 percent biotite, 0.69 percent zebraic chalcedony, 0.75 percent VRF, 0.31 percent iron, and 0.44 percent calcite.

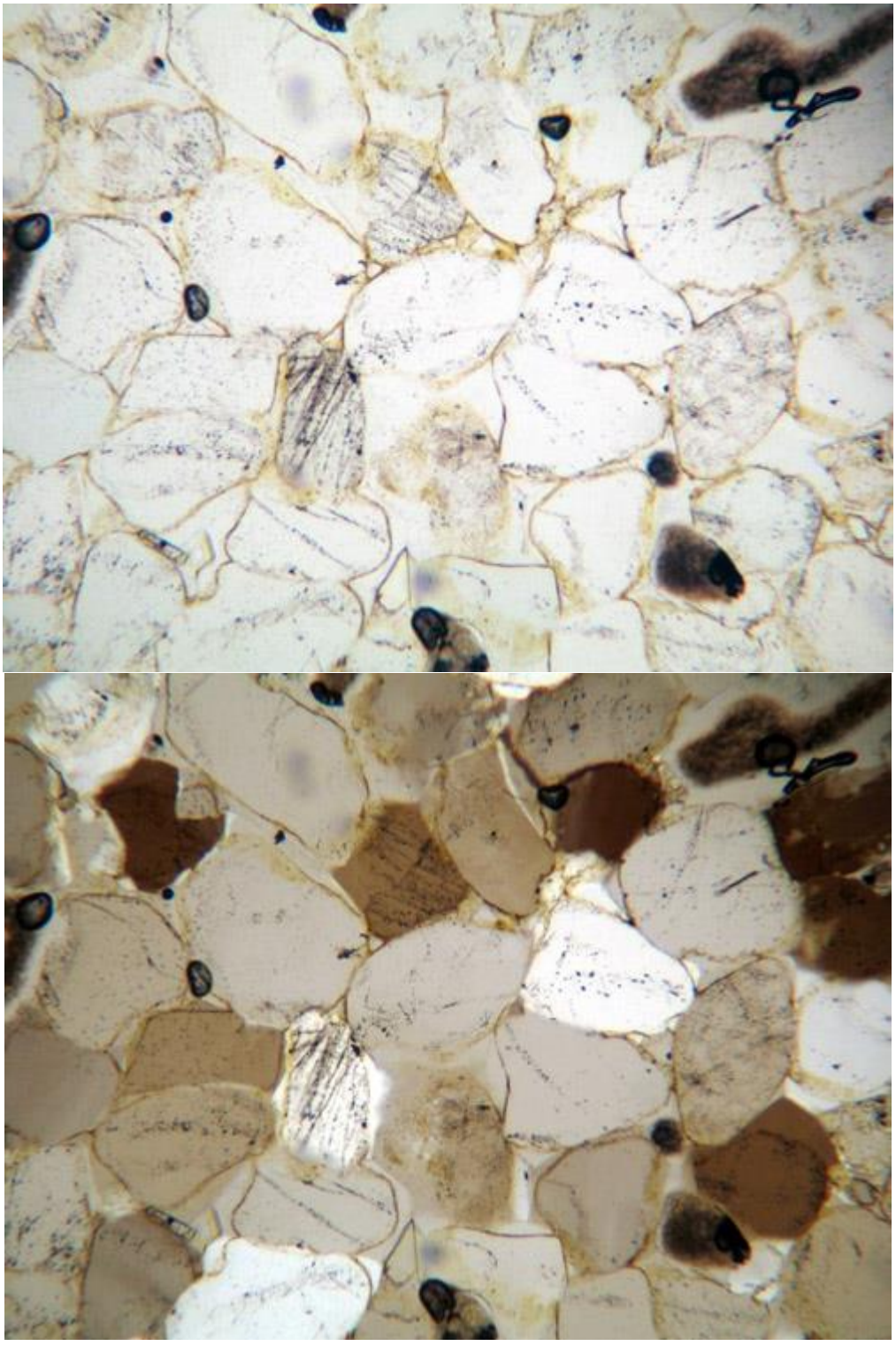

Figure 15. Sample SC09-26C with very well sorted, large the quartz grains (QMU) and overgrowths with defined dust rings. Some volcanic inclusions are visible on the margins of the photomicrograph (dark spots). Top photomicrograph is in plane light with the bottom in cross-polarized light under 10X magnification.

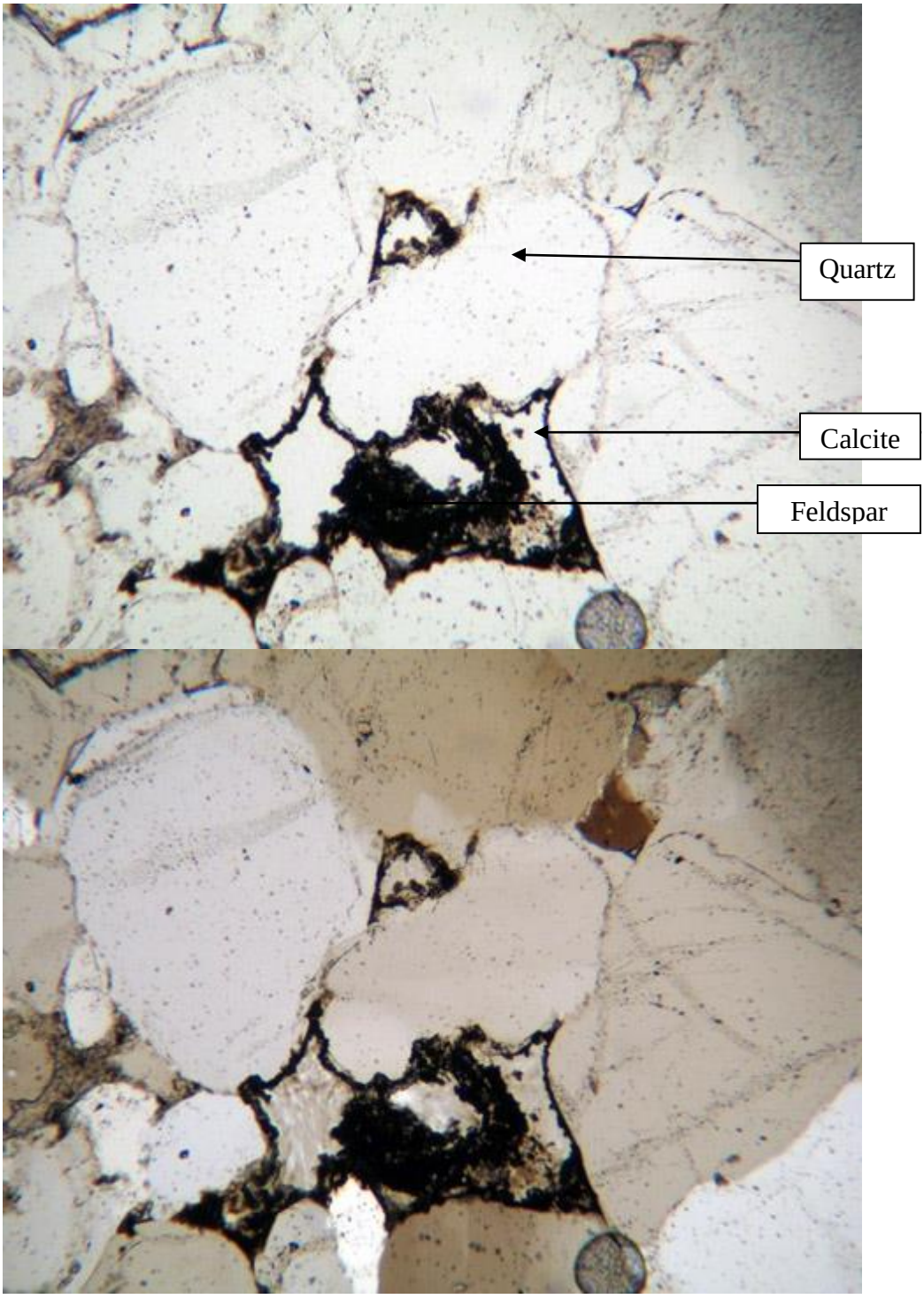

Figure 16. Sample 5GN850-3B exhibits large quartz grains with highly visible large overgrowths, degraded feldspar and calcite. Top photomicrograph is in plane light with the bottom in cross-polarized light under 10X magnification.

Group #6 (n=1) is the smallest and most unique group. A detailed point count was not completed on this group because this group is a product of field sampling error and is not quartzite or sandstone in any measure. Group #6 is a crystalline limestone carbonate, illustrated in sample SC09-24H (Figure 17). This is not on the ternary diagram (Figure 11) because its composition does not fit within the QFL parameters. It does not exhibit grain boundaries, grain relationships, or any similar composition to the rest of the samples in the study.

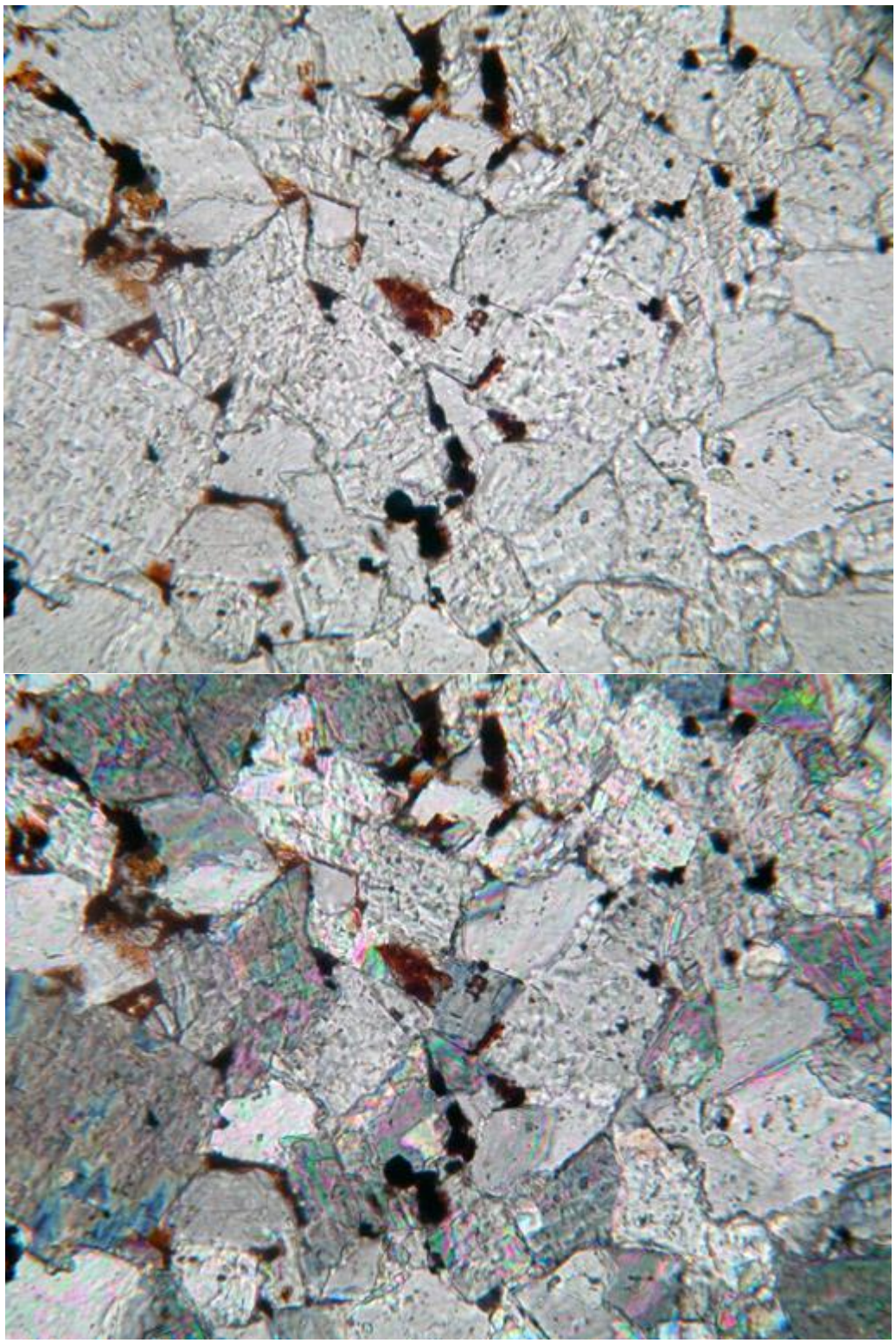

Figure 17. Sample SC09-24H, the crystalline limestone of Petrographic Group #6 with mica's and iron grains prevalent. Top photomicrograph is in plane light with the bottom in cross-polarized light under 10X magnification.

Discussion

Geologic Formation Associations

Geologic formations do not match the petrographic groups perfectly, yet they do demonstrate predictable patterns (Table 5 and 6).

Petrographic Group #1 is dominated by Tertiary sources, with Tertiary gravel cobbles making up seven of ten samples. The other samples are from a Quaternary fan (n=1) and Tertiary cobble (n=2) deposits. Petrographic Group #2 is the most lithic heavy group. It is also sampled from exclusively Quaternary age geologic formations. Petrographic Group #3 contains low amounts of lithic materials and is primarily from Cretaceous Dakota and Burro Canyon Formations, with the exception of two Tertiary gravel cobble sources. Petrographic Group #4 contains almost pure silica and is the second largest group in the study with fifteen samples. Petrographic Group #4 is dominated by Jurassic Junction Creek and Entrada samples (54 percent), with the rest sampled from Quaternary Alluvium cobbles (20 percent), Tertiary gravel deposits (13 percent), and Quaternary gravels (13%). Petrographic Group #5 is the largest group with sixteen samples, and is the most diverse when considering geologic formation sources. It is comprised of Tertiary cobble sources (44 percent), Cambrian Saguache outcrop (25 percent), Jurassic Junction Creek outcrop (19 percent), and Jurassic Junction Creek cobbles (13 percent).

Geologic formation distribution is clearer when cobble and outcrop sources are separated from each other. Separating outcrops and cobbles demonstrates that Petrographic Groups #1 and #2 are only cobble sources with some other cobbles scattered throughout the other groups as expected from their heterogeneous nature.

Petrographic Group #3 is exclusively from Cretaceous outcrops with Petrographic Group #4 exclusively from Jurassic outcrops. Petrographic Group #5 is found in both Cambrian and Jurassic outcrops. Logically, Petrographic Groups #4 and #5 have the potential to overlap slightly as the groups are separated by a continuum of the amount of feldspar. There is not clear divide with the amount of feldspar, which contributes to this overlap. Understanding that Petrographic Groups #4 and #5 overlap, the higher silica samples in Petrographic Group #5, adjacent to Petrographic Group #4, are all from Jurassic sources. The higher feldspar samples of Group #5 are primarily of Cambrian origin, although one does fit with the higher silica near the border with Group #4.

Table 5. Petrographic Groups Compared to Geologic Group/Formation. The Geologic Formations represent all Formations sampled.

Petrographic Group	Geologic Formation
1	Tertiary Gravels (70%), Tertiary Cobble (20%), Quaternary Fan (10%)
2	Tertiary Gravels (50%), Quaternary Alluvium (50%)
3	Cretaceous Dakota and Burro Canyon (67%), Tertiary gravels (33%)
4	Jurassic Junction Creek and Entrada (54%), Quaternary Alluvium (20%), Tertiary Gravels (13%), Quaternary Gravels (13%)
5	Tertiary cobbles (44 percent), Cambrian Saguache (25 percent), Jurassic Junction Creek (19 percent), and Jurassic Junction Creek cobbles (13 percent)
6	Crystalline Limestone cobble

Table 6. Petrographic Groups Compared to Geologic Group/Formation with Reference to Cobble and Outcrop Distinction.

Separating Cobbles from Outcrops	
1 and 2	Cobbles only
3	Cretaceous Dakota/Burro Canyon Outcrop
4	Jurassic Junction Creek and Entrada Outcrops
5	Cambrian Saguache (63%) and Jurassic Junction Creek (37%) Outcrops

Spatial Associations

Spatially a few patterns emerge (Figure 19). Petrographic Groups #1 and #3, the lithic heavy groups, only occur in the southern portion of the UGB. The southern portion of the UGB is distinct as the contact zone with the Uncompahgre Plateau where the uplift features that created the steep mountains around Crested Butte change to the large, high Uncompahgre Plateau. The volcanism responsible for higher lithic amounts occurred in this area. Petrographic Group #4 shows the most significant spatial pattern, the group highest in silica and best toolmaking material, occurs only at known prehistoric quarries and not commonly at non prehistoric sampled areas in the UGB. For example, it occurs in high concentrations at 5GN1, a massive quartzite quarry adjacent to the Blue Mesa Reservoir, and prehistoric Gunnison River (Figure 18). This may be the most valuable finding of the Basin-wide study beyond its role as a proof of concept that is the main objective: demonstrating that petrography can distinguish between individual quartzite sources. Chapters 5-7 focus on a closer examination of how well petrography can distinguish between individual quartzite sources with the examination of all 5GN1 samples and Parlin Flats samples collected.

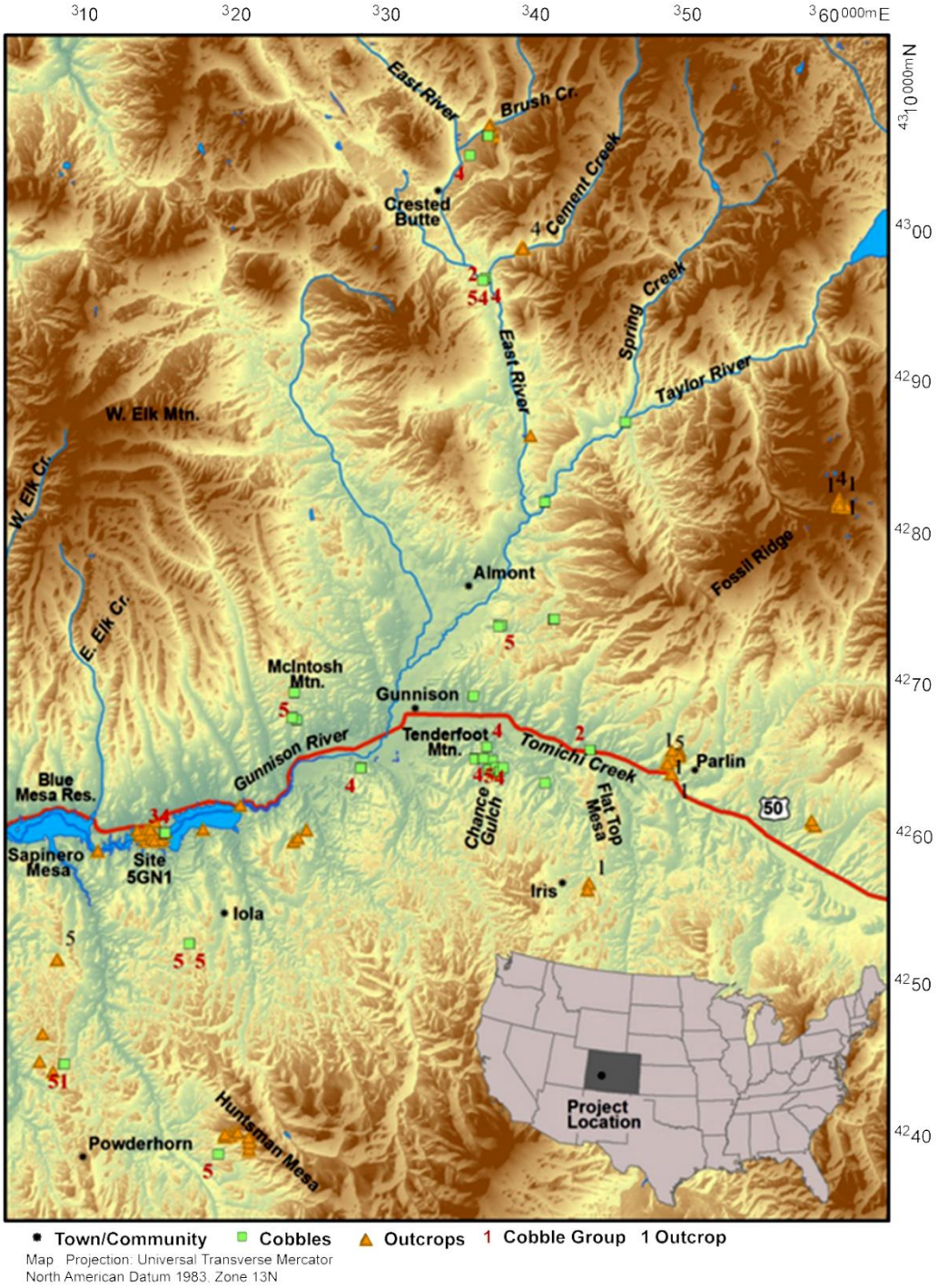

Figure 18. Spatial Distribution of Basin-Wide Study Petrographic Groups. Notice that the high lithic quantity groups #1 and 3 only occur in the southern portion of the Basin.

Chapter 5: 5GN1 Analysis

As its site number suggests, 5GN1 is the first site recorded in Gunnison County, representing a large cobble and Jurassic Junction Creek (Jj) outcrop quarry and rockshelter site used extensively throughout prehistory. The site is along on the south side of the modern Blue Mesa reservoir west of the present day Gunnison River in a parkland environment at roughly 7,700 ft. asl. (Figure 19). Prehistorically, this would have overlooked and been readily accessible to the Gunnison River. First recorded by William G. Buckles in 1962 (Buckles 1962) the site has been revisited several times by archaeologists over the years, and was it designated eligible for the National Register in 2009 by the Louis Berger Group INC. CRM firm (Anderson et al. 2009). Utah State University visited the primary site (and two other loci 5GN1.1 and 5GN1.2) during the 2009 field school to record and collect samples that are discussed in this chapter.

Figure 19. 2009 USU Field crew collecting samples and documenting 5GN1.2. Photo courtesy of Bonnie Pitblado.

Although Buckles' original site form (1962) lists the site as having been picked over by collectors, he also documented several tools including knife fragments (19), choppers (3), and a probable Late Prehistoric cottonwood triangular projectile point (1) all made from the local fine grain quartzite in addition to "a great amount of broken quartzite". When the USU field school visited the main 5GN1 site, they documented 20 quartzite projectile points dating to the Middle, Late Archaic, and unassigned prehistoric eras. Additionally, they noted over 500,000 quartzite and chert primary reduction debitage flakes and over 1,000,000 secondary quartzite and chert debitage flakes ranging in color from white, greyish pink, and red. 5GN1.1 and 5GN1.2 are both quarries and rock shelters with hearths and over 100 pieces of quartzite debitage a piece (see Peart 2013 for a detailed examination of 5GN1.2 and discussion of 5GN1 and 5GN1.1).

The description of the cobble and outcrop sample variability contributes to this petrography project, but also to a greater understanding of this important quarry and habitation site.

Results

All samples from the three 5GN1 locations including outcrop (SC09-1 and SC09-7) and cobble (SC09-6) samples are point counted in order to characterize the quarry variability. Included in this detailed look at all 5GN1 samples, 3 samples are included in the Basin-wide study with 16 additional samples introduced. New groups are made specifically for 5GN1 because it is important to understand the variability within the source itself and how that variability clusters within the geologic formation before it is placed within context of the Basin-wide study groups. The additional

samples will be placed within a new Basin-wide context in Chapter 8. The same three tiered statistical analysis applied to the Basin-wide study (Chapter 4) is applied here to the cobbles, outcrop, and total 5GN1 sample. The petrographic groups largely align with the petrographic groups from broader study of UGB quartzite, but taken in isolation vary slightly. The groups presented here are specific to the 5GN1 samples and will be compared to Parlin Flats in Chapter 6, and combined with evaluated in the broader UGB sample in Chapter 7.

K-means Cluster Analysis

K-means cluster analysis demonstrates that all 5GN1 samples (SC09-6) fit within three distinct petrographic groups. Appendix A: (Table 6) details group membership and distance from the K-cluster centroid; Table 7 shows group centroids or average. Since the number of groups is set before K-means cluster analysis is run, several iterations are run with different group sizes. Three groups is the most accurate when checked with the paired discriminant analysis discussed below. This multiple iterations and accuracy checking as completed with Basin-wide is a technique utilized for each time the paired multivariate analyses are run. 5GN1 cobbles fit into three groups (Table 8; Appendix Table 7), and outcrops fit into two statistically significant K-means clusters (Table 9; Appendix Table 8).

Table 7. 5GN1 K-Means Cluster Analysis Group Centroids.

	Group		
	1	2	3
Quartz	97.57809	86.06507	75.80571
Feldspar	0.603429	1.650962	2.938395
Lithics	1.81848	2.938395	21.25589

Table 8. 5GN1 Cobble K-Means Cluster Analysis Group Centroids.

	Group		
	1	2	3
Quartz	98.66071	86.30805	78.93471
Feldspar	0.446429	2.030015	3.058652
Lithics	0.892857	11.66194	18.00664

Table 9. 5GN1 Outcrop K-Means Cluster Analysis Group Centroids.

	Group	
	1	2
Quartz	100.0000	71.6814
Feldspar	.0000	6.1947
Lithics	.0000	22.1239

Discriminant Analysis

The first discriminant analysis on the ten 5GN1 quartzite cobble samples classification with K-means groups are classified correctly with 100 percent accuracy (Figure 20; Appendix A: Table 9). Second, the nine outcrop sample accuracy is also perfect at 100 percent (Appendix A: Table 10). As two outcrop groups are optimal no discriminant plot is made. With the third discriminant analysis for the total 5GN1 samples (n=19), the accuracy drops to 94.7 percent. Sample SC09-1D originally belonged to petrographic group #1, but the discriminant analysis reclassified SC09-1D to group #3 based on the analyses greater discretionary power (Figure 21; Appendix A: Table 11).

5GN1 Cobble Samples

The ten 5GN1 cobble samples separate into three petrographic groups (Figure 22). The groups, as with Basin-wide study (Chapter 4) are derived from the K-means and Discriminant analyses. Each group reflects the samples' QFL mineral composition.

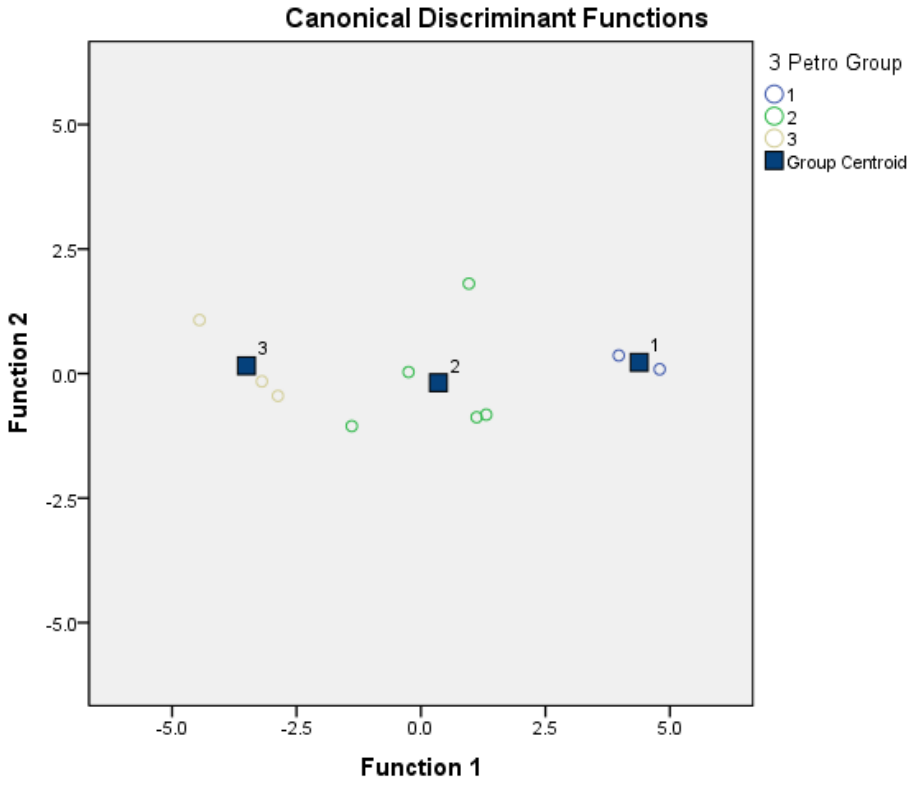

Figure 20. 5GN1 Cobble Discriminant Analysis Plot. Petro Group indicates the Petrographic groups.

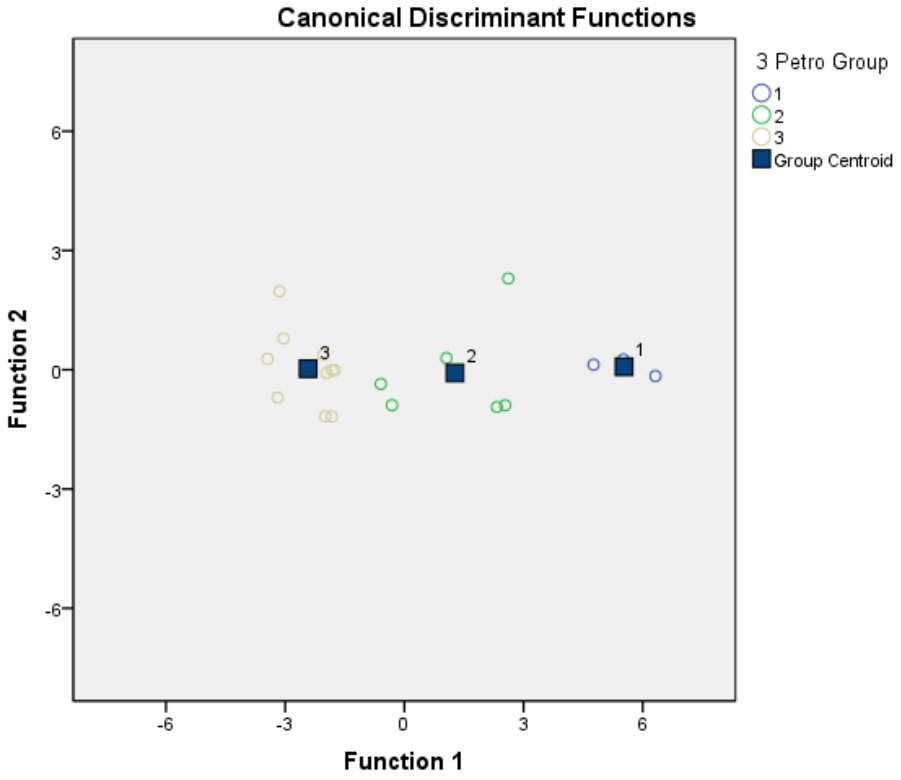

Figure 21. Total 5GN1 Discriminant Analysis Plot. Petro Group indicates the Petrographic groups.

5GN1 cobble group #1 is represented by two samples. These are characterized by an almost entirely quartz composition with a group average of 98.7 percent, well within the traditional geologic definition of quartzite. In fact sample SC09-6E is 100 percent silica quartz. The other sample within this group, SC09-6B, is a textbook example of geologic sedimentary quartzite with thick quartz overgrowths surrounding well defined quartz grains with thick dust rings and thick quartz overgrowths as the cement (Figure 23). Rounded to sub-angular grains vary in size from fine to medium sand (174 to 460 microns) with an average of 280 microns (medium sand). Group samples are pure silica or at minimum 98 percent making them an ideal toolstone aligning with Basin-wide study petrographic group #4, geologically described as a

quartz arenite (Figure 5). This is not to say the other cobbles would not have been utilized, but these samples would have been what a discerning knapper was after when quarrying toolstone.

5GN1 cobble group #2 contains five samples characterized by an average 87 percent quartz, 1.6 percent feldspar, and 11.4 percent lithic, geologically characterized as a sublithic arenite. These samples all contain moderately well sorted rounded to sub-angular grains within a usually thick zebraic chalcedony cement (Figure 24). The little feldspar present is highly degraded and dispersed. Often the feldspar is only identifiable with the help of the K-spar stain. Chert fragments are present in the samples, although always make up less than 7.8 percent of total composition. Complex quartz grains (QPS and QPC) are notably absent from this group inferring limited strain during diagenesis. Unstrained quartz grains (QMN) are present in low amounts (0.03 percent). I noted other (QMN and QPC) grains while point counting, yet I did not record them because these grains were never under the crosshairs used to pin point grains in the systematic point count. Grain size is variable between very fine sand to coarse sand (74 to 598 microns) with an average of 276 microns (medium sand). This group is roughly equivalent to group #3 in the Basin-wide Study.

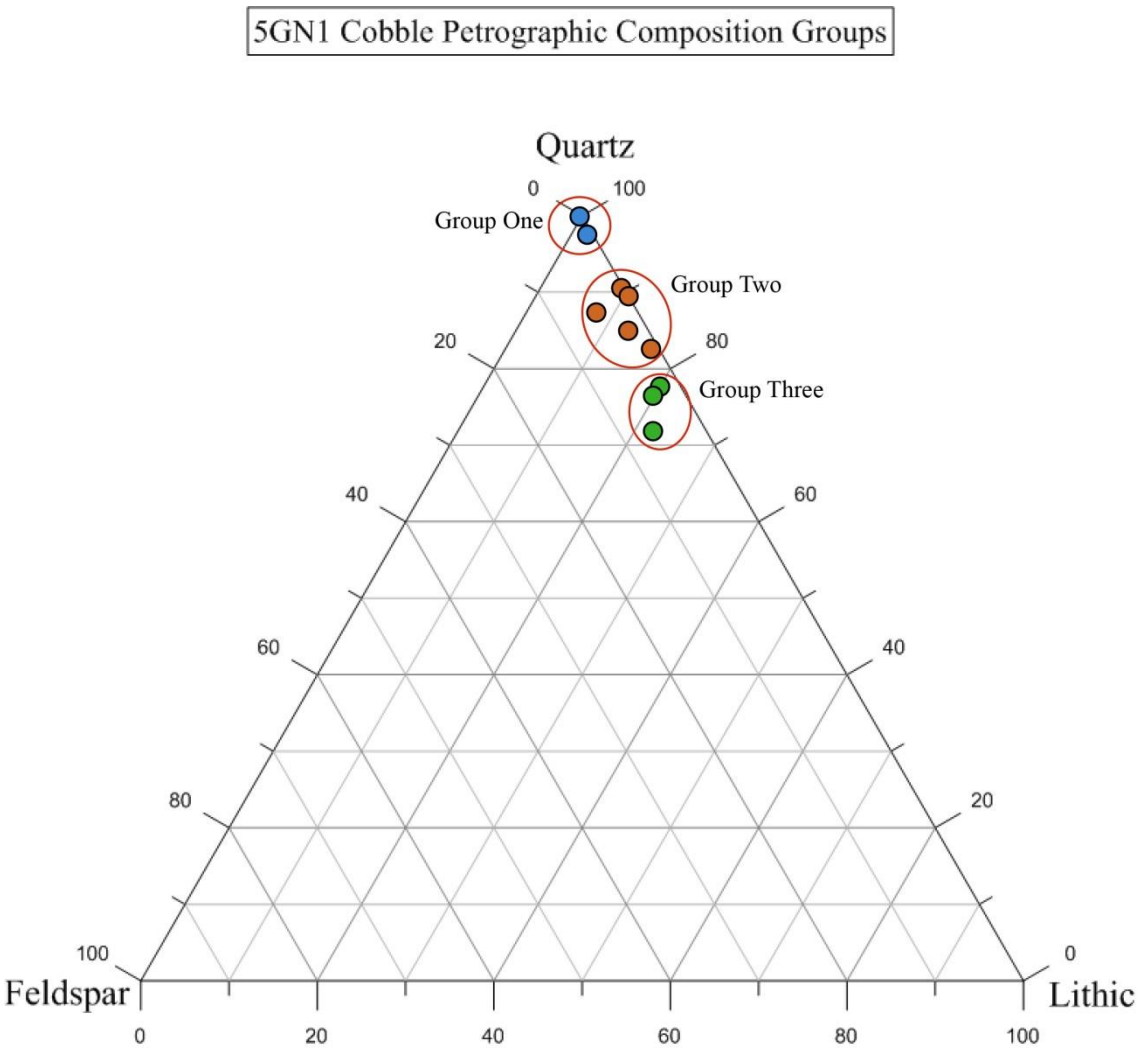

Figure 22. Ternary Diagram for 5GN1 Cobble samples. The top and right axis represents quartz, right and bottom axis represents lithic, and the left axis representing feldspar sample composition.

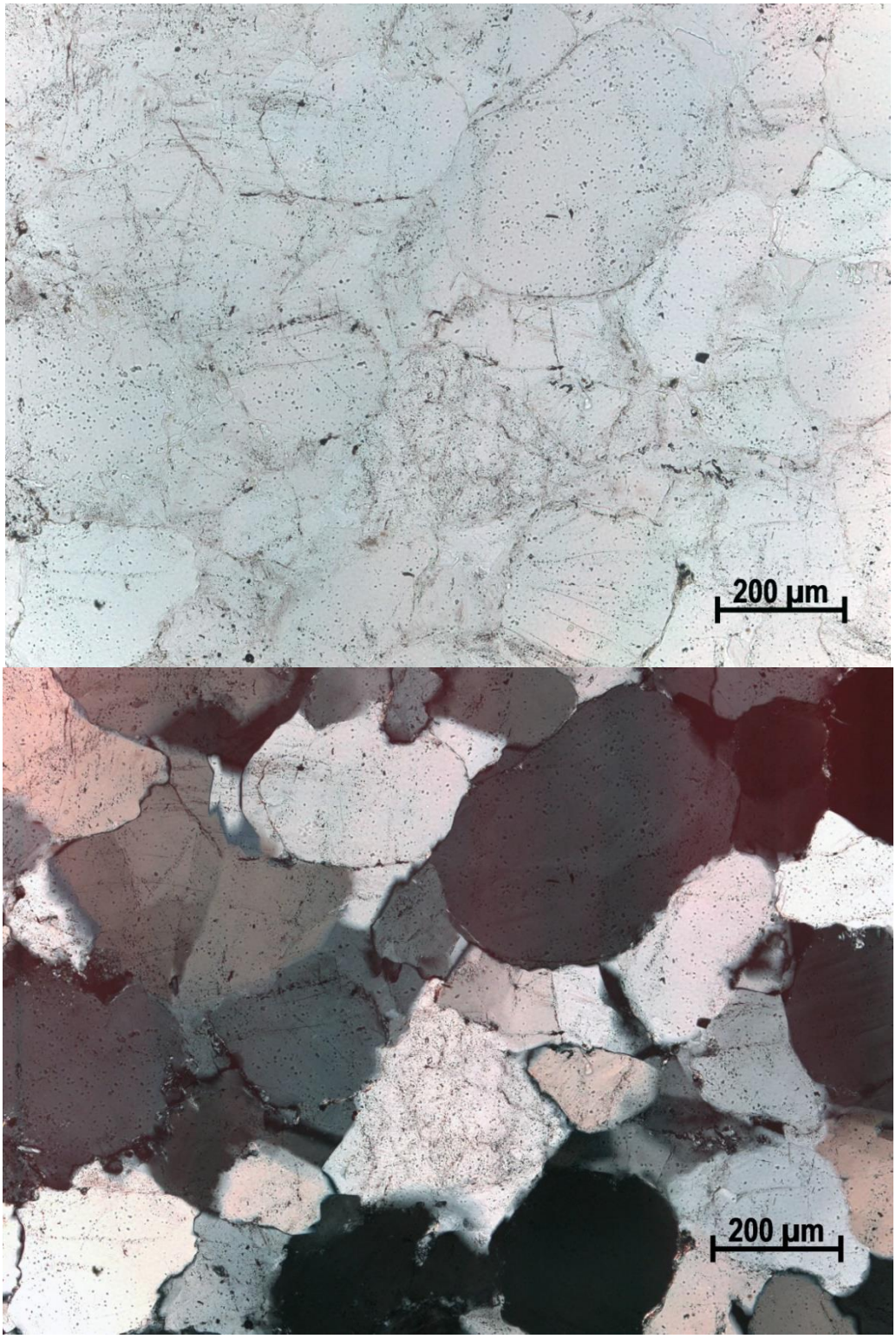

Figure 23. 5GN1 Cobble sample SC09-6B displaying rounded to sub-rounded quartz grains with thick overgrowths and lack of chalcedony. Top photomicrograph is in plane light with the bottom in cross-polarized light under 10X magnification.

5GN1 cobble group #3 contains three cobble samples with thin zebraic cement surrounding moderately well sorted, rounded to sub-rounded grains (Figure 25). This sublithic arenite to volcanic arenite has an average sample composition of 76 percent quartz, 3 percent feldspar, and 21 percent lithic, contributing to it being the most mixed composition equivalent to group #1 in the Basin-wide Study. This group contains the most feldspar, although still just 6 percent or less. As with other samples in the study the feldspar is highly degraded and difficult to see without the K-spar stain (introduced when the thin sections are manufactured to identify feldspar easier), with the exception of the few plagioclase grains that display twinning. Mica is present in very low amounts missing any points on the point count. Quartz grains are notably unstrained compared to other samples, although complex quartz grains (QPS and QPC) are still poorly represented in the point count at 0.03 percent of group sample composition. Grain size ranges from very fine sand to medium sand (80 to 457 microns) with an average of 255 microns (just within the medium sand category from fine sand).

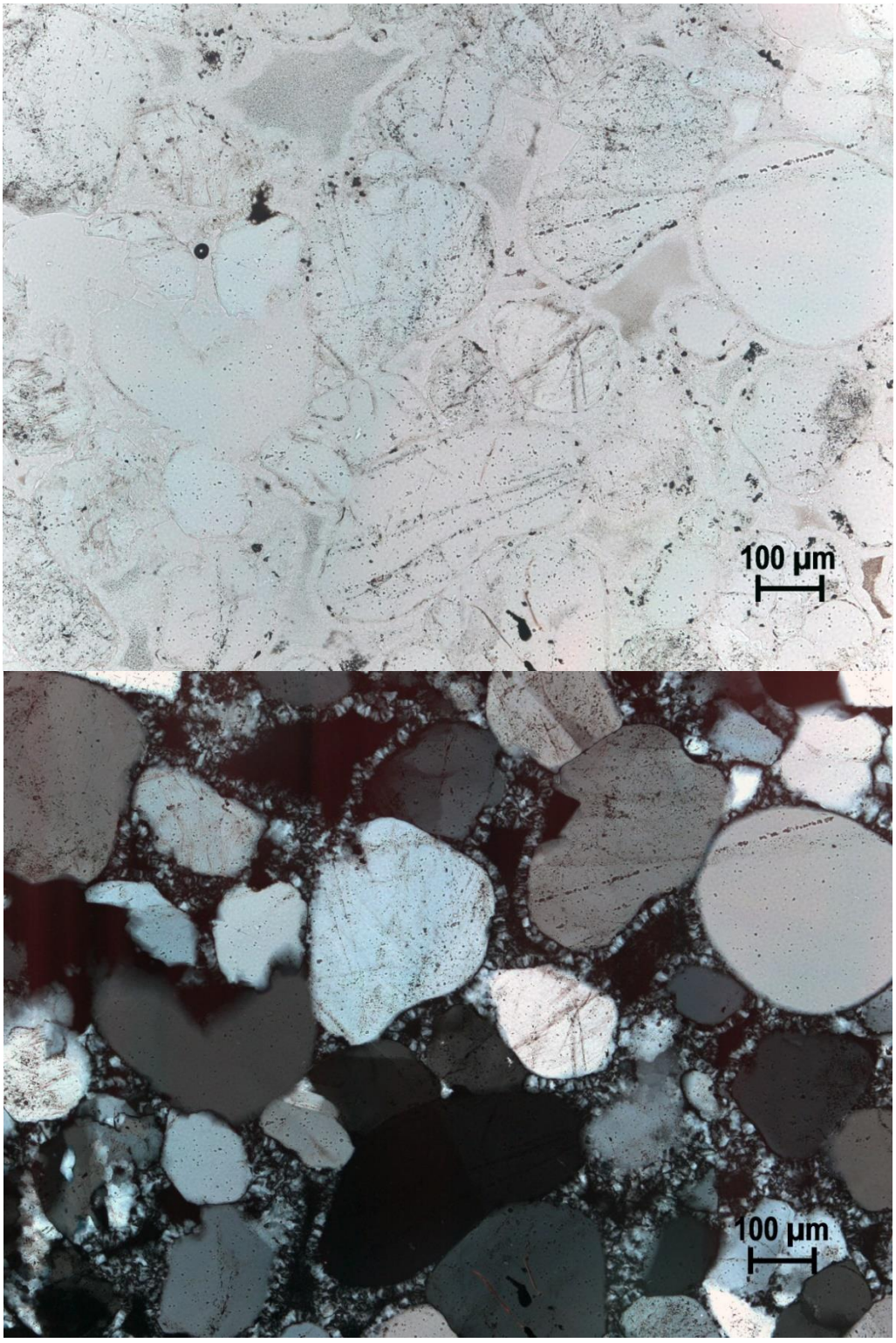

Figure 24. 5GN1 cobble sample SC09-6C with quartz grains surrounded by a thin zebraic chalcedony cement. The two quartz grains in the top center are demonstrating ungulatory extinction. Top photomicrograph is in plane light with the bottom in cross-polarized light under 10X magnification.

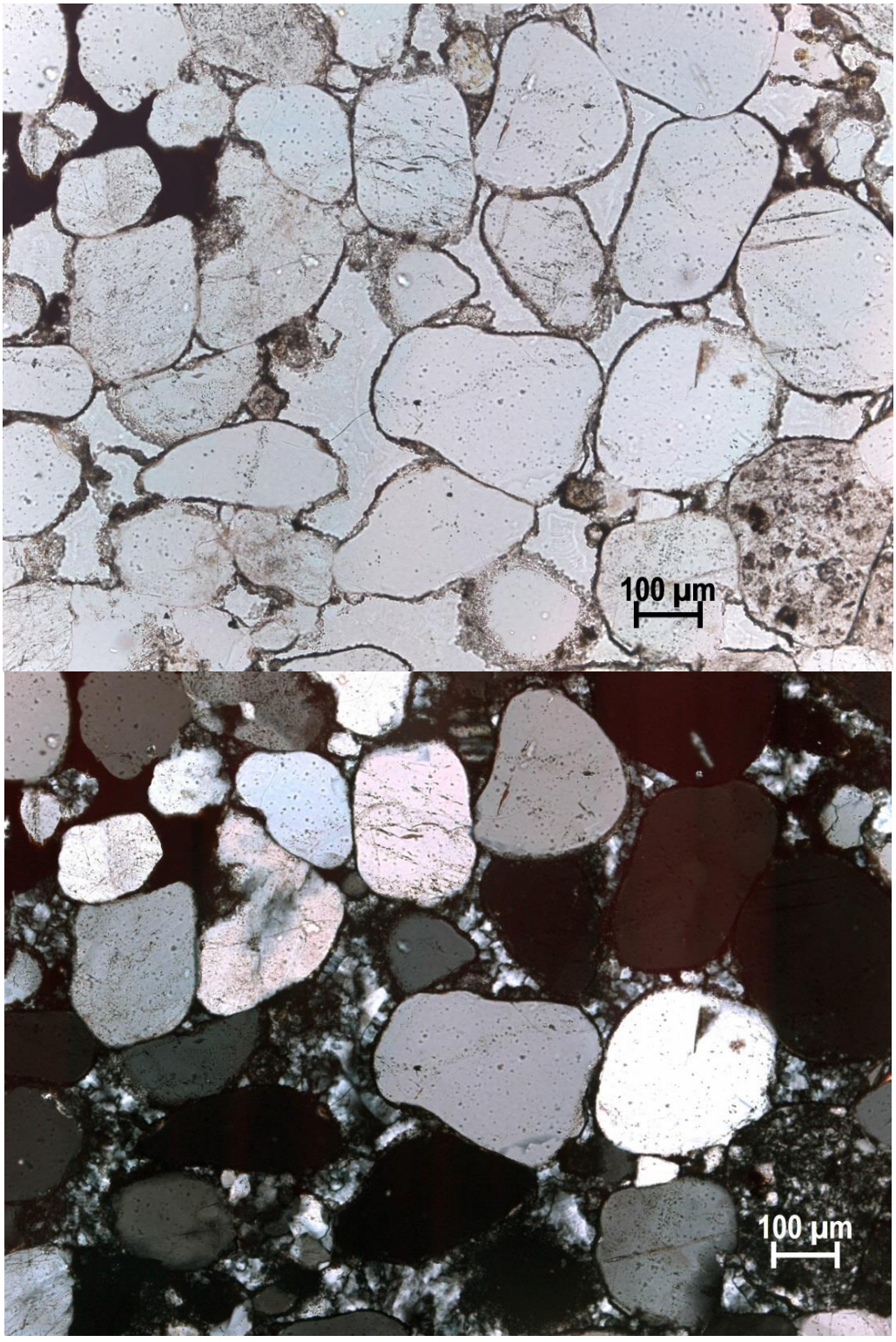

Figure 25. 5GN1 Cobble sample SC09-6F average composition. Note the black and white chalcedony cement around quartz grains with a chert fragment in the lower right corner near the scale. Top photomicrograph is in plane light with the bottom in cross-polarized light under 10X magnification.

5GN1 Outcrop Samples

Outcrop samples at 5GN1 are fairly homogenous as might be expected given that all outcrop samples belong to Jurassic Junction Creek Formation (Jj). Nonetheless the samples divide into two uneven groups with group #1 containing one sample (SC09-7B) and group #2 with the other eight samples (Figure 26).

Outcrop Group #1 is equivalent to 5GN1 cobble group #1, a quartz arenite, although this particular sample shows a slightly more mixed mineralogical composition with 95.4 percent quartz, 0.9 percent feldspar, and 3.7 percent lithic. This fits well within the geologic definition of quartzite, as demonstrated by the nearly pure quartz grain composition shown in Figure 27 of SC09-7B. From a knappers perspective this represents a prime toolstone that would concordially fracture across the nearly pure silica grains. What is characteristic of this group is medium to thick quartz overgrowths that surround quartz grains. Lithics constitute 4.6 percent of the sample and are all rounded chert grains. Biotite was noted, although it was not accounted for in the point count as the microscope crosshairs used to identify what is to be counted never fell on it. This well sorted sample's grains vary from fine to medium sand (126 to 404 microns) with an average of medium sand (261 microns).

Two

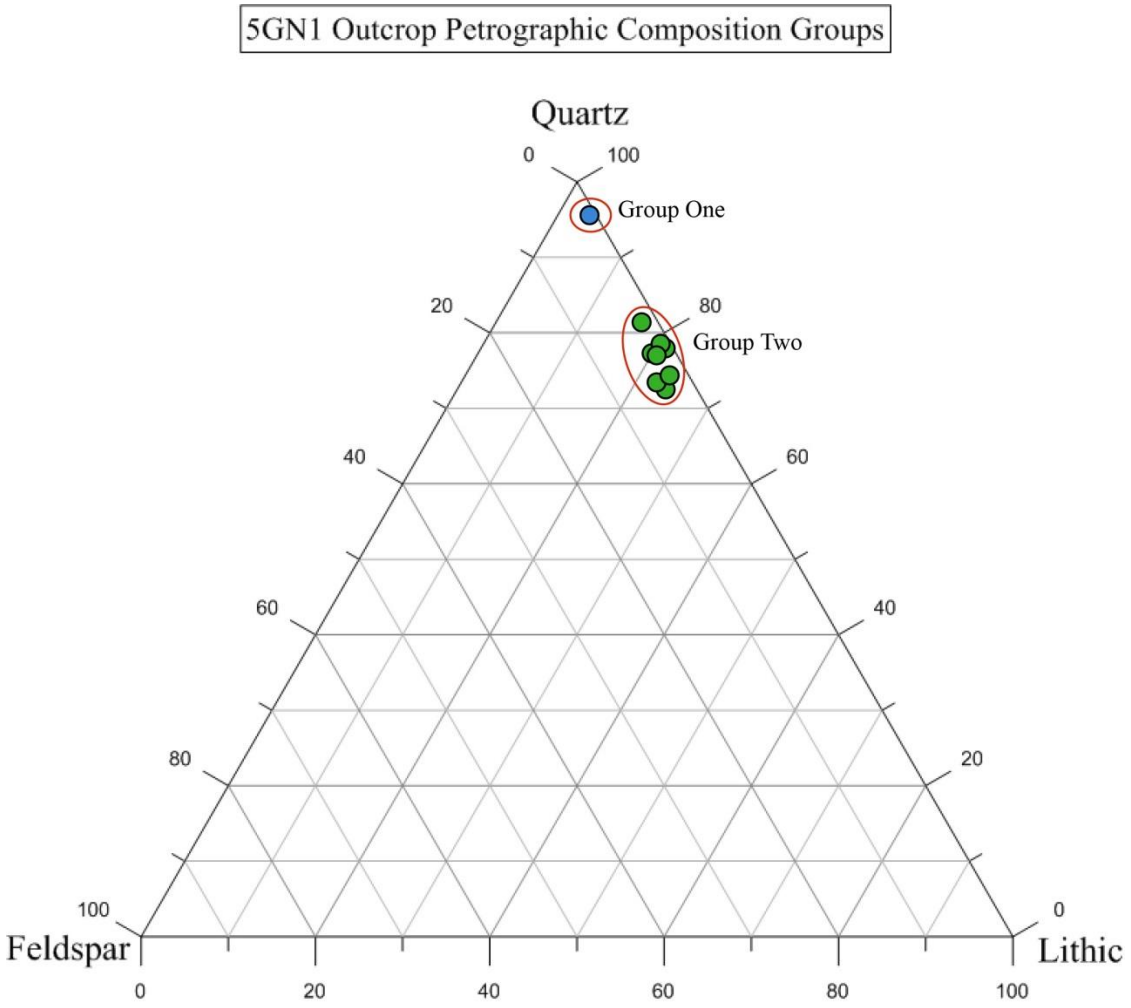

Figure 26. Ternary Diagram for 5GN1 Cobble samples. The top and right axis represents quartz, right and bottom axis represents lithic, and the left axis representing feldspar sample composition.

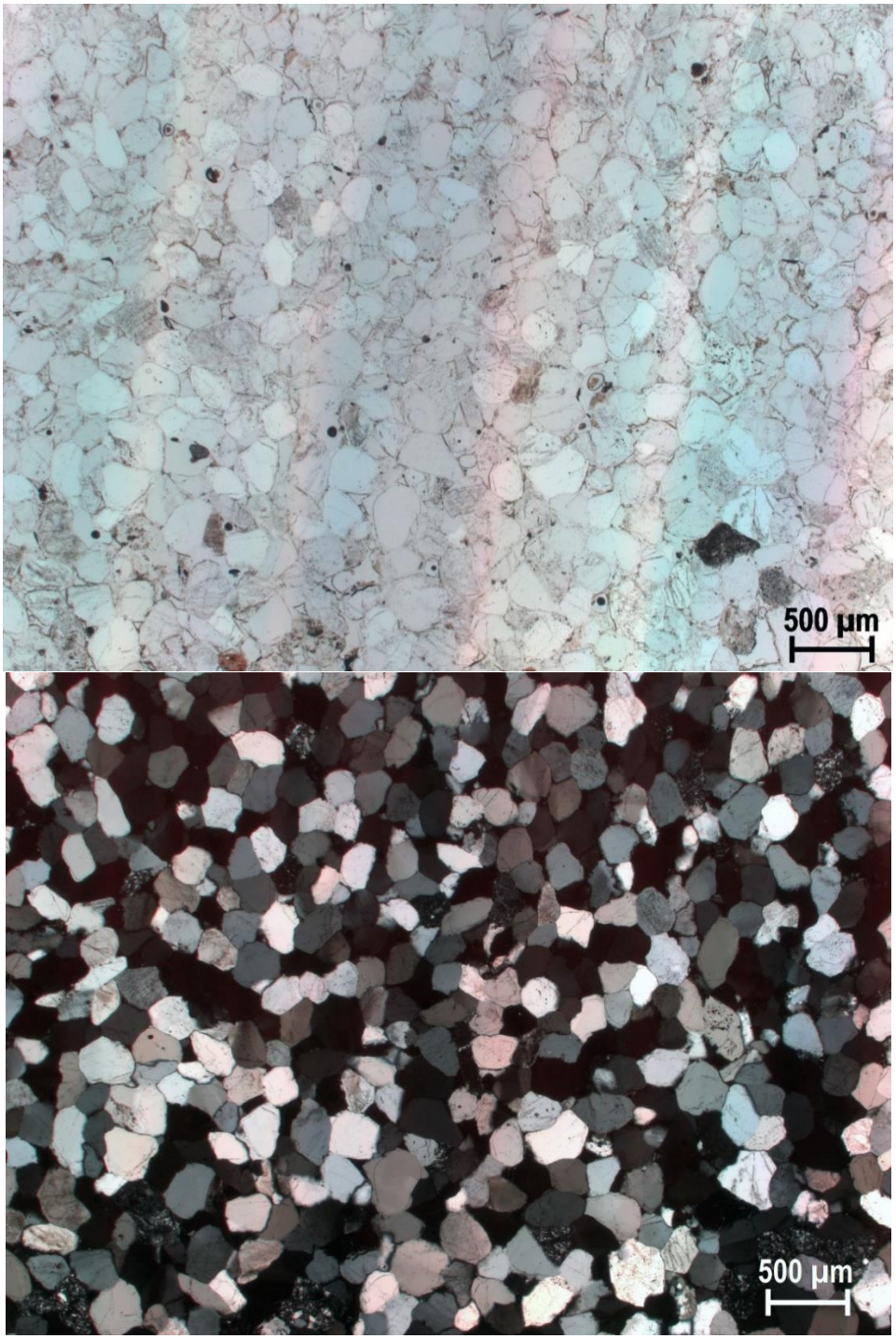

Figure 27. 5GN1 Outcrop sample SC09-7B demonstrating a nearly pure quartz grain composition. Quartz grains exhibit medium to large quartz overgrowths comprising the cement. Top photomicrograph is in plane light with the bottom in cross-polarized light under 2.5X magnification. The dark grains in the top (plane light) photomictograph are K-spar stain feldspar (top lower right) chert (bottom lower right), and biotite (lower left), although the biotite was not recorded in the point count.

5GN1 outcrop group #2 is statistically significant for this small subset, but crosses the boundary of what is two 5GN1 cobble groups (2 and 3) and Basin-wide study groups (1 and 3) of sublithic anrenite and lithic arenite. SC09-1D is 81 percent quartz, which would be grouped with 5GN1 cobble group 2, for which the break point is 80 percent quartz. Because it is the only sample within the 80 to 90 percent quartz range with sample SC09-1D (normally within a septate group as with the 5GN1 cobble samples), it is grouped with the other sub 80 percent quartz grain samples. Similar to cobble group #3 the outcrop group #2 samples are still predominantly quartz grains at 76.7 percent quartz, 2.4 percent feldspar, and 20.9 percent lithics. The cement is zebraic chalcedony in thin multicrystilalline ribbons around quartz grains with some small pore space present in the middle of such matrix ribbons of black calcite. Feldspar is present in small amounts (4 percent or less), with a few fragments displaying plagioclase twining (Figure 28). Small chert fragments occur in quantities less than 7 percent of sample composition, with chert grains larger on average than quartz grains. The quartz grains are normally rounded to sub rounded, some with small volcanic vacuoles (needle like volcanic inclusions). Many grains have thick dust rings (boundaries), with some having small to medium quartz overgrowths. For the most part quartz grains are unstressed. A few polycrystalline quartz grains (QPC) are present, likely from secondary deposition. Grain size ranges from very fine sand to medium sand (116 to 494 microns) with an average of 214 microns or fine sand.

A Collective View of 5GN1 Samples

All 5GN1 samples fit within three petrographic groups and are notable for containing less than 5 percent feldspar (Figure 29). These samples are mainly composed

of silica quartz grains and chalcedony cement contributing to a relatively high lithic quantity. This is not surprising, given that this trend was observed with the broader Basin-wide study on UGB quartzite, how lithic-high samples tend to occur near the southern portion of the basin near higher volcanism. An important result of the Basin-wide study is that it allows for these spatial understandings to be known, and tested as in this case with 5GN1. The total 5GN1 petrographic groups mirror the cobble groups discussed above with group #1 of nearly pure quartz grains, group # 2 representing a sublithic arenite with thin zebraic chalcedony cement, and group #3 below 80 percent quartz straddling the border between a sublithic arenite and a lithic arenite. The main difference between the 5GN1 groups and the outcrop groups is sample SC09-1D is now groups in 5GN1 group #2, as it contains more than 80 percent quartz as discussed above.

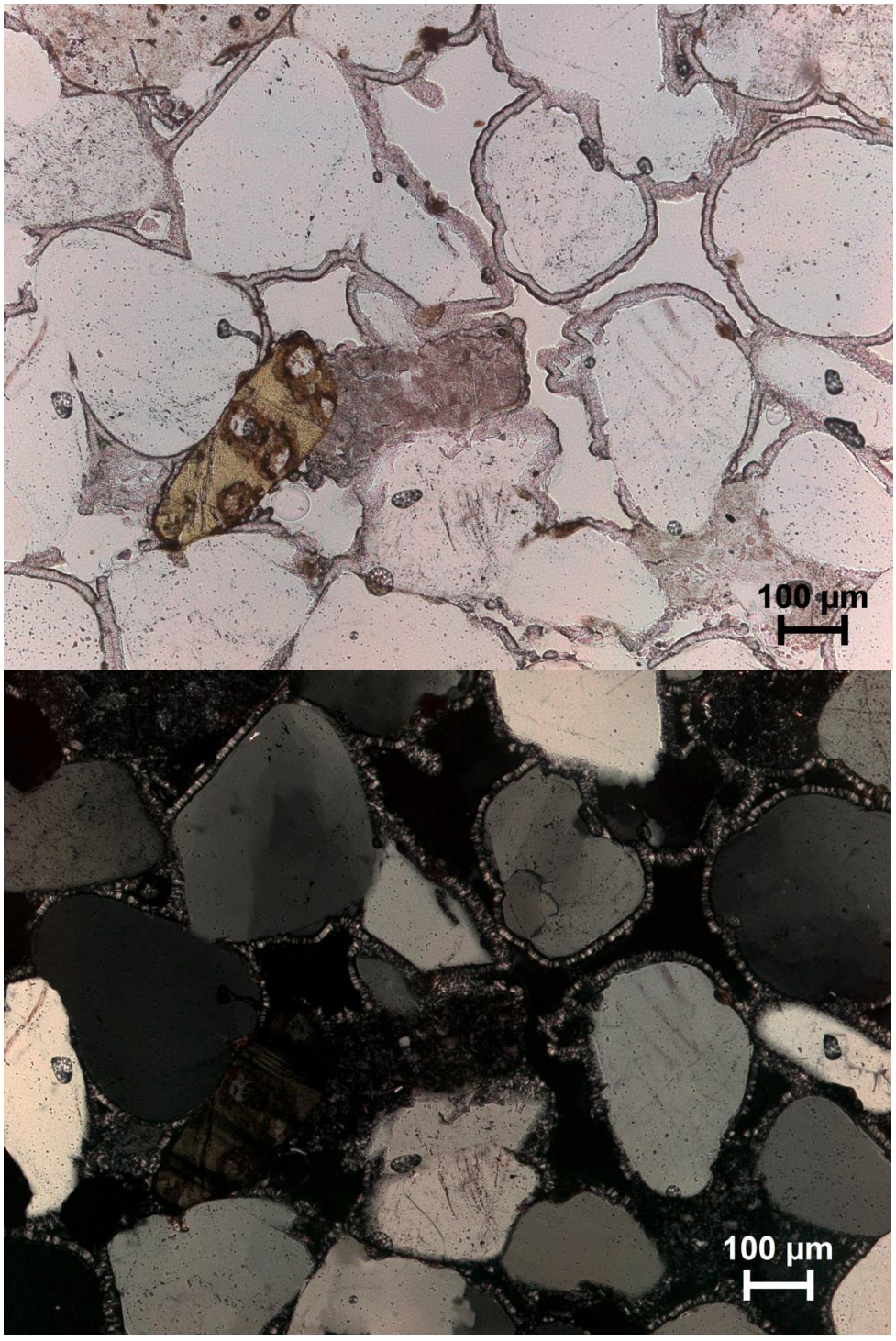

Figure 28. 5GN1 Outcrop sample SC09-1G with quartz grains surrounded by a thin zebraic chalcedony cement. Note the Plagioclase fledspar in the lower left of frame exhibiting twinning with a yellow brown (from the stain) and black color. Additionally, the large quartz grain in the upper left is demonstrating a textbook ungulatory extinction in the cross-polarized image. Top photomicrograph is in plane light with the bottom in cross-polarized light under 10X magnification.

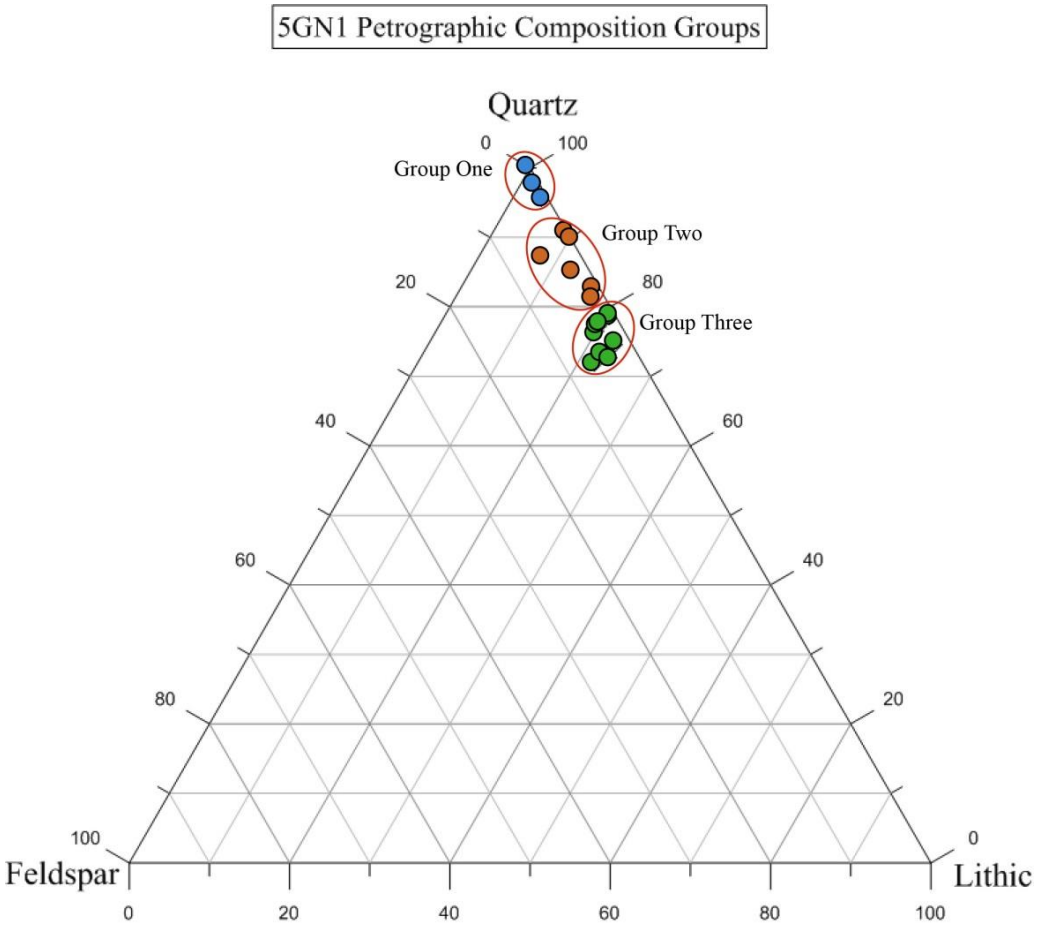

Figure 29. Ternary Diagram showing all 5GN1 samples. The top and right axis represents quartz, right and bottom axis represents lithic, and the left axis representing feldspar sample composition.

Discussion

In the context of the Basin-wide study petrographic groups, 5GN1 groups #1, 2 and 3 primarily align with Basin-wide groups #4 (primarily quartz), 3 (quartz and lithic), and 1 (lithic heavy) respectively. Absent from the samples is the feldspar-heavy category. Although, 5GN1 samples contain feldspar, it is only in small amounts less than 5 percent.

Of significant geologic interest here is that the *cobble* groups and Jurassic Junction Creek *outcrop* groups are the same petrographically and geochemically (Pitblado et al. 2013). This is an unusual and unexpected outcome. Cobbles are nearly always more heterogeneous UGB wide when compared to outcrops, as demonstrated with Basin-wide petrographic study and previously obtained geochemical results. Additionally, the cobbles rarely match the nearest outcrop, except in few only a few cases that includes the 5GN1 samples. Therefore, this result is an anomaly in the larger quartzite study (Pitblado and Dehler 2006; Pitblado et al. 2008 and 2013). The near absence of a group characterizing the 80 to 90 percent quartz groups at 5GN1 is notable in the outcrop samples. I believe this to be an artifact of sampling and not characteristic of an actual difference, especially since the geochemistry and petrography agree that these are the same material. Mineralogical and textural characteristics are similar in the 5GN1 samples such as quartz grain weathering and variability of chalcedony and lithics. The outcrop in this instance and not, for example the Paleo Gunnison River or another formation process, is most likely the parent source for the cobbles.

Chapter 6: Parlin Flats Analysis

Parlin Flats refers to sample locations CD09-3, 4, and 5 from the 2009 USU fieldschool. Located on cliffs near the unincorporated community of Parlin, east of the city of Gunnison in the eastern portion of the UGB, Parlin Flats consists of a series of sampled Cretaceous Dakota and Burro Canyon (Kdb) deposits. It is still a part of the intermountain basin, sagebrush parkland environmental zone at nearly 8,000 ft. asl. (Figure 30). The outcrops were sampled in three separate locations laterally and vertically. Samples CD09-3 were collected laterally, whereas CD09-4 and CD09-5 capture potential vertical variability. One archaeological site was recorded at sample site CD09-3 and it consisted of more than 1,000 quartzite debitage flakes, 300 chert debitage flakes, and one Late Archaic corner notched serrated knife, in addition to tested cobbles and outcrops (Figure 31).

Figure 30. Test location CD09-3 and 2009 USU fieldschool crew sampling CD09-5B left and right respectively. Photos courtesy of Bonnie Pitblado.

Figure 31. 2009 USU Fieldschool crew flagging out the site near CD09-3. Photo courtesy of Bonnie Pitblado.

Results

The fifteen Parlin Flats samples demonstrate interesting variability within the Cretaceous Dakota and Burro Canyon Formations, despite the fact that all the samples are geochemically indistinguishable (Pitblado et al. 2013). From the Basin-wide study (chapter 4) 4 samples were included in this more detailed analysis with an additional 11 samples. Similar to 5GN1, new specific Parlin Flats groups are made to fully understand the variability within the source and how that variability clusters within the geologic formation. I utilized the same statistic approach is utilized as the Basin-wide and 5GN1 analysis, except I ran it only once because all Parlin Flats samples are from the same outcrop formation. Although the groups I obtained mirror the petrographic

groups outlined in the Basin-wide Study, these are statistically distinct groups specific to the Parlin Flats data.

K-means Cluster Analysis

As in the case of 5GN1, the Parlin Flats samples discriminated into three groups (Table 10; Appendix A: Table 12). These groups are spread out along the quartz and lithic axes of the ternary diagram (Figure 33) due to an overall lack of feldspar in the samples (1.4 percent).

Table 10. Parlin Flats K-Means Cluster Analysis Group Centroids.

	Final Cluster Centers		
	Cluster		
	1	2	3
Quartz	93.3967	77.5163	66.4269
Feldspar	.8557	1.3428	2.3980
Lithic	5.7490	21.1408	31.1751

Discriminant Analysis

The K-means cluster analysis groups were again 100 percent accurate as verified through discriminant analysis (Figure 32; Appendix A: Table 13). There is a clear distinction between the groups.

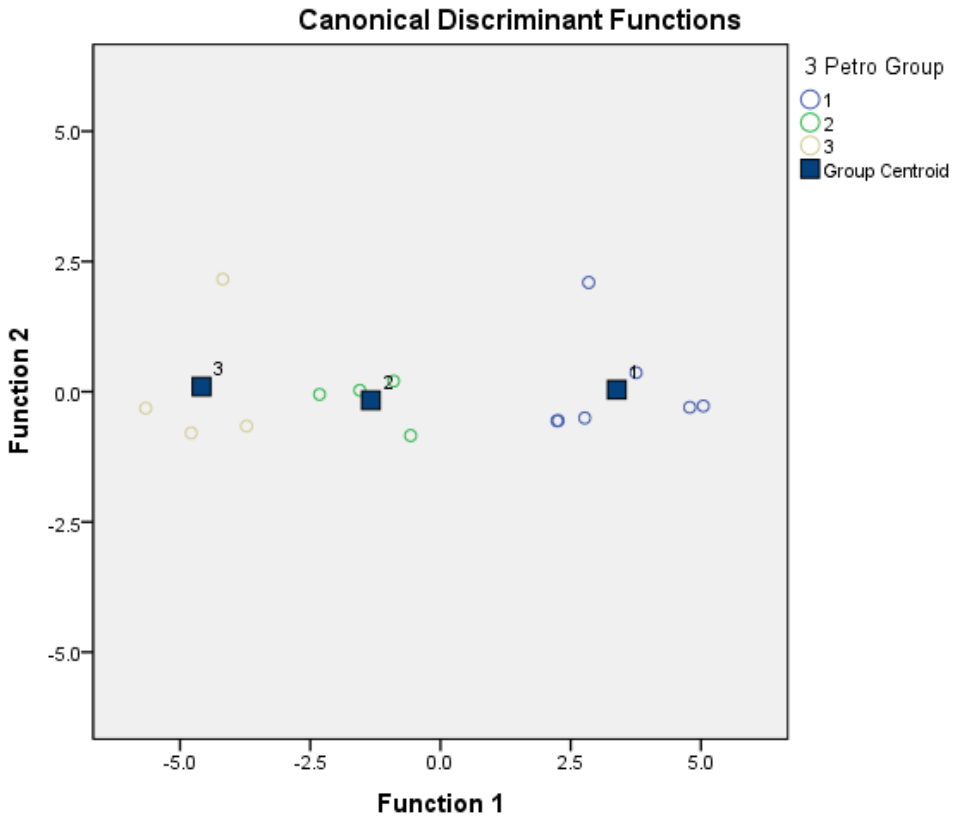

Figure 32. Parlin Flats Discriminant Analysis Plot. Petro Group indicates the Petrographic groups.

Parlin Flats Petrographic Groups

When compared with the 5GN1 samples the Parlin Flats samples constitute similar groups, although in the case of Parlin Flats, there is a drop off in quartz grains between 80 and 89 percent quartz (Figure 34). What is a gradual transition in quartz composition in the Basin-wide study and at 5GN1 is much sharply distinct in this Cretaceous Dakota and Burro Canyon Formations.

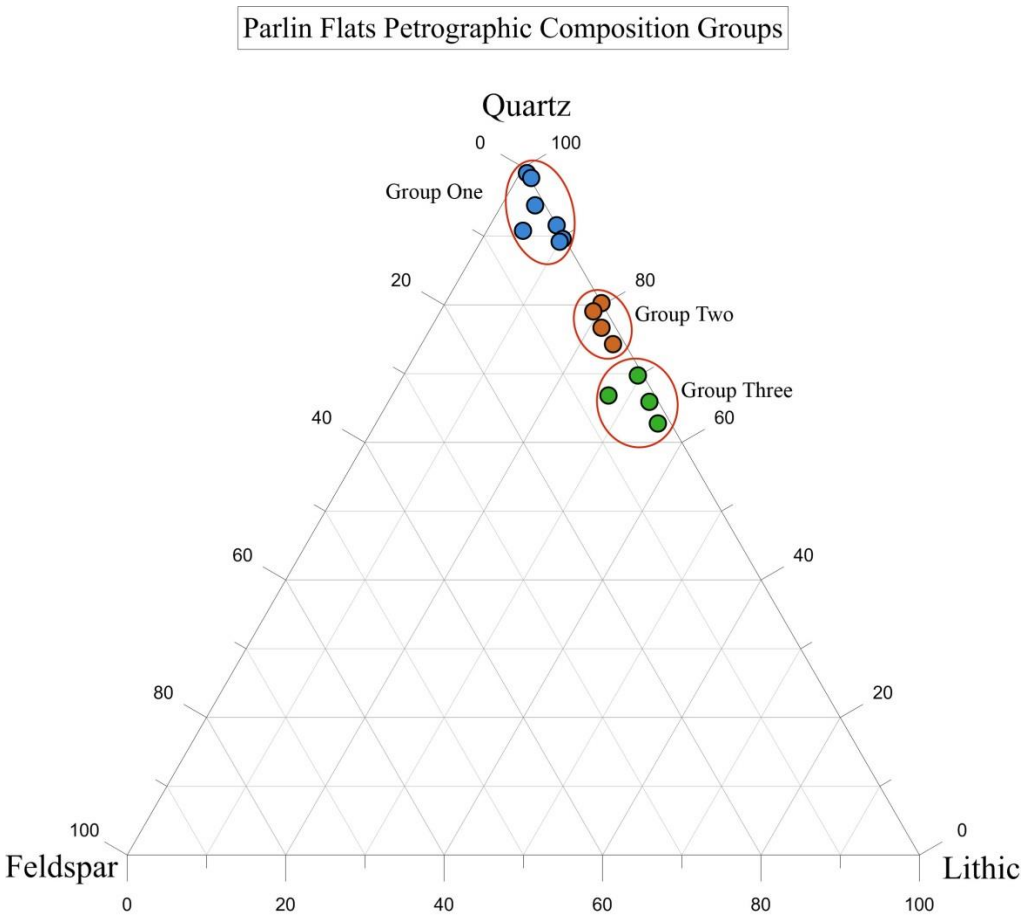

Figure 33. Parlin Flats samples ternary diagram. The top and right axis represents quartz, right and bottom axis represents lithic, and the left axis representing feldspar sample composition.

The Parlin Flats group #1 consists of seven samples primarily from CD09-3 (5), with two more from CD09-4. Notably absent from this group are samples from the CD09-5B location. Parlin Flats group #1 samples are a quartz arenite with nearly pure, well sorted rounded to sub-rounded silica quartz grains with a group average of 93 percent quartz, 1 percent feldspar, and 6 percent lithic primarily chalcedony, chert, and VRF's (Figure 34). Grain size is notable for the furthest west sample in the CD09-3 collection group, CD09-3A. The grains in sample CD09-3A are notably small at an average of 97 microns (very fine sand) and total range of 51 to 169 microns (coarse silt

to fine sand) (Figure 34). The rest of Parlin Flats group #1 average grain size is around 274 microns (medium sand) with a variable range of 67-521 microns (very fine to coarse sand). CD09-3A was collected near a fault plane, which likely caused increased pressure and heat during the initial formation of its diagenesis. This caused the grains to become closely aligned facilitating the growth of quartz overgrowths and not allowing the presence of a cement. The increased pressure can also make the sample more homogenous overall and with grain size as it will preferentially select for similar grain size minerals (in this case quartz grains) during the formation process. Additionally, CD09-3A is 98 percent quartz making it nearly pure silica. Otherwise this sample is characterized by thick dust rings around quartz grains and thick well developed quartz overgrowths preventing the inclusion of a chalcedony or calcite cement as observed in other samples from the UGB. All six other samples in this group have moderate quartz overgrowths and thin to barely visible dust rings. This is unusual for samples that contain primarily quartz grains and no chalcedony cement.

Parlin Flats group #2 contains four samples with an average composition of 77 percent quartz, 1.5 percent feldspar, and 21.5 percent lithic, making these sublithic and lithic arenite samples. They show a thin chalcedony cement around moderately well to well sorted quartz grains (Figure 35). Biotite and mica occurs in small, fragmented quantities with three out of the four samples containing 1 percent mica or biotite. This suggests less pressure during rock formation, in contrast to Parlin Flats group #1. Grain size ranges from very fine sand to medium sand (86 to 414 microns) with an average grain size of 210 microns (fine sand) on sub-rounded to sub-angular grains. Quartz overgrowths are present, but are fairly small or absent.

Parlin Flats group #3 containing four lithic arenite samples is the most mixed composition group, showing 66.4 percent quartz, 2.4 percent feldspar, and 31.2 percent lithic. Thick chalcedony cements are common with sub-rounded to sub-angular quartz, chert, and VRF grains (Figure 36). The mixed composition of these samples suggest less heat and pressure samples during formation. Dust rings are thin and difficult to notice. Mica and biotite are noted with some whole grains present, although this still remains less than 1 percent of total sample composition. Volcanic inclusions are very common on quartz grains. Grain size varies from 96 to 502 microns (very fine sand to medium-coarse sand) with an average grain size of 233 microns (fine sand). Both CD09-5 samples are within this group, suggesting that it was not an area that would have been prehistorically quarried.

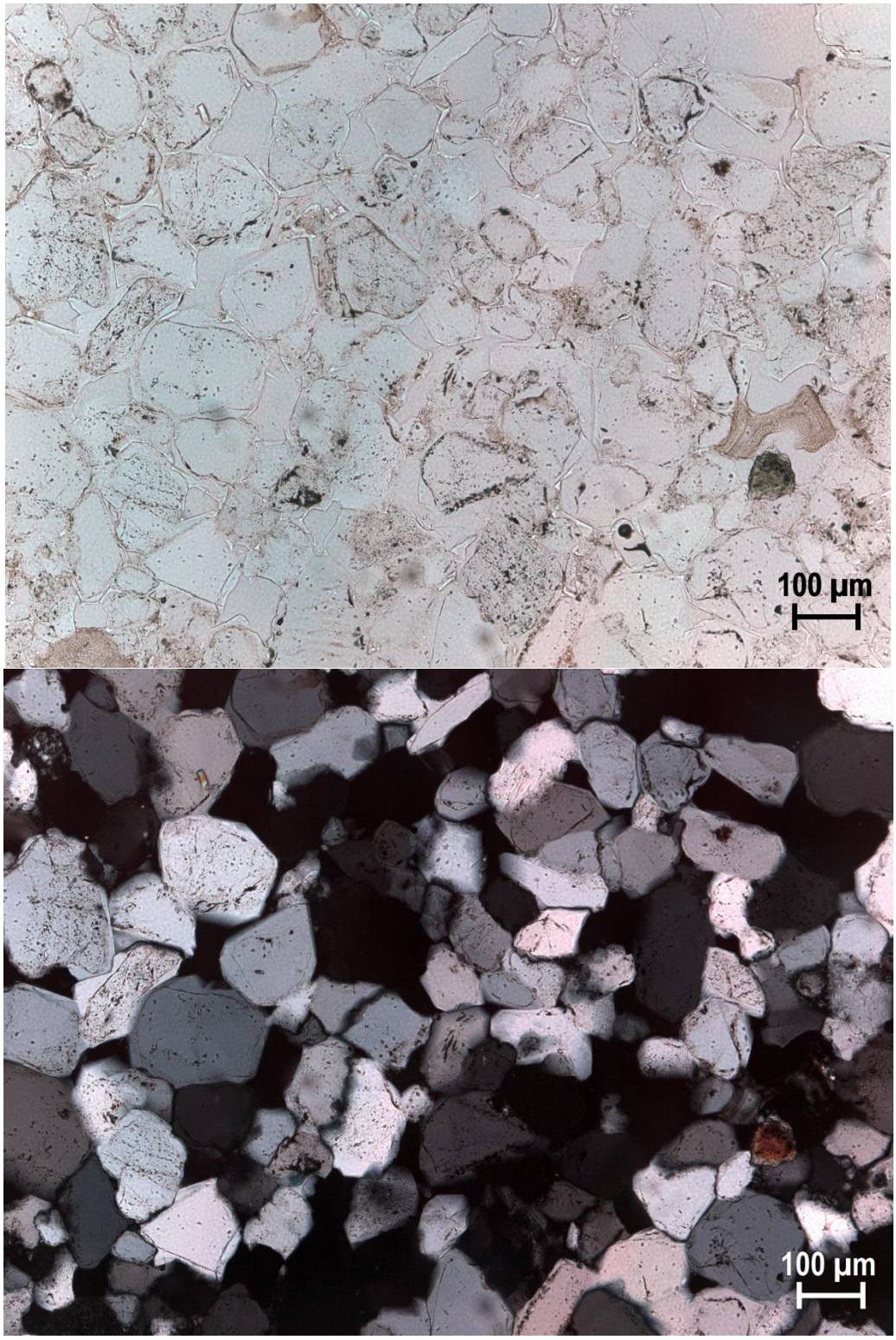

Figure 34. CD09-3A demonstrating the ubiquitous rounded to sub-rounded quartz grains with thick overgrowths. The bright mineral in the lower left is a mica fragment, unusual for this sample. Top photomicrograph is in plane light with the bottom in cross-polarized light under 10X magnification.

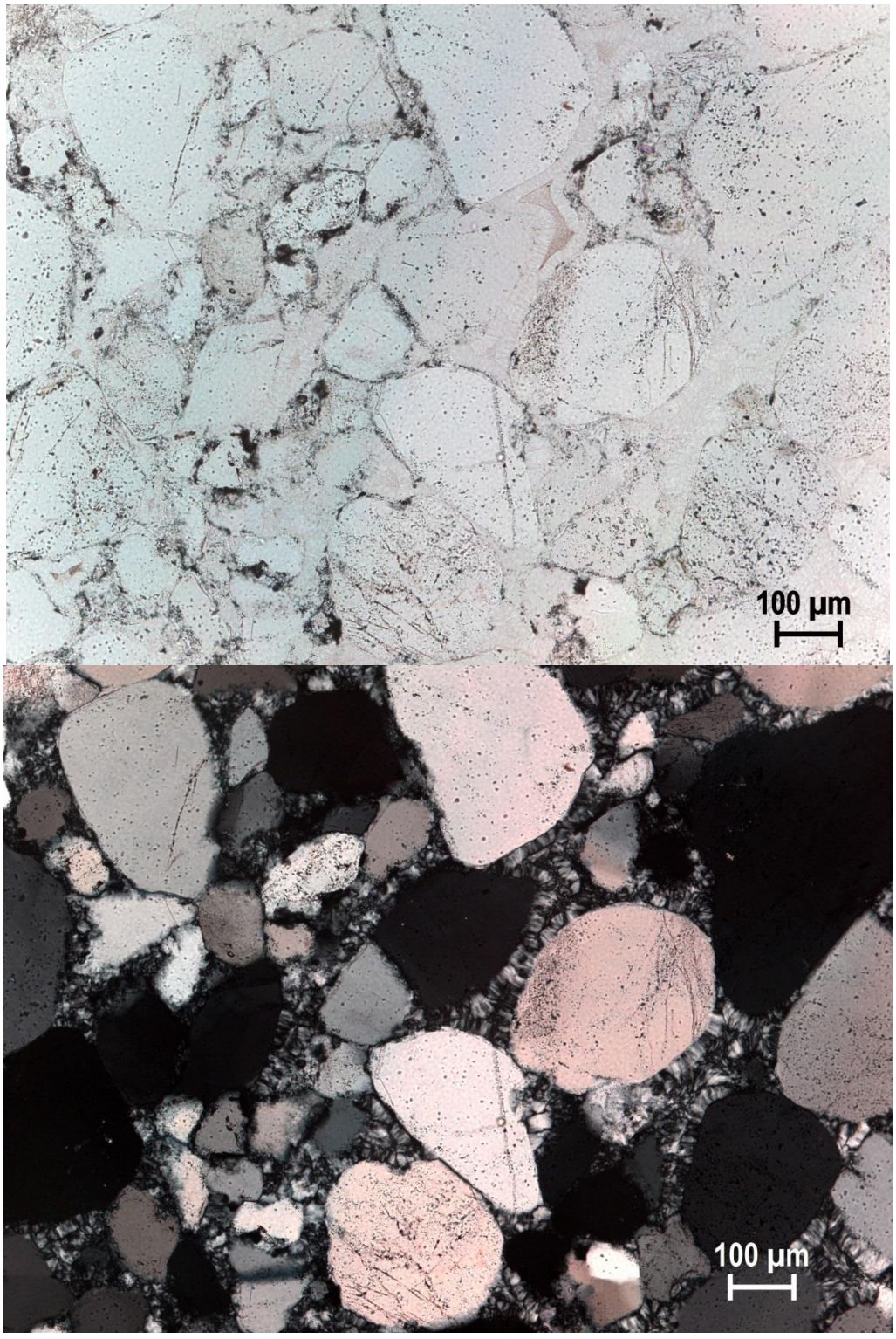

Figure 35. CD09-3D exhibiting vibrant thin ribbons of zebraic chalcedony around quartz grains, a few with small overgrowths. Top photomicrograph is in plane light with the bottom in cross-polarized light under 10X magnification.

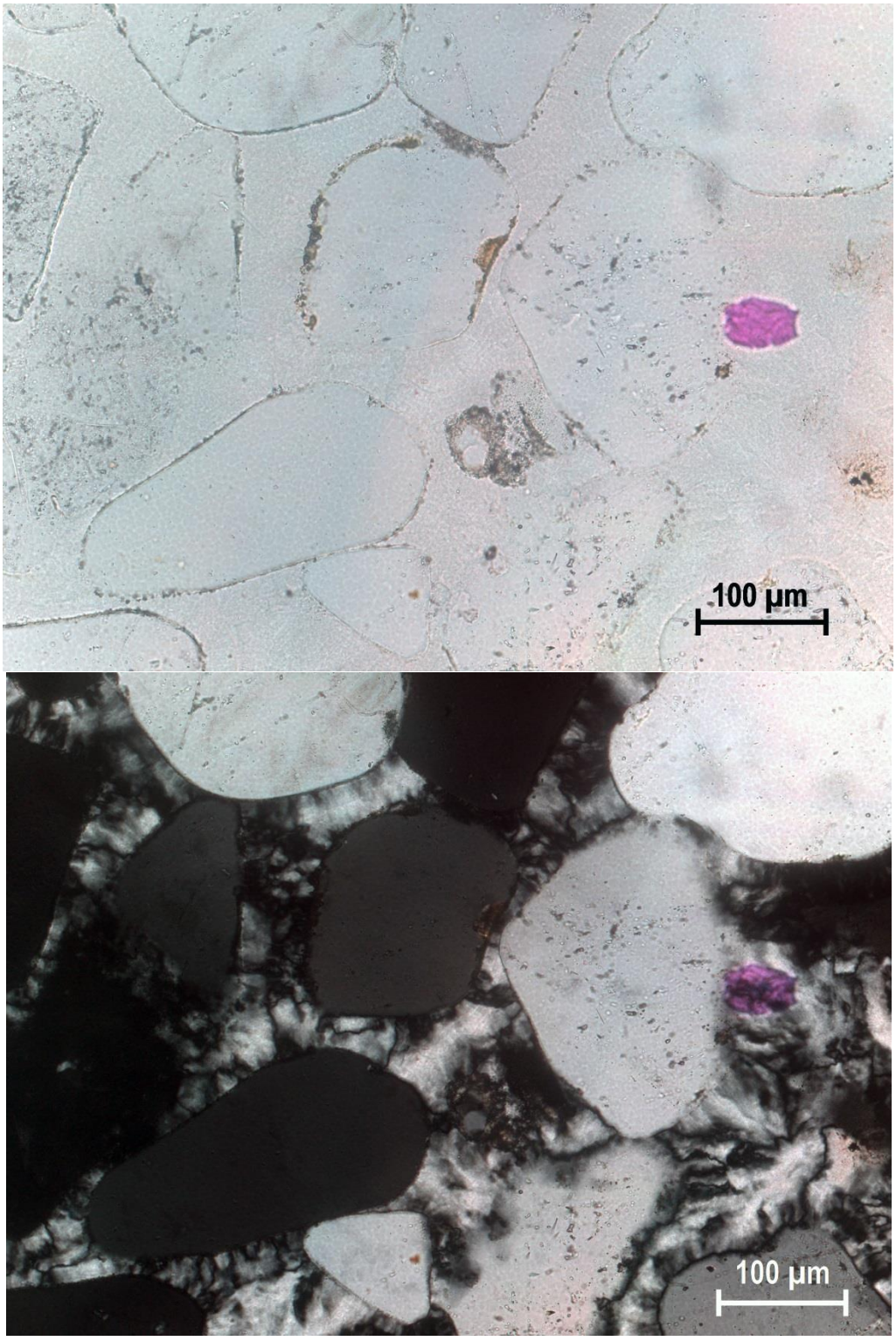

Figure 36. CD09-3F demonstrating characteristic thick zebraic chalcedony surrounding sub-rounded to sub-angular quartz grains. Notice the bright purple piece of mica in the center right of frame. Top photomicrograph is in plane light with the bottom in cross-polarized light under 10X magnification.

Discussion

A clear trend captured by the vertical sampling of the Parlin flats samples is that the finest-grain and purest quartzite from the Cretaceous Dakota and Burro Canyon Formation occurs at or near the contact with the Jurassic Morrison Formation. The further away from the contact zone sample, the more mixed in composition the samples become. For example, CD09-4A is part of Parlin Flats group #1, and came from meter mark 1. CD09-4B, part of Parlin Flats group #2 is from meter mark 3. CD09-4C, from meter mark 16, belongs to Parlin Flats group #3. The exception to this pattern is CD09-4D, from meter mark 41, which belongs to Parlin Flats group #1, and represents a completely different depositional event that likely occurred long after any of the other samples. CD09-4D is the only sample collected from the archaeological site CD09, which has quartzite consisting of 99 percent silica quartz. This demonstrates the same tendency we saw at 5GN1 that prehistoric peoples of the UGB desired in a toolstone. The event that created CD09-4D at meter mark 41 was a return to a quick high pressure formation that contributed to its different diageneses. CD09-5A and B samples belong to Parlin Flats group #3 despite being collected from 7 and 10.5 meter marks. These samples were likely collected from the same area in the formation as CD09-4C with the contact zone not exposed in this collection area.

In the regard to the Basin-wide results, Parlin Flats groups #1, 2, and 3 primarily align with petrographic groups #4, and 1 respectively.

Chapter 7: A Tale of Two Sources-Comparison of 5GN1 and Parlin Flats

Both 5GN1 and Parlin Flats were prehistorically quarried, although with different degrees of intensity. The extensively and consistently quarried 5GN1 was a primary lithic source within the UGB with its many loci driving archaeological research since Buckles's first recording in 1962 (Anderson et al. 2009; Buckles 1962; Peart 2013; Stiger 2001). Parlin Flats as a quartzite source on the other hand, was not recorded as having any prehistoric activity until the 2009 Utah State University Fieldschool collected samples for this geologic study. While used prehistorically, Parlin Flats does not compare to 5GN1 is exploitation, although both were clearly utilized. A comparison of these quarries entails comparing a Cretaceous Dakota and Burro Canyon Formation (Kdb) in Parlin Flats to a Jurassic Junction Creek Formation (Jj) at 5GN1. Parlin Flats is of direct interest in comparison to 5GN1 because on the initial coarse grain geochemical analysis it grouped with Jurassic sources despite being Cretaceous in age (Figure 3) (Pitblado et al. 2013).

Despite both areas having some geochemical characteristic composition, petrography reveals a big difference between the two sources in the absence of samples with quartz grains between 80 and 90 percent at Parlin Flats versus 5GN1. This is similar to a gap noted within the 5GN1 outcrop sample, which is likely due to sampling error. Why this is not the case at Parlin Flats is because the clear pattern demonstrated throughout the formation from near the contact with the Jurassic Morrison Formation from nearly pure quartz grains to a more mixed composition (Figure 33), while 5GN1 outcrops are more homogenous. Parlin Flats exhibits a greater range of differences in sample composition than 5GN1. Further, the associated cobbles at 5GN1 do occur in

the 80 to 90 percent quartz range and overlap with the other recorded petrographic groups present (Figure 26).

Other differences between the quarry sites relate to individual mineral composition. Samples from Parlin Flats group #1, while having a nearly identical mineralogical composition 5GN1 group #1 in the QFL groups, nonetheless display some notable differences. Both sources' groups include nearly pure quartz grains, making them quartz arenites and fulfilling the geologic definition of quartzite. However, the Parlin Flats group #1 samples have moderate quartz overgrowths and quartz grain dust rings that are thin to nonexistent. Conversely, samples from 5GN1 group #1 have thick overgrowths and thick dust rings signifying a different depositional process (Figure 37).

Feldspar occurs in small amounts at each source location, although feldspar occurs in amounts 2 and 3 times that at Parlin Flats in several 5GN1 samples. Lithic-heavy or lithic arenite samples that occur in Parliln Flats group #3 all exhibit thick zebraic chalcedony cements (Figures 36 and 37). In 5GN1 group #3 of similar composition, the zebraic chalcedony is notably thinner (Figures 25 and 28). Quartz grains on the 5GN1 group #3 have small to medium quartz overgrowths and thick dust rings with both of these attributes absent in the Parlin Flats group #2 and 3. Parlin Flats quartz grains throughout every group (#1-3) contain more volcanic intrusions within quartz grains in addition to volcanic rock fragments (VRFs). The presence of more volcanic intrusions and VRFs in the Parlin Flats samples is expected as the outcrop is near a fault. Additionally, the Parlin Flats assemblage contains four samples with higher lithics and a more mixed composition overall with quartz grains between 60 and 70

percent (Figure 34). This more mixed composition does not occur at 5GN1 (Figure 29). In short, petrography *can* account for source differences and variability. While the geochemistry on the first coarse grain analysis did not find major differences, it is likely that further geochemical analysis will verify the differences found with petrography.

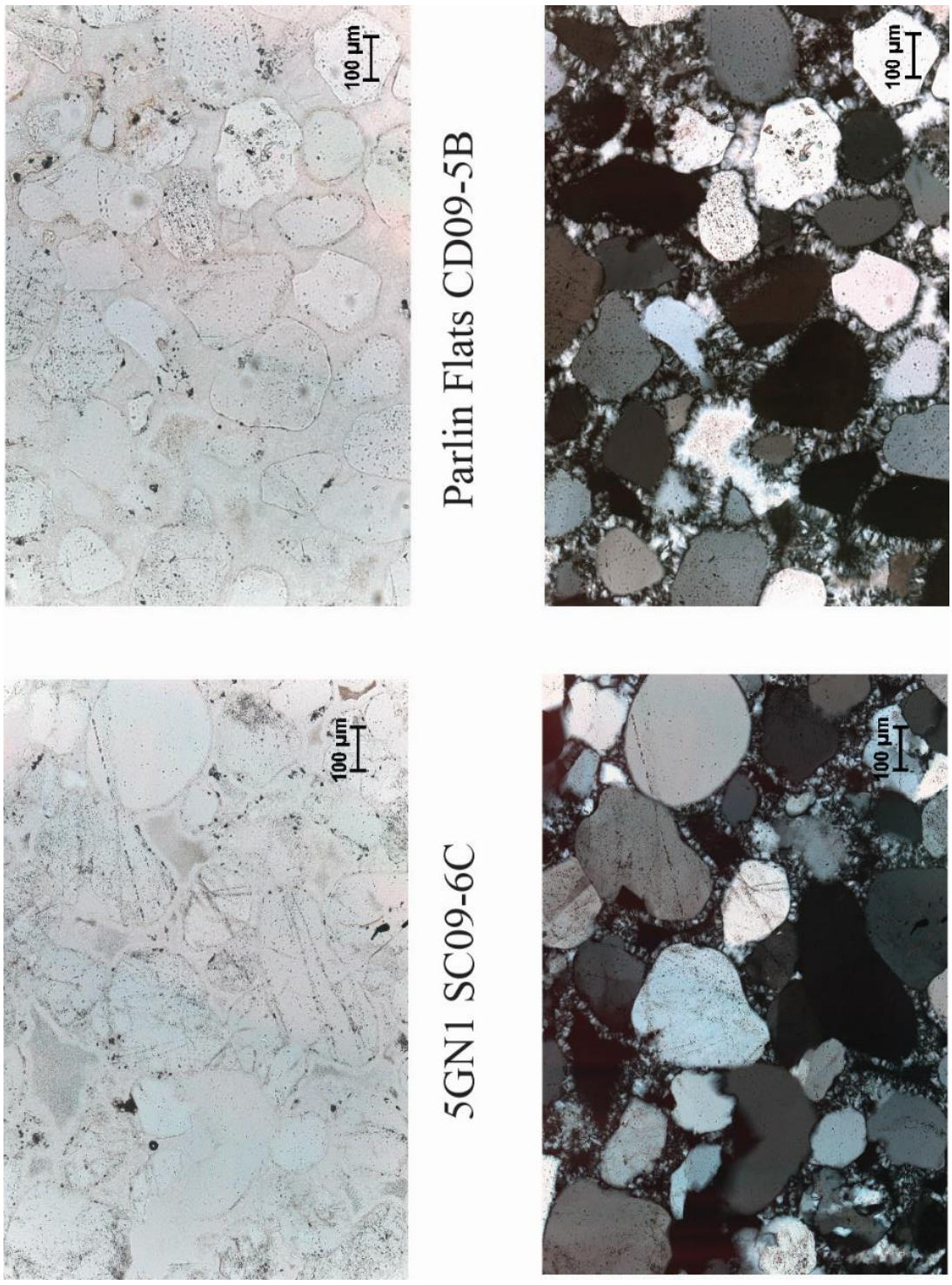

Figure 37. Comparison of 5GN1 and Parlin Flats with differential thickness in the chalcedony cement. Notice the intrusions in the Parlin Flats quartz grain in the center right. Both are taken at 10X with plane and cross-polarized top and bottom respectively.

Chapter 8: Discussion and Conclusions

Basin-Wide Study: UGB Quartzite Variability

The previously obtained LA-ICP-MS geochemistry results are encouraging from a sourcing-potential perspective, classifying the 402 quartzite samples from 48 source localities by geologic era, cobble or source origin, and demonstrating meaningful spatial differences (Neff 2010; Pitblado et al. 2013). The petrographic study yielded six distinct petrographic groups based on the samples' mineralogical and textual characteristics. The Basin-wide study on samples from across the UGB study demonstrated that significant differentiation among sources is achievable (Figure 11). In addition, from a prehistoric toolmakers-and thus archaeological-perspective, Basin-wide Groups #3, #4, and #5 are of the highest quality (i.e. have the greatest percentage of silica) and are the best-controlled quartzite among the sample population.

Petrographic Group #4 correlates with known prehistoric quartzite quarries. This is archaeologically important and a significant outcome of this study, because Petrographic Group #4 consists of nearly pure silica, making it the optimal quartzite toolstone in the UGB. The correlation between petrographic groups and geologic formations is very encouraging. When considering only outcrop sources, the petrographic groups align well with the various UGB formations according to geologic age. Petrographic Group #3 characterizes with Cretaceous sources, Group #4 Jurassic sources, and Group #5 Cambrian (and infrequently Jurassic) sources. Petrographic Groups #1 and #2 both capture secondarily deposited cobble sources.

5GN1

The detailed analysis of 5GN1 offers a first step in understanding the petrographic variability within this well-known quartzite quarry. While this is mainly a

descriptive exercise, valuable information has been forthcoming/resulted. All of the samples from 5GN1 lack feldspar and show a higher than average amount of lithics versus other UGB samples. This is consistent with the observation that higher lithic amounts occur in the southern portion of the basin than to the north.

Parlin Flats

The Parlin Flats analysis contributes important information to be used by archaeologists and geologists alike to understand the composition of the Cretaceous Dakota and Burro Canyon Formation near/at its contact with the Jurassic Morrison Formation. Additionally, the knowledge of how the formation consistently changes as it approaches the shale of the Upper Cretaceous will assist in a greater understanding of its variability through geologic time. It should be noted that this trend is based on a small sample size that should be further tested. The predictable variability the further from the contact with the Morrison Formation contributes a good test for where the finest, purest quartz is found and if this was what was prehistorically quarried whereas other areas at Parlin Flats are sampled for this geologic study where less pure and unquarried. The archaeological site CD09-3 demonstrates that this group (petrographic group #4 from the Basin-wide study) was prehistorically quarried. CD-4A represents a slightly different scenario. Its presence near a fault shows that the high quality quartzite and silicified sandstone formations near faults can contain smaller grain, nearly pure quartz grain stone. Simply stated, areas near faults can contain very high quality toolstone because of the higher heat and pressure during rock formation squeezing out not quartz grains and controlling for grain size.

Comparison of 5GN1 and Parlin Flats

The mineralogical and petrographic composition clearly demonstrate attributes particular to 5GN1 and Parlin Flats. Textural and mineralogical differences combined with quantifiable compositional differences demonstrate the separate formation process or diagenesis that occurred at each quarry. This shows that as originally hypothesized, petrography is a powerful tool that when coupled with the previous LA-ICP-MS geochemical analysis, can achieve fine grain source differentiation even within and between similar sources. The initial coarse grain geochemical results are explained and refined by petrography as in this case, and in the example of Basin-wide study group #6, the crystalline limestone that stood alone geochemically.

Consideration of All 77 Samples

The results from 5GN1 and Parlin Flats, in combination with Basin-wide study results led to significant conclusions. By using the paired analysis of K-means cluster analysis and discriminant analysis one last time, the 77 total samples (the crystalline limestone is excluded from statistical analysis discussed in Chapter 4) from the UGB represent 23 percent of the total 402 sample assemblage. One misclassification was detected in the discriminant analysis on the K-means clusters for an accuracy of 97.4 percent (Figure 38; Appendix A: Tables 14 and 15). With this corrected, the final petrographic groupings shifted slightly to accommodate the additional samples that are heavy on the lithics axis (Figure 38). Still the groups the groups are largely the same as described in Chapter 4 (Table 11). This robust classification of quartzite can only help with the future of quartzite chipped stone research within the UGB and beyond.

Table 11. Total Project K-Means Cluster Analysis Group Centroids.

	Petrographic Group				
	1	2	3	4	5
Quartz	69.3475	52.0000	79.7432	94.6415	85.2522
Feldspar	4.7298	1.5000	1.7637	1.5473	11.8061
Lithics	25.9227	46.5000	18.4931	3.8116	2.9412

This study demonstrates that petrographic analysis can effectively discriminate among different geologic sources of quartzite in the UGB, establishing a direction for inter-and intra-source differentiation for future research. The differences between 5GN1 and Parlin Flats quartzite sources show that it is possible to discriminate between these two despite similar compositions. Mineralogical differences clearly demonstrate that discrimination *between* these two quarries is possible, due to distinctions in the amount and presence of feldspar, volcanic inclusions, and quartz grain characteristics at the two localities. Results from this research have aided in the creation of a robust petrographic database that complements the existing geochemical version, but which also serves as a platform for future petrographic analysis of UGB quartzite.

It is the hope that this research will lead to additional sourcing studies in the UGB and a greater understanding of hunter-gather mobility. The variability within geologic formations as demonstrated with both 5GN1 and Parlin Flats sources allows for a detailed understanding of source distribution than was previously attempted. A greater understanding of Jurassic and Cretaceous deposits in the UGB is demonstrated with the characteristics and differences at each source. While this can be applied to the sourcing of artifacts, I advise caution. For an accurate application to the sourcing of

artifacts, a complete study that includes the analysis of a greater number of the 402 samples needs to be completed for a fine grain source database to work with rather than the subset that is available at the conclusion of this thesis.

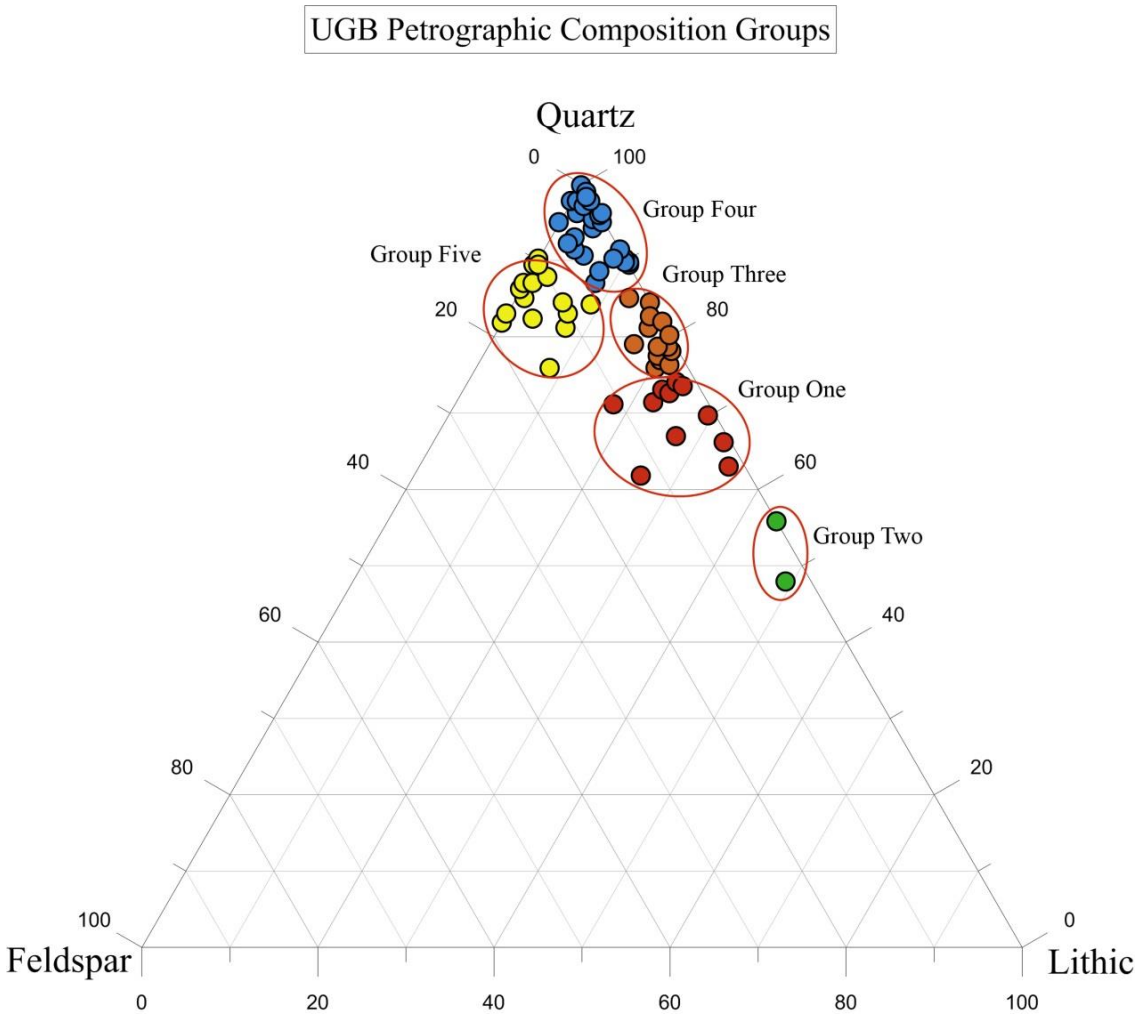

Figure 38. Total Study Upper Gunnison Basin Petrographic Composition Groups. The top and right axis represents quartz, right and bottom axis represents lithic, and the left axis representing feldspar sample composition.

Anthropological Considerations

What is fascinating with the UGB is the continued occupation from Folsom to Late Prehistoric. Many questions remain unanswered because of the inability to address human mobility through chipped stone assemblages in this lithic environment. One

hypothesis is that the high usage of quartzite within the UGB indicates a more isolated population than other neighboring intermountain basins. While this is likely a wrong assumption, the ability to test it could allow the archaeological record to speak in ways unavailable to archaeologists working with these quartzite assemblages before.

The Folsom period within the Basin and the greater Southern Rocky Mountains is of great interest to researchers. A detailed sourcing study would add a valuable line of evidence to understanding Folsom mobility and occupation in the mountains. In particular, a challenge to the ultra-mobile model of Folsom mobility based on exotic chert artifacts primarily from sites on the Plains (Hofman et al. 1991; Kelly and Todd 1988; Goodyear 1989) would be a welcome addition to the archaeological record. Interesting research questions tied to the ability to source quartzite artifacts at Folsom sites in the UGB and neighboring basins focus on the idea of bifacial reduction strategies tied to the conservation of exotic chert raw materials. The presence of local quartzite artifacts within Folsom assemblages could indicate that this model of ultra-mobile Folsom hunter-gathers is less applicable to the Southern Rocky Mountains demonstrating more variability in the archaeological record than has been previously afforded. To then compare the changes or continuity in mobility to the relatively better represented Late Paleoamerican period in the UGB could demonstrate interesting cultural changes over time.

For later periods in the UGB, the ability to use stone assemblages as a proxy for mobility could demonstrate cultural ties to neighboring regions. This is especially important with population density hypothesized to be growing during the Late Archaic and Late Prehistoric periods (i.e. Stiger 2001). Are certain types of UGB quartzite

valued over others? And if so do these types of quartzite travel outside of the Basin and if so how far? Cultural contact between areas in the UGB and greater Southern Rocky Mountains that has not been researched in this way previously, and quartzite sourcing could open up the archaeological record for new interpretations.

Human behavior is not exclusive to just obsidian and fine grain volcanic artifacts, or exotic stone artifacts. Human behavior encompasses everything that was available to the people of the past and all artifacts should be investigated/sourced if possible to understand the complexity of past human technology and variation.

Future Research Directions

As with all research, this study is one step of many in expanding our knowledge of geological processes and materials that have influenced prehistoric human behaviors. This work has the potential to provide powerful results, allowing archaeologists to apply provenance analysis to quartzite artifacts/assemblages for the application of prehistoric land use questions with petrography and/or LA-ICP-MS in the Rocky Mountains and potentially around the world.

Future research objectives include:

- Complete petrographic analysis on all 402 quartzite samples, explaining geochemical outliers
- Fully describe all outcrop and prehistoric quarry sources in the UGB
- Apply provenience analysis to the Late Paleoamerican Chance Gulch archaeological assemblage (95% quartzite),
- Apply to other Gunnison Basin sites covering all periods of human occupation,

- Compare sourcing information among UGB sites spatially and temporally,
- Build quartzite source databases for other basins in the Southern Rocky Mountains,
- Compare mobility among the intermountain basins,
- Compare mobility between larger regions.

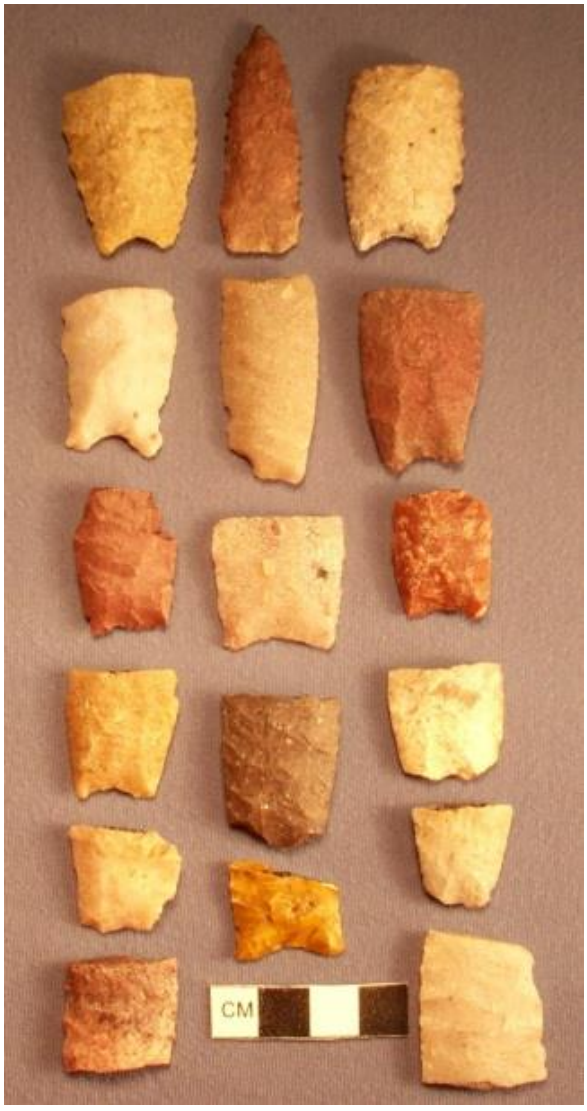

Figure 39. Late Paleoamerican projectile points from the Chance Gulch site in the Upper Gunnison Basin, Colorado. Photo courtesy of Bonnie Pitblado.

References

Andrefsky, William, Jr.
1994 Raw-material Availability and the Organization of Technology. *American Antiquity* 59: 21-34.

Anderson, Stephen R., Amanda D. Herron, and Michaela L. Grillo
2009 Curecanti National Recreation Area Motorized Vehicle Access Plan/Environmental Assessment Class III Inventory Cultural Resources Report, Gunnison and Montrose Counties, Colorado (Vols. 1 and 2). *Louis Berger Group, INC. for the National Park Service*. Manuscript on file, Colorado Historical Society, Denver.

Andrews, Brian
2010 *Folsom Adaptive Systems in the Upper Gunnison Basin, Colorado: An Analysis of the Mountaineer site.* PhD dissertation, Southern Methodist University, Dallas, Texas.

2013 *The Mountaineer Folsom Site.* Paper presented, 11th Biennial Rocky Mountain Anthropological Conference, Sagebrush Inn, Taos, New Mexico.

Andrews, Brian, Jason M. Labelle, and John D. Seebach
2008 Spatial Variability in the Folsom Archaeological Record: A Multi-Scalar Approach. *American Antiquity* 73:464-490.

Bamforth, Douglas B.
1986 Technological Efficiency and Tool Curation. *American Antiquity* 51: 38-50.

2002 High Tech Foragers? Folsom and Later Paleoindian Technology on the Great Plains. *Journal of World Prehistory* 16:55-98.

2006 The Windy Ridge Quartzite Quarry: Hunter-Gatherer Mining and Hunter-Gatherer Land Use on the North American Continental Divide. *World Archaeology* 38:511-527.

Beck, Charlotte and George T. Jones
2011 The Role of Mobility and Exchange in the Conveyance of Toolstone During the Great Basin Paleoarchaic. In *Perspectives on Prehistoric Trade and Exchange in California and the Great Basin*, edited by Richard E. Hughes, pp. 55-82. University of Utah Press, Salt Lake City.

Benedict, Audrey DeLella
2013 *A Sierra Club Naturalist's Guide: The Southern Rockies.* Sierra Club Books, San Francisco.

Benedict, James B.
1981 *The Fourth of July Valley: Glacial Geology and Archaeology of the Timberline Ecotone.* Research Report No. 2, Center for Mountain Archaeology, Ward.

1992a Footprints in the Snow: High-Altitude Cultural Ecology of the Colorado Front Range, U.S.A. *Arctic and Alpine Research* 24:1-16.

1992b Along the Great Divide: Paleoindian Archaeology of the High Colorado Front Range. In *Ice Age Hunters of the Rockies,* edited by Dennis Stanford and Jane S. Day, pp. 343-360. Denver Museum of Natural History and University Press of Colorado, Niwot.

Black, Kevin D.
1983 Shelter and Subsistence at 5GN344, a High Altitude Short-Term Camp near Almont, Colorado. *Southwestern Lore.* 49:26-33.

1991 Archaic Continuity in the Colorado Rockies: The Mountain Tradition. *Plains Anthropologist.* 36:1-29.

2000 Lithic Sources in the Rocky Mountains of Colorado. In *Intermountain Archaeology,* edited by David B. Madsen and Michael D. Metcalf, pp. 132-141. University of Utah Archaeological Papers Number 122, Salt Lake City.

Blatt, Harvey and John M. Christie
1963 Undulatory Extinction in Quartz of Igneous and Metamorphic Rocks and its Significance in Provenance Studies of Sedimentary Rocks. *Journal of Sedimentary Petrology* 33:559-579.

Brunswig, Robert H., Jr.
1992 Paleoindian Environments and Paleoclimates in The High Plains and Central Rocky Mountains. *Southwestern Lore* 58:5-23.

Buckles, William G.
1962 5GN1 Archaeological Survey Sheet. *University of Colorado*. Manuscript on file, Colorado Historical Society, Denver.

Cackler, Paul R., Michael D. Glascock, Hector Neff, Harry Iceland, K. Anne Pyburn, Dale Hudler, Thomas R. Hester, and Beverly M. Chiarulli
1999 Chipped Stone Artefacts, Source Areas, and Provenance Studies of the Northern Belize Chert-bearing Zone. *Journal of Archaeological Science* 26:389-397.

Carozzi, A.V.
1993 *Sedimentary Petrography*. PTR Prentice Hall, Englewood Cliffs.

Cassells, E. Steve
1983 *The Archaeology of Colorado.* Johnson Books, Boulder.

Church, Tim
1994 Ogalalla Orthoquartzite: An Updated Description. *The Plains Anthropologist.*39:53- 62.

1996 Lithic Resources of the Bearlodge Mountains, Wyoming: Description, Distribution and Implications. *Plains Anthropologist* 41:135-164.

Cooper, Judith R.
2006 A possible Clovis-age quartzite workshop (5GN149) in Gunnison County, Colorado. *Current Research in the Pleistocene.* 23:85-88.

Cooper Judith R. and Meltzer David J.
2009 Investigations at 5GN149, a lithic workshop in the Upper Gunnison Basin, Colorado. *Southwestern Lore*. 75:3–29.

Crabtree, Don E.
1967 Notes on Experiments in Flint knapping: The Flintknapper's Raw Materials. Tebiwa. 10.

Cullers, Robert L.
1995 The controls on the major-and trace-element evolution of shales, siltstones and sandstones of Ordovician to Tertiary age in the Wet Mountains region, Colorado, U.S.A. *Chemical Geology* 123:107-131.

2000 The Geochemistry of shales, siltstones and sandstones of Pennsylvanian-Permian age, Colorado, USA: implications for provenance and metamorphic studies. *Lithos* 51:181-203.

Dalpra, Cody
2015 *The Distribution of Quartzite Toolstone Throughout Prehistory and Across the Landscape, Upper Gunnison Basin, Colorado.* Poster presented at the 73rd Annual Plains Anthropological Conference, Iowa City, Iowa.

Dalpra, Cody L., and Bonnie L. Pitblado
2016 Discriminating Quartzite Sources Petrographically in the Upper Gunnison Basin, Colorado: Implications for Paleoamerican Lithic-Procurement Studies. *PaleoAmerica*.

Dapples, E.C., W.C. Krumbein, and L.L. Sloss
1953 Petrographic and Lithologic Attributes of Sandstones. *The Journal of Geology* 21:291-317.

Dehler, Carol
2012 *Personal Communication,* Logan, Utah.

DeWitt, E., Stoneman, R.J., Clark, R.
1985 *Mineral Resource Potential Map of the Fossil Ridge Wilderness Study Area, Gunnison County, Colorado*, Map MF-1629-A.

Dickinson William R.
1970 Interpreting Detrital Modes of Graywacke and Arkose. *Journal of Sedimentary Petrology* 40:695-707.

1985 Interpreting Provenance Relation from Detrital Modes of Sandstones. In *Provenance of Arenites: NATO ASI Series.* Edited by Gian Gaspare Zuffa, pp. 333-363. D.Reidel Publishing Company, Dordrecht.

Dickinson, William R. and Christopher A. Suczek
1979 Plate Tectonics and Sandstone Compositions. *American Association of Petroleum Geologist* 63:2164-2182.

Dott, R. H., Jr.
1964 Wacke, Greywacke and Matrix—What Approach to Immature Sandstone Classification? *Journal of Sedimentary Petrology.* 34:625-632.

Dunteman, George H.
1989 Principal Components Analysis- *Series: Quantitative Applications in the Social Sciences.* Sage Publications, Beverly Hills.

Ebright, Carol A.
1987 Quartzite Petrography and its Implications for Prehistoric Use and Archaeological Analysis. *Archaeology of Eastern North America.* 15:29-45.

Eerkens, J. W. and J. S. Rosenthal
2004 Are Obsidian Subsources Meaningful Units of Analysis?: Temporal and Spatial Patterning of Subsources in the Coso Volcanic Field, Southeastern California. *Journal of Archaeological Science* 31:21-29.

English, Joseph M. and Stephan T. Johnston
2004 The Laramide Orogeny: What Were the Driving Forces? *International Geology Review* 46: 833-838.

Epis, Rudy C. and Charles E. Chapin
1975 Geomorphic and Tectonic Implications of the Post-Laramide, Late Eocene Erosion Surface in the Southern Mountains. *Geological Society of America Memoir* 144:45-74.

Euler, R. T., Mark Stiger
1981 *1978 Test Excavations at Five Archaeological Sites in Curecanti National Recreation Area, Intermountain, Colorado*. Boulder, CO: University of Colorado Bureau of Applied Anthropological Research.

Fitzpatrick, Scott M., William R. Dickinson, and Geoffrey Clark
2003 Ceramic Petrography and Cultural Interaction in Palau, Micronesia. *Journal of Archaeological Science* 30:1175-1184.

Frison, George C., Gary A. Wright, James B. Griffin, and Adon A. Gordus
1968 Neutron Activation Analysis of Obsidian: An Example of its Relevance to Northwestern Plains Archaeology. *Plains Anthropologist* 13:209-217.

Gaskill, D.L.
1977 *Chapter 1: Geology of the West Elk Wilderness and vicinity, Delta and Gunnison counties, Colorado*. USGS Open File Report 77-751: 4-31.

Gaskill, D.L., S.M. Colman, J.E. DeLong, Jr., C.H. Robinson
1986 *Geologic Map of the Crested Butte Quadrangle, Gunnison, Colorado*, Map GQ-1580, 1:24,000.

Gaskill, D.L., J.E. DeLong, Jr., D.M. Cochran
1987 *Geologic Map of the Mount Axtell Quadrangle, Gunnison, Colorado*, Map GQ-1604, 1:24,000.

Glascock, M. D., G. E. Braswell and R. H. Cobean
1998 A Systematic Approach to Obsidian Source Characterization. In *Archaeological Obsidian Studies: Method and Theory*. Edited by M. S. Shackley, pp. 15-65. Plenum Press, New York.

Glascock, M. D. and H. Neff
2003 Neutron Activation Analysis and Provenance Research in Archaeology. *Measurement Science and Technology* 14:1516-1526.

Glascock, M. D., H. Neff and K. J. Vaughan
2004 Instrumental Neutron Activation Analysis and Multivariate Statistics for Pottery Provenance. *Hyperfine Interactions* 154:95-104.

Goldstein, August
1948 Cementation of Dakota Sandstones of the Colorado Front Range. *Journal of Sedimentary Petrology* 18:108-125.

Golonka, J. and D. Ford
2000 Pangean (Late Carnoniferous-Middle Jurassic paleoenvironment and lithofacies. *Palaeogeography, Palaeoclimatology, Palaeoecology* 161:1-34.

Goodyear, A.C.
1989 A Hypothesis for the Use of Cryptocrystalline Raw Materials among Paleoindian Groups of North America. In *Eastern Paleoindian Resource Use*, ed. by C. Ellis and J. Lothrop, pp. 1-10. Westview Press, Boulder.

Graham Stephan A., William R. Dickinson, and Raymond V. Ingersoll
1974 Himalayan-Bengal Model for Flysch Dispersal in Appalachian-Ouachita system. *Geological Society of America Bulletin* 86:273-286.

Healy, Paul F., Heather I McKillop, and Bernie Walsh
1984 Analysis of Obsidian from Moho Cay, Belize: New Evidence on Classic Maya Trade Routes. *Science* 225:414-417.

Herz, Norman and Ervan G. Garrison
1998 *Geological Methods for Archaeology.* Oxford University Press, Oxford.

Hedlund, D. C., and J. C. Olson
1974 *Geologic Map of the Iris NW Quadrangle, Gunnison and Saguache Counties, Colorado,* Map GQ-1134, 1:24,000 scale.

1981 Precambrian Geology Along Parts of the Gunnison Uplift of Southwestern Colorado. In *New Mexico Geological Society Guidebook, 32 Field Conference, Western Slope Colorado,* edited by Rudy C. Epis and Jonathan F. Callender, pp. 267-277. New Mexico Geological Society, Las Cruces.

Heidke, James M. and Elizabeth J. Miksa
2000 Correspondence and Discriminant Analyses of Sand and Sand Temper Compositions, Tonto Basin, Arizona. *Archaeometry* 42:273-299.

Hoard, Robert J., Steven R. Holen, Michael D. Glascock, Hector Neff, and J. Michael Elam
1992 Neutron Activation Analysis of Stone From Chadron Formation and a Clovis Site on the Great Plains. *Journal of Archaeological Science* 19:655-665.

Hofman, Jack L., Lawence C. Todd, and Michael B. Collins
1991 Identification of Central Texas Edwards Chert at the Folsom and Lindenmeier Sites. *Plains Anthropologist* 36:297-308.

Holen, Steven R., and Kathleen Holen
2013 The mammoth Steppe Hypothesis: The Middle Wisconsin (Oxygen Isotope Stage 3) Peopling of North America. In *Paleoamerican Odyssey,* edited by Kelly E. Graf, Caroline V. Ketron, and Michael R. Waters, pp. 429-444. Center for the Study of the First Americans, Texas A&M University, College Station.

Howard, Jeffrey L.
2005 The Quartzite Problem Revisited. *The Journal of Geology.* 113(6):707-713.

Hughes, Richard E., and Robert L. Smith
1993 Archaeology, Geology, and Geochemistry in Obsidian Provenance Studies. In *Effects of Scale on Archaeological and Geoscientific Perspectives,* edited by J. K. Stein and A.R. Linse, pp. 79-91. Geological Society of America Special Paper 283, Boulder.

Hughes, Richard E.
1998 On Reliability, Validity, and Scale in Obsidian Sourcing Research. In *Unit Issues in Archaeology: Measuring Time, Space, and Material* edited by A. F. Ramenofsky and A. Steffen, pp. 103-114. University of Utah Press, Salt Lake City.

2011 *Perspectives on Prehistoric Trade and Exchange in California and the Great Basin*. University of Utah Press, Salt Lake City.

Huckell, Bruce B., J. David Kilby, Matthew T. Boulanger, Michael D. Glascock
2011 Sentinel Butte: neutron activation analysis of White River Group chert from a primary source and artifacts from a Clovis cache in North Dakota, USA. *Journal of Archaeological Science* 38:965-976.

Ingersoll, Raymond V., Tom F. Bulard, Richard L. Ford, J.P. Grimm, J.P. Pickle, and S.W. Sares
1984 The Effect of Grain Size on Detrital Modes: A Test of the Gazzi-Dickinson Point Counting Method. *Journal of Sedimentary Petrology* 54:103-116.

Jodry Margret
1999 Folsom Technological and Socioeconomic Strategies: Views from Stewart's Cattle Guard and the Upper Rio Grande Basin, Colorado. Unpublished PhD dissertation, Department of Anthropology. American University, Washington, DC.

Jodry Margret and Dennis Stanford
1992 Stewart's Cattle Guard Site: An Analysis of Bison Remains in a Folsom Kill-Butchery Campsite. In *Ice Age Hunters of the Rockies,* edited by Dennis Stanford and Jane Day, pp. 101-168. Denver Museum of Natural History and University Press of Colorado, Niwot, Co.

1996 Changing Hydrological Regimes and Prehistoric Landscape Use in the Northern San Luis Valley, Colorado. In *Hydrogeology of the San Luis Valley and environmental issues downstream from the Summittville Mine, South-Central Colorado,* pp. 1–11. Geologic excursions to the Rocky Mountains and beyond, Field trip guidebook for the 1996 Annual Meeting Geological Society of America, Denver, Special Publication 44. Denver: Colorado Geological Survey, Department of Natural Resources.

Jodry, Margret, Mort D. Turner, V. Spero, J. C. Turner, and Dennis Stanford
1996 Folsom in the Colorado High Country. *Current Research in the Pleistocene* 13:25-27.

Jones, George T., Charlotte Beck, Eric E. Jones, and Richard E. Hughes
2003 Lithic Resource Use and Paleoarchaic Foraging Territories in the Great Basin. *American Antiquity* 68:5-38.

Jones, George T., Lisa M. Fontes, Rachael A. Horowitz, Charlotte Beck, and David G. Bailey
2012 Reconsidering Paleoarchaic Mobility in the Central Great Basin. *American Antiquity* 77:351-367.

Jorge, Ana, Maria Isabel Dias, and Peter M. Day
2013 Plain Pottery and Social Landscapes: Reinterpreting the Significance of Ceramic Provenance in the Neolithic. *Archaeometry 55*:825-851.

Kelly, Robert L.
1992 Mobility/Sedentism: Concepts, Archaeological Measures and Effects. *Annual Review of Anthropology* 21:43-66.

1995 *The Foraging Spectrum: Diversity in Hunter-Gather Lifeways,* pp. 65-160. Smithsonian Institution Press, Washington D.C.

King, Robert J. and D. F. Merriam
1969 Origin of the "Welded Chert", Morrison Formation (Jurassic), Colorado. *Geological Society of America Bulletin.* 80: 1141-1148.

Kelly, Robert L. and Lawrence C. Todd
1988 Coming into the Country: Early Paleoindian Hunting and Mobility. *American Antiquity* 53: 231-244.

Klecka, William R.
1980 *Discriminant Analysis-Series: Quantitative Applications in the Social Sciences.* Sage Publications, Beverly Hills.

Kornfeld, Marcel
2013 *The First Mountaineers: Coloradans before Colorado.* University of Utah Press, Salt Lake City.

Kornfeld, Marcel, George C. Frison, and Mary Lou Larson
2010 *Prehistoric Hunter-Gathers of the High Plains and Rockies, Third Edition.* Left Hand Press, Walnut Creek.

Kroll, Herbert, Ilse Schmiemann, and Gisela von Cölln
1986 Feldspar solid solutions. *American Mineralogist.* 71:1-16.

Lamphere, M.A.
1988 High-resolution 40Ar/39Ar chronology of Oligocene volcanic rocks, San Juan Mountains, Colorado. *Geochemica et Cosmochinica Acta*. 52:1425-1434.

Larsen Jr., Esper S. and Whitman Cross
1956 Geology and Petrology of the San Juan Region Southwestern Colorado. *Geological Survey Professional Paper 258,* Department of the Interior, U.S. Government Printing Office, Washington D.C.

Lister, G.S. and B.E. Hobbs
1980 The Simulation of Fabric Development During Plastic Deformation and its Application to Quartzite: The Influence of Deformation History. *Journal of Structural Geology* 2:355-370.

Liestman, Terri
1985 Biface Technology at Curecanti: A Study of the Acquisition of Raw Materials and the Production of Lithic Tools. *Midwest Archaeological Center Report, National Park Service,* Lincoln, Nebraska. Manuscript on file, Anthropology Program, University of Oklahoma, Norman, Oklahoma.

Lipe, William D. and Bonnie L. Pitblado
1999 Paleoindian and Archaic periods. In *Colorado Prehistory: a Context for the Southern Colorado River Basin*, edited by William D. Lipe, M. D.Varien R. H. Wilshusen, Colorado Council of Professional Archaeologists, Denver pp. 95-131.

Livaccari, Richard F.
1991 Role of crustal thickening and extensional collapse in the tectonic evolution of the sevier-Laramide orogeny, western United States. *Geology* 19:1104-1107.

Luedtke, Barbra E.
1978 Chert Sources and Trace-Element Analysis. *American Antiquity* 43:413-423.

1979 The Identification of Sources of Chert Artifacts. *American Antiquity* 44:744-756.

MacKenzie, David B.
1975 Tidal sand flat deposits in Lower Cretaceous Dakota Group near Denver, Colorado. In *Tidal Deposits: A Casebook of Recent Examples and Fossil Counterparts*, edited by Robert N. Ginsburg, pp. 117-125. Springer-Verlag, Berlin and Heidelberg.

Meltzer, David J.
2006 *Folsom: New Archaeological Investigations of a Classic Paleoindian Bison Kill.* University of California Press.

Metcalf, Michael D. and Jim Moses
2012 Building an Archaeological Business. In *Archaeology in Society: Its Relevance in the Modern World*, edited by Marcy Rockman and Joe Flatman, pp. 89-96. Springer, New York.

Miksa, Elizabeth J. and James M. Heidke
2001 It All Comes Out in the Wash: Actualistic Petrofacies Modeling of Temper Provenance, Tonto Basin, Arizona. *Geoarchaeology* 16:177-222.

Miller, D. Shane, Vance T. Holliday, and Jordon Bright
2013 Clovis across the Continent. In *Paleoamerican Odyssey,* edited by Kelly E. Graf, Caroline V. Ketron, and Michael R. Waters, pp. 207-220. Center for the Study of the First Americans, Texas A&M University, College Station.

Mutel, Cornelia Fleischer and John C. Emerick
1992 *From Grassland to Glacier: The Natural History of Colorado.* Johnson Books, Boulder, CO.

Neff, Hector
1998 Units in Chemistry-Based Ceramics Provenance. In *Unit Issues in Archaeology: Measuring Time, Space, and Material*, edited by A. F. Ramenofsky and A. Steffen, pp. 115-128. University of Utah Press, Salt Lake City.

2010 LA-ICP-MS Analysis of Quartzite from the Gunnison Basin, Colorado. Manuscript on file, Anthropology Program, University of Oklahoma, Norman, Oklahoma.

Odell, George H.
2000 Stone Tool Research at the End of the Millennium: Procurement and Technology. *Journal of Archaeological Research* 8:269-331.

Peart, Jonathan M.
2013 Late Prehistoric Technology, Quartzite Procurement, and Land Use in the Upper Gunnison Basin, Colorado: View from site 5GN1.2. Unpublished MS thesis, Department of Anthropology, Utah State University, Logan.

Pettijohn, F. Francis John, Paul Edwin Potter, and Raymond Siever
1987 *Sand and Sandstone,* 2nd ed. Springer-Verlag, New York.

Pitblado, Bonnie L.
2002 The Chance Gulch Late Paleoindian Site, Gunnison Basin, Colorado. *Current Research in the Pleistocene* 19:74-76.

2003 *Late Paleoindian Occupation of the Southern Rocky Mountains*. University Press of Colorado, Niwot.

2016 Paleoindian Archaeology of the Upper Gunnison Basin, Colorado Rocky Mountains. *North American Archaeologist* 37:20-60.

Pitblado, Bonnie and Carol Dehler
2006 Petrographic , ICP-MS, and LA-ICP-MS Sourcing of Quartzite Sources, Gunnison Basin, Colorado. NSF Grant. Manuscript on file, Anthropology Program, Utah State University, Logan, Utah.

Pitblado, Bonnie, Carol Dehler, Hector Neff and Stephen T. Nelson
2008 Pilot Study Experiments Sourcing Quartzite, Gunnison Basin, Colorado. *Geoarchaeology.* 23:742-778.

Pitblado, Bonnie, Molly Boeka Cannon, Hector Neff, Carol M. Dehler, and Stephan T. Nelson
2013 LA-ICP-MS Analysis of Quartzite from the Upper Gunnison Basin, Colorado. *Journal of Archaeological Science*.

Porat, Naomi, Joseph Yellin, and Lisa Heller-Kallai
1991 Correlation Between Petrography, NAA, and ICP Analyses: Application to Early Bronze Egyptian Pottery from Canaan. *Geoarchaeology* 6:133-149.

Powers, M.C.
1953 A New Roundness Scale for Sedimentary Particles. *Journal of Sedimentary Petrology.* 23:117-119.

Prather, Thomas
1982 *Geology of the Gunnison Country.* B & B Printers. Gunnison.

Rath, Michael M., Peter Raase, and Jurgen Reinhardt
2012 *Guide to Thin Section Microscopy.* Rath, Raase, and Reinhardt. Ebook, www.minsocam.org/msa/openaccess_publications.html.

Reed, Lori Stephens
2001 Aztec Ruins Ceramic Provenance and Raw Materials Study. Final Report for Western National Parks Association Grant 10-01. Manuscript on file, PaleoResearch Institute, Golden, Colorado.

Reed, Alan D., and Michael D. Metcalf
1999 *Colorado Prehistory: A Context for the Northern Colorado River Basin.* Colorado Council of Professional Archaeologists, Denver.

Riederer, J.
2004 Thin Section Microscopy Applied to the Study of Archaeological Ceramics. *Hyperfine Interactions.* 154:143-158.

Riley, N. Allen
1947 Structural Petrology of the Baraboo Quartzite. *The Journal of Geology.* 55:453-475.

Roll, Tom E., Michael P. Neeley, Robert J. Speakman, and Michael D. Glascock.
2005 Characterization of Montana Cherts by LA-ICP-MS. In *Laser Ablation ICP-MS in Archaeological Research*, edited by Robert J. Speakman and Hector Neff, pp. 59-79. University of New Mexico Press, Albuquerque.

Sahlen, Daniel
2013 Selected with Care?-The Technology of Crucibles in Late Prehistoric Scotland. A Petrographic and Chemical Assessment. *Journal of Archaeological Science.* 40:4207-4221.

Scholle, Peter A.
1979 *A Color Illustrated Guide to Constituents, Textures, Cements, and Porosities of Sandstones and Associated Rocks*. American Association of Petroleum Geologists Memoir 28 Tulsa.

Shackley, M. Steven
1995 Sources of Archaeological Obsidian in the Greater American Southwest: An Update and Quantitative Analysis. *American Antiquity* 60:531-551.

1998 *Archaeological Obsidian Studies: Method and Theory.* Springer, New York.

Simmons, George C.
1957 Contact of Burrow Canyon Formation with Dakota, Slickrock District, Colorado and Correlation of Burro Canyon Formation. *Bulletin of the American Association of Petroleum Geologists* 41:2519-2529.

Smith, Geoffrey M.
2010 Footprints Across the Black Rock: Temporal Variability in Prehistoric Foraging Territories and Toolstone Procurement Strategies in the Western Great Basin. *American Antiquity* 75:865-885.

Speakman, Robert J., Hector Neff, Michael D. Glasscock, and Barry J. Higgins
2002 Characterization of Archaeological Materials by Laser Ablation-Inductively Coupled Plasma-Mass Spectrometry. In *Archaeological Chemistry: Materials, Methods, and Meaning*, edited by Kathryn A. Jakes, American Chemical Society, Washington, D.C.

Speer, Charles A.
2014a Experimental Sourcing of Edwards Plaeau Chert Using LA-ICP-MS. *Quaternary International* 342:199-213.

2014b LA-ICP-MS Analysis of Colvis Period projectile Points from the Gault Site. *Journal of Archaeological Science* 52: 1-11.

Stamm, John F., Bonnie L. Pitblado, and Beth Ann Camp.
2004 The geology and soils of the Chance Gulch archaeological site near Gunnison, Colorado. *The Mountain Geologist* 41:63-74.

Stiger, Mark
2001 *Hunter-Gatherer Archaeology of the Colorado High Country*. University Press of Colorado, Niwot.
2006 A Folsom Structure in the Colorado Mountains. *American Antiquity* 71:321-351.

Streufert, R.K.
1999 *Geology and mineral resources of Gunnison county, Colorado*. Colorado Geological Survey, Resource Series 37, 1:150,000-scale map, 76 pp.

Stross, Fred H., Thomas R. Hester, Robert F. Heizer and Robert N. Jack
1976 Chemical and Archaeological Studies of Mesoamerican Obsidians. In *Advances in Obsidian Glass Studies*, edited by R.E. Taylor, Noyes Press, Park Ridge.

Stross, Fred H., Richard L. Hay, Frank Asaro, H. R. Bowman, H. V. Michel
1988 Sources of the Quartzite of Some Ancient Egyptian Sculptures. *Archaeometry* 30:109-119.

Surovell, Todd A., and Nicole M. Waguespack
2007 Folsom Hearth-Centered Use of Space at Barger Gulch, Locality B. In *Frontiers in Colorado Paleoindian Archaeology*, edited by Robert H. Brunswig and Bonnie L. Pitblado, pp. 219-260. University of Colorado Press, Boulder.

Surovell, Todd A., Nicole M. Waguespack, James H. Mayer, Marcel Kornfeld, and George C. Frison
2005 Shallow Site Archaeology: Artifact Dispersal, Stratigraphy, and Radiocarbon Dating at the Barger Gulch Locality B Folsom Site, Middle Park, Colorado. *Geoarchaeology* 20:627-649.

Tucker, Maurice E.
2001 *Sedimentary Petrology: An Introduction to the Origin of Sedimentary Petrology.* Blackwell Publishing, Malden.

Tweto, Ogden
1987 *Rock units of the Precambrian Basement in Colorado*. USGS Professional Paper 1321-A, 54 pp.

Vale, T. R.
1995 Mountains and Moisture in the West. In *The Mountainous West: Explorations in Historical Geography,* edited by William Wyckoff and Lary Dilsaver, pp. 141-165. University of Nebraska Press, Lincoln.

Weigand P. C., G. Harbottle and E. V. Sayre
1977 Turquoise sources and source analysis: Mesoamerica and the Southwestern USA. In *Exchange Systems in Prehistory,* edited by T. K. Earle and J. E. Eriscon, Academic Press, New York.

Wentworth, Chester K.
1922 A Scale of Grade and Class Terms for Clastic Sediments. *The Journal of Geology* 30:377-392.

Wyckoff, William, and Lary Dilsaver
1995 *The Mountainous West: Explorations in Historical Geography.* University of Nebraska Press, Lincoln.

Zech, R.S.
1988 *Geologic Map of the Fossil Ridge Area, Gunnison County, Colorado,* Map I-1883, 1:24,000.

Appendix A: Additional Tables

Table 12. Master Basin-Wide Study Petrographic Data.

Sample No.	Petrographic Group	Geologic Formation	QMU	QMN	Wx Feldspar	Wx VRF	Matrix	QPS	QPC	Cement (overgrowths, silica)	Chalcedony	Calcite	SRF (chert)	Biotite	Iron	Chlorite	Sericite	Total
CD08-3G	1	Cobbles (Tg)	61	6	1	3	0	0	2	1	26	0	0	0	0	0	0	100
CD08-3I	1	Cobbles (Tg)	65	2	0	8	0	1	2	1	21	0	0	0	0	0	0	100
CD08-4A	1	Cobbles (Tg)	55	3	5	5	0	1	2	0	29	0	0	0	0	0	0	100
MP09-1H	1	Cobbles (Tg)	63	1	3	0	0	1	1	9	20	0	0	0	2	0	0	100
SC09-1E	1	Cobbles (Tg)	73	0	2	0	0	0	0	2	0	22	0	0	1	0	0	100
SC09-18B	1	Cobbles (Tg)	60	1	5	5	2	0	4	5	16	0	0	1	1	0	0	100
SC09-18 Spot1	1	Cobbles (Tg)	65	0	4	1	0	1	2	4	13	0	0	0	8	0	0	98
SC09-22H	1	Cobbles (Tg)	56	2	12	18	0	1	1	2	0	6	0	1	0	0	0	99
SC08-4C	1	Cobbles (Qg)	59	2	6	2	0	2	4	0	0	0	0	22	3	0	0	100
SGN852-1B	1	Cobbles (Tg)	69	0	10	7	0	1	2	0	0	4	0	7	0	0	0	100
CD09-2D	2	Cobbles (Qg)	47	0	0	0	0	3	6	0	0	38	0	0	6	0	0	100
SC09-13F	2	Cobbles (Tg)	46	1	3	2	0	0	1	0	0	16	0	29	2	0	0	100
CD09-4C	3	Kdh Outcrop	73	0	6	3	0	0	2	10	6	0	0	0	0	0	0	100
SC09-10spot3	3	Kdh Outcrop	67	2	3	2	0	1	0	21	0	1	0	0	3	0	0	100
SC09-5 Spot1	3	Kdh Outcrop	70	3	0	6	0	2	2	0	0	16	0	1	0	0	0	100
SC09-6G	3	Kdh Outcrop	74	0	2	11	0	0	0	0	13	0	0	0	0	0	0	100
SGN3510-E	3	Cobbles (Tg)	73	1	0	1	0	0	2	10	0	5	7	1	0	0	0	100
SC09-18 Spot3	3	Cobbles (Tg)	65	0	1	0	0	0	0	0	0	0	0	6	5	14	9	100
SGN2269-A	4	Jj Outcrop	71	2	0	3	0	0	0	24	0	0	0	0	0	0	0	100
SGN850-1I	4	Jj Outcrop	77	7	0	1	1	4	0	11	0	0	0	0	0	0	0	101
SGN850-2B	4	Jj Outcrop	81	2	0	1	0	5	3	8	0	0	0	0	0	0	0	100
SGN850-4H	4	Ja Outcrop	88	0	5	1	0	0	1	3	0	2	0	0	0	0	0	100
BF09-4G	4	Cobble (Qg?)	77	5	0	0	1	2	0	14	0	0	1	0	0	0	0	100

BP09-8D	4	Cobble (Qa)	76	6	5	0	0	0	1	10	0	0	2	0	0	0	0	100
SC09-10spot5	4	Cobble (Qa)	69	1	0	0	0	0	1	26	0	0	0	0	3	0	0	100
SC09-11C	4	Cobbles (Tg)	73	3	1	0	0	0	1	21	0	0	0	1	0	0	0	100
SC09-12B	4	Cobbles (Tg)	84	0	2	0	0	0	1	13	0	0	0	0	0	0	0	100
SC09-13D	4	Jj Outcrop	67	3	2	1	0	2	3	22	0	0	0	0	0	0	0	100
5GN3510-	4															0	0	
F(BF09-3F)		Jj Outcrop	83	1	0	0	0	3	1	11	1	0	0	0	0			100
SC09-23A	4	Jj Outcrop	80	2	5	1	0	0	0	11	0	0	0	1	0	0	0	100
SC09-23F	4	Jj Outcrop	70	3	4	0	22	0	0	2	0	0	0	0	0	0	0	101
SC09-26C	4	Cobble (Qa)	72	1	0	4	0	1	3	19	0	0	0	0	0	0	0	100
	4	Modern														0	0	
		River																
SC09-6E		Cobbles	70	3	0	0	0	3	0	19	5	0	0	0	0			100
	5	Modern														0	0	
		River																
5GN1982-G		Cobbles	83	1	13	0	0	2	1	0	0	0	0	0	0			100
5GN850-3B	5	Es Outcrop	69	5	9	0	0	1	2	10	4	0	0	0	0	0	0	100
5GN852-1D	5	Es Outcrop	60	4	14	0	0	2	2	18	0	0	0	0	0	0	0	100
BP09-2C	5	Es Outcrop	77	2	13	1	2	0	1	4	0	0	0	0	0	0	0	100
BP09-4G	5	Es Outcrop	77	4	11	0	0	1	0	11	0	0	0	1	0	0	0	105
MP09-1F	5	Jj Outcrop	72	0	10	0	0	0	1	10	0	7	0	0	0	0	0	100
5GN840-F	5	Cobbles (Qf)	73	4	9	4	0	0	1	7	1	0	0	1	0	0	0	100
SC09-10 T3B	5	Cobbles (Qf)	75	4	9	0	0	1	1	8	0	0	0	0	2	0	0	100
SC09-10 T3D	5	pE Outcrop	82	0	9	0	0	1	2	6	0	0	0	0	0	0	0	100
SC09-13A	5	Jj Outcrop	72	1	9	3	0	0	1	11	0	0	0	0	3	0	0	100
SC09-22A	5	Cobbles (Jj)	62	2	10	0	0	0	3	0	0	0	0	23	0	0	0	100
SC09-23I	5	Cobbles (Jj)	73	0	15	4	4	0	0	3	0	0	0	4	0	0	0	103
SC09-23B	5	Tertiary	71	0	8	0	20	0	0	1	0	0	0	0	0	0	0	100

		Cobbles																
	5	Cobbles (Tg)														0	0	
		Green River																
SC09-3B		Formation	67	3	15	0	0	1	0	13	1	0	0	0	0			100
	5	Cobbles (Tg,														0	0	
SC09-3I		Tw)	75	0	12	0	0	0	1	7	5	0	0	0	0			100
SC09-8I	5	Jj Outcrop	80	0	13	0	0	3	1	0	0	2	0	1	0	0	0	100
	6	Cobbles (Qt,	Lime-															
SC09-24H		Qdf)	stone															

Table 13. Results of Basin-Wide Study K-means cluster analysis (excludes non-quartzite group 6).

Petrographic Group	Sample No.	Distance to Cluster Centroid
1	CD09-3G	5.040
1	CD09-3I	6.029
1	CD09-4A	10.326
1	MP09-1H	4.191
1	SC09-1E	6.590
1	SC09-4C	2.590
1	SC09-18B	.854
1	SC09-18 Spot1	4.221
1	SC09-22H	10.463
1	5GN852-1B	10.455
2	CD09-2D	4.950
2	SC09-13F	4.950
3	CD09-4C	5.281
3	SSC09-5 Spot1	7.476
3	SC09-6G	.816
3	SC09-10spot3	5.555
3	SC09-18 Spot3	6.043
3	5GN3510-E	4.399
4	BF09-4G	3.176
4	BP09-8D	5.546
4	SC09-6E	4.508
4	SC09-10spot5	2.903
4	SC09-11C	1.406
4	SC09-12B	2.344
4	SC09-13D	.923
4	SC09-23A	5.655
4	SC09-23F	4.105
4	SC09-26C	3.822
4	5GN2269-A	2.817
4	5GN3510-F(BF09-3F)	3.236
4	5GN850-1I	3.236
4	5GN850-2B	3.267
4	5GN850-4H	5.777

Petrographic Group	Sample No.	Distance to Cluster Centroid
5	BP09-2C	1.782
5	BP09-4G	2.591
5	MP09-1F	6.941
5	SC09-3B	6.509
5	SC09-3I	2.831
5	SC09-8I	3.364
5	SC09-10 T3B	4.027
5	SC09-10 T3D	6.509
5	SC09-13A	5.436
5	SC09-22A	3.010
5	SC09-23I	11.326
5	SC09-23B	5.806
5	5GN1982-G	3.005
5	5GN840-F	5.244
5	5GN850-3B	5.392
5	5GN852-1D	5.524

Table 14. Basin-Wide Study Quartzite Cobble Discriminant Analysis Table.

Sample Number	Actual Group	Predicted Group	Highest Group				Squared Mahalanobis Distance to Centroid	Second Highest Group		Squared Mahalanobis Distance to Centroid	Discriminant Scores				
			P(D>d | G=g)		P(G=g | D=d)			Group	P(G=g | D=d)		FUNC 1	FUNC 2	FUNC 3	FUNC 4	Type
			p	df											
5GN1982-G	5	5	.913	4	1.000		.981	4	.000	64.020	-4.622	-1.496	2.185	-.313	Cobble
5GN2269-A	4	4	.595	4	1.000		2.780	5	0.000	90.391	.725	-7.037	-2.408	.984	Cobble
5GN850-1I	4	4	.638	4	1.000		2.537	5	.000	54.883	-1.444	-5.349	-2.605	.140	Cobble
5GN850-2B	4	4	.461	4	1.000		3.611	5	0.000	87.672	.688	-5.240	-4.162	-.356	Cobble
5GN850-3B	5	5	.494	4	1.000		3.395	4	.000	61.983	-4.987	-1.093	.888	-1.239	Cobble
5GN850-4H	4	4	.080	4	1.000		8.336	5	.000	32.172	-1.988	-4.433	-1.162	.140	Cobble
5GN852-1D	5	5	.782	4	1.000		1.749	1	0.000	81.664	-4.739	-.492	3.199	-1.361	Cobble
BF09-4G	4	4	.459	4	1.000		3.628	5	0.000	102.062	1.633	-6.843	-3.035	-.057	Cobble
BP09-2C	5	5	.993	4	1.000		.239	1	.000	73.709	-4.357	-.589	2.549	-.932	Cobble
BP09-4G	5	5	.483	4	1.000		3.466	1	.000	68.998	-2.971	-.687	3.614	-.040	Cobble
BP09-8D	4	4	.218	4	1.000		5.755	5	.000	69.693	1.612	-5.423	-1.169	-1.041	Cobble
CD09-2D	2	2	.894	4	1.000		1.100	1	0.000	283.127	-2.770	22.015	-2.817	-.683	Cobble
MP09-1H	1	1	.150	4	1.000		6.738	5	.000	78.869	-2.166	7.132	-.920	1.469	Cobble
MP09-1F	5	5	.279	4	1.000		5.086	1	.000	40.785	-2.850	.509	1.513	.598	Cobble
SC09-12B	4	4	.768	4	1.000		1.825	5	0.000	76.727	-.361	-7.125	-2.078	-.350	Cobble
SC09-13F	2	2	.894	4	1.000		1.100	1	0.000	331.127	-2.832	22.741	-3.822	-2.374	Cobble
SC09-13D	4	4	.765	4	1.000		1.840	5	.000	61.757	-.122	-5.316	-2.396	-1.233	Cobble
5GN3510-F (BF09-3F)	4	4	.787	4	1.000		1.719	5	0.000	90.683	.027	-6.715	-3.563	.327	Cobble
5GN840-F	5	5	.140	4	1.000		6.916	4	.000	45.591	-4.766	-2.348	.545	.165	Cobble
SC09-13A	5	5	.664	4	1.000		2.393	1	.000	66.861	-4.250	.154	1.553	-1.606	Cobble
SC09-22H	1	1	.062	4	1.000		8.982	5	0.000	116.031	-1.812	7.283	.519	6.150	Cobble
SC09-22A	5	5	.943	4	1.000		.767	1	.000	57.486	-4.338	.144	2.433	-.116	Cobble
SC09-3B	5	5	.198	4	1.000		6.013	1	0.000	95.847	-6.236	-1.284	3.543	-.236	Cobble

SC09-3I	5	5	.824	4	1.000	1.517	1	.000	50.932	-3.741	.226	2.250	.229	Cobble
SC09-6E	4	4	.818	4	1.000	1.551	5	.000	73.909	-.635	-6.095	-3.066	.870	Cobble
SC09-6G	3	3	.995	4	1.000	.199	4	0.000	1066.108	31.332	2.121	1.894	-.375	Cobble
5GN3510-E	3	3	.995	4	1.000	.199	4	0.000	1018.108	30.644	2.053	1.396	-.108	Cobble
5GN852-1B	1	1	.120	4	1.000	7.309	5	.000	35.558	-1.775	3.683	1.444	2.683	Cobble
SC09-8I	5	5	.371	4	1.000	4.270	1	.000	77.413	-2.901	-.496	3.677	-1.335	Cobble

u. Unselected case

**. Misclassified case

Table 15. Basin-Wide Study Quartzite Outcrop Discriminant Analysis Table.

Sample Number	Actual Group	Predicted Group	Highest Group P(D>d | G=g) p	df	P(G=g | D=d)	Squared Mahalanobis Distance to Centroid	Second Highest Group	P(G=g | D=d)	Squared Mahalanobis Distance to Centroid	Discriminant Scores Function 1	Function 2	Function 3	Type
CD09-3G	1	1	.473	3	1.000	2.511	3	0.000	175.259	-9.778	-1.170	-1.034	Outcrop
CD09-3I	1	1	.781	3	1.000	1.084	3	0.000	167.619	-9.763	-.668	.368	Outcrop
CD09-4A	1	1	.515	3	1.000	2.288	3	0.000	194.172	-10.632	1.468	-.154	Outcrop
CD09-4C	3	3	.033	3	.999	8.725	4	.001	23.034	1.556	.102	-.618	Outcrop
SC09-1E	1	1	.987	3	1.000	.137	3	0.000	172.629	-9.938	.320	.108	Outcrop
SC09-10spot3	3	3	.292	3	.964	3.734	4	.036	10.330	4.927	-.287	1.474	Outcrop
SC09-10spot5	4	4	.516	3	.997	2.279	3	.003	13.715	4.330	-3.020	.221	Outcrop
SC09-11C	4	4	.274	3	1.000	3.886	3	.000	37.059	6.359	-4.406	-.661	Outcrop
SC09-18B	1	1	.528	3	1.000	2.221	3	0.000	141.824	-8.680	1.009	.262	Outcrop
SC09-10 T3B	5	5	.562	3	1.000	2.053	3	.000	26.166	5.936	3.478	-.539	Outcrop
SC09-10 T3D	5	5	.316	3	1.000	3.534	4	.000	47.999	9.011	3.311	-1.254	Outcrop
SC09-18 Spot1	1	1	.996	3	1.000	.057	3	0.000	175.614	-9.974	.233	-.404	Outcrop
SC09-23I	5	5	.754	3	1.000	1.195	3	.000	34.817	7.239	3.744	.017	Outcrop
SC09-23A	4	4	.575	3	1.000	1.986	3	.000	18.228	5.565	-1.363	-1.261	Outcrop
SC09-23B	5	5	.344	3	.999	3.326	4	.001	16.635	6.811	1.205	-1.096	Outcrop
SC09-23F	4	4	.365	3	1.000	3.176	5	.000	19.557	6.297	-1.306	-1.536	Outcrop
SC09-26C	4	4	.827	3	1.000	.892	3	.000	16.767	4.955	-3.061	-.011	Outcrop
SC09-4C	1	1	.967	3	1.000	.261	3	0.000	178.343	-10.026	.131	-.688	Outcrop
SC09-5 Spot1	3	3	.552	3	1.000	2.101	4	.000	31.773	2.687	.249	3.295	Outcrop

SC09-18 Spot3	3	3	.466	3	1.000	2.553	4	.000	30.079	3.118	.028	3.513	Outcrop

u. Unselected case

**. Misclassified case

Table 16. Basin-Wide Study Quartzite Cobble and Outcrop Discriminant Analysis Table.

Sample Number	Actual Group	Predicted Group	Highest Group P(D>d | G=g) p	df	P(G=g | D=d)	Squared Mahalanobis Distance to Centroid	Second Highest Group	P(G=g | D=d)	Squared Mahalanobis Distance to Centroid	Discriminant Scores Function 1	Function 2	Function 3	Function 4	Type
5GN1982-G	5	5	.939	4	1.000	.798	4	.000	33.970	-1.072	-3.294	-.591	.741	Cobble
5GN2269-A	4	4	.518	4	1.000	3.241	3	.000	39.193	-4.957	2.656	-.217	-1.450	Cobble
5GN850-1I	4	4	.844	4	1.000	1.399	5	.000	36.665	-4.720	1.866	-.638	-1.519	Cobble
5GN850-2B	4	4	.660	4	1.000	2.416	3	.000	28.579	-3.069	2.325	-1.931	-.719	Cobble
5GN850-3B	5	5	.939	4	1.000	.799	4	.000	19.815	-1.639	-2.186	-.652	-.034	Cobble
5GN850-4H	4	4	.447	4	.983	3.705	5	.017	11.849	-2.971	.027	-.249	-.854	Cobble
5GN852-1D	5	5	.487	4	1.000	3.441	4	.000	40.890	-1.071	-3.708	-1.258	1.474	Cobble
BF09-4G	4	4	.976	4	1.000	.469	3	.000	32.393	-4.283	2.084	-1.150	-.813	Cobble
BP09-2C	5	5	.899	4	1.000	1.071	4	.000	30.542	-1.673	-3.315	-.293	.432	Cobble
BP09-4G	5	5	.258	4	1.000	5.302	4	.000	23.365	-3.029	-2.537	.026	1.496	Cobble
BP09-8D	4	4	.210	4	.914	5.855	5	.086	10.592	-2.799	.004	-1.345	.670	Cobble
CD09-2D	2	2	.322	4	1.000	4.674	1	0.000	169.857	16.712	1.091	-1.879	.277	Cobble
CD09-3G	1	1	.856	4	1.000	1.333	3	.000	43.177	3.730	.414	2.325	-2.055	Outcrop
CD09-3I	1	1	.173	4	1.000	6.367	3	.000	43.299	3.948	2.331	2.603	-2.109	Outcrop
CD09-4A	1	1	.080	4	1.000	8.344	5	0.000	82.522	6.781	-.232	2.230	-2.735	Outcrop
CD09-4C	3	5**	.151	4	.962	6.721	4	.024	14.125	-.718	-.075	.063	-.327	Outcrop
MP09-1H	1	1	.407	4	1.000	3.989	3	.000	43.364	4.962	.289	.137	-.388	Cobble
MP09-1F	5	5	.910	4	1.000	1.000	3	.000	24.439	-.154	-2.172	.005	.583	Cobble
SC09-1E	1	1	.949	4	1.000	.719	3	.000	33.807	3.748	.484	1.391	-1.047	Outcrop

SC09-10spot3	3	3	.200	4	.888	5.992	4	.109	10.192	-1.284	1.615	.137	.702	Outcrop
SC09-10spot5	4	4	.187	4	.976	6.167	3	.024	13.555	-3.563	2.692	-.031	1.260	Outcrop
SC09-11C	4	4	.739	4	1.000	1.985	5	.000	37.588	-5.284	1.561	-.949	-1.153	Outcrop
SC09-12B	4	4	.959	4	1.000	.637	5	.000	30.365	-4.690	1.337	-.960	-.891	Cobble
SC09-13F	2	2	.322	4	1.000	4.674	1	0.000	257.857	18.176	1.863	-5.751	1.259	Cobble
SC09-13D	4	4	.906	4	1.000	1.023	5	.000	26.278	-3.811	1.440	-1.831	-.368	Cobble
5GN3510-F(BF09-3F)	4	4	.943	4	1.000	.763	3	.000	32.370	-3.785	2.158	-1.199	-1.263	Cobble
5GN840-F	5	5	.312	4	.995	4.768	4	.005	15.429	-1.859	-1.454	.484	-1.104	Cobble
SC09-18B	1	1	.523	4	1.000	3.210	3	.000	39.194	4.848	.106	.744	.072	Outcrop
SC09-10 T3B	5	5	.613	4	1.000	2.677	4	.000	23.621	-.558	-1.819	-1.603	-.157	Outcrop
SC09-10 T3D	5	5	.557	4	.996	3.006	4	.004	13.877	-2.246	-1.568	-1.107	.379	Outcrop
SC09-18 Spot1	1	1	.847	4	1.000	1.385	5	.000	52.562	4.807	-.281	2.750	-1.630	Outcrop
SC09-13A	5	5	.039	4	.997	10.073	1	.003	22.011	1.434	-.949	-1.492	-.051	Cobble
SC09-22H	1	1	.311	4	1.000	4.776	3	.000	56.334	4.655	-.338	3.898	-1.589	Cobble
SC09-22A	5	5	.092	4	1.000	7.985	1	.000	24.080	.147	-2.387	1.896	-.887	Cobble
SC09-23I	5	5	.287	4	1.000	5.006	3	.000	31.078	-.063	-3.297	1.288	1.359	Outcrop
SC09-23A	4	4	.565	4	.999	2.959	5	.001	17.260	-3.966	.062	-.078	-.973	Outcrop
SC09-23B	5	5	.364	4	.960	4.323	4	.040	10.695	-2.458	-1.137	-.933	.396	Outcrop
SC09-23F	4	4	.732	4	1.000	2.023	5	.000	17.372	-4.031	.191	-.998	-.337	Outcrop
SC09-26C	4	4	.771	4	1.000	1.806	3	.000	30.706	-3.736	2.816	-1.134	-1.064	Outcrop
SC09-3B	5	5	.569	4	1.000	2.931	4	.000	45.114	-.786	-4.196	-.291	.596	Cobble
SC09-3I	5	5	.918	4	1.000	.943	3	.000	31.370	-.282	-2.970	-.077	.771	Cobble
SC09-4C	1	1	.532	4	1.000	3.158	5	.000	33.562	3.982	-.130	.086	-1.221	Outcrop

SC09-5 Spot1	3	3	.597	4	1.000	2.773	1	.000	36.139	.972	2.624	1.850	3.017	Outcrop
SC09-6E	4	4	.897	4	1.000	1.085	3	.000	30.241	-3.440	2.054	-.826	-1.490	Cobble
SC09-6G	3	3	.472	4	1.000	3.541	4	.000	46.702	-.500	2.677	2.056	4.254	Cobble
5GN3510-E	3	3	.573	4	1.000	2.912	4	.000	40.208	-.847	3.217	2.022	3.665	Cobble
5GN852-1B	1	1	.054	4	.956	9.318	5	.044	15.472	2.004	-1.448	1.896	-.112	Cobble
SC09-8I	5	5	.971	4	1.000	.529	4	.000	32.691	-1.066	-3.165	-.478	.684	Cobble
SC09-18 Spot3	3	3	.472	4	1.000	3.541	4	.000	46.702	-.500	2.677	2.056	4.254	Outcrop

u. Unselected case

**. Misclassified case

Table 17. Results of 5GN1 Cobble K-means Cluster Analysis.

Petrographic Group	Sample No.	Distance to Cluster Centroid
3	SC09-6A	1.472
3	SC09-6F	4.427
3	SC09-6H	2.955
2	SC09-6B	1.67
2	SC09-6E	1.67
3	SC09-6C	6.846
1	SC09-6D	3.537
1	SC09-6G	2.449
1	SC09-6I	4.174
1	SC09-6J	4.777

Table 18. Results of 5GN1 Outcrop K-means Cluster Analysis.

Petrographic Group	Sample No.	Distance to Cluster Centroid
1	SC09-7B	0
2	SC09-1A	2.163
2	SC09-1B	1.42
2	SC09-1C	4.949
2	SC09-1D	6.087
2	SC09-1E	3.359
2	SC09-1F	2.619
2	SC09-1G	4.188
2	SC09-7A	0.962

Table 19. Results of 5GN1 K-means Cluster Analysis.

Petrographic Group	Sample No.	Distance to Cluster Centroid
1	SC09-6B	0.388
1	SC09-6E	3.088
1	SC09-7B	2.866
2	SC09-1D	6.716
2	SC09-6C	5.524
2	SC09-6D	4.722
2	SC09-6G	1.248
2	SC09-6I	5.405
2	SC09-6J	5.573
3	SC09-1A	3.235
3	SC09-1B	2.216
3	SC09-1C	3.954
3	SC09-1E	2.728
3	SC09-1F	3.71
3	SC09-1G	3.102
3	SC09-6A	1.343
3	SC09-6F	5.326
3	SC09-6H	2.485
3	SC09-7A	1.785

Table 20. Results of 5GN1 Quartzite Cobble Discriminant Analysis.

Sample Number	Actual Group	Predicted Group	Highest Group				Second Highest Group			Discriminant Scores	
			P(D>d | G=g)	p	df	P(G=g | D=d)	Squared Mahalanobis Distance to Centroid	Group	P(G=g | D=d)	Squared Mahalanobis Distance to Centroid	Function 1	Function 2
SC09-6B	1	1	.910		2	.997	.188	2	.003	13.427	3.973	.363
SC09-6E	1	1	.910		2	1.000	.188	2	.000	19.826	4.794	.087
SC09-6C	2	2	.150		2	.830	3.788	3	.170	5.942	-1.391	-1.055
SC09-6D	2	2	.586		2	.998	1.069	1	.002	11.877	1.118	-.876
SC09-6G	2	2	.816		2	.996	.406	3	.004	10.618	-.250	.031
SC09-6I	2	2	.513		2	.996	1.334	1	.004	10.553	1.310	-.826
SC09-6J	2	2	.114		2	.997	4.337	1	.003	14.207	.963	1.807
SC09-6A	3	3	.907		2	.997	.195	2	.003	12.570	-3.195	-.156
SC09-6F	3	3	.421		2	1.000	1.731	2	.000	24.616	-4.449	1.074
SC09-6H	3	3	.682		2	.987	.765	2	.013	10.460	-2.873	-.448

Squared Mahalanobis distance is based on canonical functions.

Table 21. Results of 5GN1 Quartzite Outcrop Discriminant Analysis.

Sample Number	Actual Group	Predicted Group	Highest Group P(D>d | G=g) p	df	P(G=g | D=d)	Squared Mahalanobis Distance to Centroid	Second Highest Group Group	P(G=g | D=d)	Squared Mahalanobis Distance to Centroid	Discriminant Scores Function 1
SC09-7B	1	1	1.000	1	1.000	.000	2	.000	68.399	7.351
SC09-1A	2	2	.754	1	1.000	.099	1	.000	73.691	-1.233
SC09-1B	2	2	.506	1	1.000	.442	1	.000	57.846	-.254
SC09-1C	2	2	.325	1	1.000	.970	1	.000	85.657	-1.904
SC09-1D	2	2	.066	1	1.000	3.370	1	.000	41.405	.917
SC09-1E	2	2	.173	1	1.000	1.856	1	.000	92.792	-2.281
SC09-1F	2	2	.897	1	1.000	.017	1	.000	70.555	-1.048
SC09-1G	2	2	.861	1	1.000	.031	1	.000	71.326	-1.094
SC09-7A	2	2	.642	1	1.000	.217	1	.000	60.919	-.454

Squared Mahalanobis distance is based on canonical functions.

Table 22. Results of 5GN1 Total Discriminant Analysis.

			Highest Group				Second Highest Group		
			P(D>d | G=g)			Squared Mahalanobis Distance to			Squared Mahalanobis Distance to
Sample Number	Actual Group	Predicted Group	p	df	P(G=g | D=d)	Centroid	Group	P(G=g | D=d)	Centroid
SC09-6B	1	1	.983	2	1.000	.033	2	.000	18.063
SC09-6E	1	1	.713	2	1.000	.676	2	.000	25.463
SC09-7B	1	1	.744	2	.994	.592	2	.006	12.218
SC09-1D	2	3**	.174	2	.632	3.493	2	.368	3.556
SC09-6C	2	2	.205	2	.635	3.167	3	.365	5.293
SC09-6D	2	2	.397	2	.995	1.847	1	.004	11.261
SC09-6G	2	2	.911	2	.996	.187	3	.004	12.174
SC09-6I	2	2	.323	2	.989	2.262	1	.011	9.892
SC09-6J	2	2	.024	2	.975	7.466	1	.025	13.432
SC09-1A	3	3	.446	2	.996	1.617	2	.004	11.855
SC09-1B	3	3	.837	2	.994	.355	2	.006	9.614
SC09-1C	3	3	.575	2	1.000	1.105	2	.000	22.367
SC09-1E	3	3	.570	2	1.000	1.123	2	.000	20.327
SC09-1F	3	3	.407	2	.993	1.798	2	.007	10.815
SC09-1G	3	3	.619	2	1.000	.958	2	.000	19.334
SC09-6A	3	3	.876	2	.997	.265	2	.003	11.184
SC09-6F	3	3	.115	2	1.000	4.320	2	.000	23.713
SC09-6H	3	3	.800	2	.992	.447	2	.008	9.168
SC09-7A	3	3	.893	2	.996	.225	2	.004	10.446

Squared Mahalanobis distance is based on canonical functions.

**. Misclassified case

Table 23. Results of Parlin Flats K-means Cluster Analysis.

Parlin Flats Petrographic Group	Sample No.	Distance to Cluster Centroid
1	CD09-3A	6.362
1	CD09-3B	5.744
1	CD09-3C	3.415
1	CD09-3G	2.052
1	CD09-3I	5.87
1	CD09-4A	4.727
1	CD09-4D	7.577
2	CD09-3D	3.481
2	CD09-3E	0.97
2	CD09-3H	2.399
2	CD09-4B	4.532
3	CD09-3F	2.455
3	SC09-4C	5.544
3	CD09-5A	5.327
3	CD09-5B	3.941

Table 24. Results of Parlin Flats Discriminant Analysis.

Sample Number	Actual Group	Predicted Group	Highest Group P(D>d | G=g) p	df	P(G=g | D=d)	Squared Mahalanobis Distance to Centroid	Second Highest Group Group	P(G=g | D=d)	Squared Mahalanobis Distance to Centroid	Discriminant Scores Function 1	Function 2
CD09-3A	1	1	.354	2	1.000	2.075	2	.000	37.485	4.785	-.300
CD09-3B	1	1	.446	2	.998	1.614	2	.002	13.097	2.261	-.555
CD09-3C	1	1	.714	2	1.000	.674	2	.000	16.967	2.769	-.504
CD09-3G	1	1	.886	2	1.000	.243	2	.000	26.198	3.754	.365
CD09-3I	1	1	.432	2	.998	1.679	2	.002	12.905	2.234	-.558
CD09-4A	1	1	.104	2	1.000	4.530	2	.000	22.596	2.844	2.097
CD09-4D	1	1	.240	2	1.000	2.854	2	.000	40.733	5.045	-.274
CD09-3D	2	2	.595	2	.999	1.039	1	.001	16.445	-.574	-.842
CD09-3E	2	2	.960	2	.990	.082	3	.010	9.234	-1.549	.027
CD09-3H	2	2	.849	2	.998	.327	3	.001	13.598	-.901	.204
CD09-4B	2	2	.611	2	.889	.986	3	.111	5.147	-2.323	-.051
CD09-3F	3	3	.660	2	.997	.832	2	.003	12.286	-4.785	-.792
CD09-4C	3	3	.110	2	.989	4.422	2	.011	13.500	-4.180	2.161
CD09-5A	3	3	.516	2	1.000	1.322	2	.000	18.707	-5.659	-.317
CD09-5B	3	3	.517	2	.910	1.321	2	.090	5.936	-3.722	-.659

Squared Mahalanobis distance is based on canonical functions.

Table 25. Total Project K-means Cluster Analysis. Note this is for 76 of the 77 samples excluding the Crystalline Limestone Outlier.

Petrographic Group	Sample No.	Distance to Cluster Centroid
1	SC09-22H	10.699
1	SC09-4C	2.878
1	5GN852-1B	10.362
1	SC09-1C	4.224
1	SC09-1E	6.3
1	SC09-1G	5.284
1	SC09-6F	4.693
1	CD09-3F	8.742
1	CD09-4B	5.93
1	SC09-4C	2.878
1	CD09-5A	11.612
1	CD09-5B	5.23
2	CD09-2D	4.95
2	SC09-13F	4.95
3	SC09-5 Spot1	2.823
3	5GN3510-E	5.811
3	SC09-1A	2.805
3	SC09-1B	2.788
3	SC09-1D	2.147
3	SC09-1F	2.28
3	SC09-6A	4.009
3	SC09-6C	3.591
3	SC09-6G	7.926
3	SC09-6H	2.534
3	SC09-18 Spot1	3.699
3	SC09-7A	3.176
3	CD09-3D	2.193
3	CD09-3E	4.298
3	CD09-3H	1.172
4	SC09-10spot3	7.465
4	SC09-18 Spot3	6.282
4	5GN2269-A	2.097
4	5GN850-1I	5.254
4	5GN850-2B	5.293
4	5GN850-4H	4.676
4	BF09-4G	5.175

4	BP09-8D	4.95
4	SC09-10spot5	2.04
4	SC09-11C	3.813
4	SC09-12B	4.945
4	SC09-13D	3.116
4	5GN3510-F(BF09-3F)	6.755
4	SC09-23A	5.033
4	SC09-23F	5.275
4	SC09-26C	1.96
4	SC09-6B	3.423
4	SC09-6D	8.015
4	SC09-6E	6.755
4	SC09-6I	7.294
4	SC09-7B	1.006
4	CD09-3A	4.448
4	CD09-3B	8.122
4	CD09-3C	5.818
4	CD09-3G	0.368
4	CD09-3I	8.246
4	CD09-4A	5.008
4	CD09-4D	5.586
4	MP09-1H	3.318
5	SC09-18B	8.171
5	5GN1982-G	3.624
5	5GN850-3B	5.361
5	5GN852-1D	6.462
5	BP09-2C	2.767
5	BP09-4G	2.732
5	MP09-1F	6.408
5	5GN840-F	3.251
5	SC09-10 T3B	3.532
5	SC09-10 T3D	6.361
5	SC09-13A	4.661
5	SC09-22A	3.625
5	SC09-23I	11.337
5	SC09-23B	5.726
5	SC09-3B	7.415
5	SC09-3I	3.639
5	SC09-8I	3.784
5	SC09-6J	8.679

Table 26. Results of Total Project Discriminant Analysis. Note this is for 76 of the 77 samples excluding the Crystalline Limestone Outlier.

			Highest Group					Second Highest Group			Discriminant Scores	
			P(D>d | G=g)			P(G=g | D=d)	Squared Mahalanobis Distance to Centroid		P(G=g | D=d)	Squared Mahalanobis Distance to Centroid	Function	
Sample Number	Actual Group	Predicted Group	p	df				Group			1	2
5GN852-1B	1	1	.020	2	.909	7.875	2	.086	13.047	-2.755	2.580	
CD09-3F	1	1	.095	2	.998	4.697	2	.002	18.135	-6.147	-1.012	
CD09-4B	1	1	.332	2	.525	2.207	2	.475	2.857	-3.577	-.838	
SC09-4C	1	1	.786	2	.997	.482	2	.003	12.486	-4.935	.863	
CD09-5A	1	1	.033	2	.982	6.838	3	.018	11.237	-6.904	-.585	
CD09-5B	1	1	.305	2	.975	2.376	2	.025	10.179	-5.076	-1.060	
SC09-1C	1	1	.645	2	.773	.877	2	.227	3.769	-3.650	-.110	
SC09-1E	1	3**	.307	2	.545	2.364	4	.455	2.274	-3.413	-.729	
SC09-1G	1	1	.532	2	.687	1.264	2	.313	3.283	-3.362	.127	
SC09-4C	1	1	.786	2	.997	.482	2	.003	12.486	-4.935	.863	
SC09-6F	1	1	.554	2	.886	1.181	2	.114	5.735	-3.496	.848	
SC09-22H	1	1	.009	2	1.000	9.382	2	.000	29.558	-5.312	3.297	
CD09-2D	2	2	.536	2	1.000	1.246	4	.000	25.907	-9.330	-1.137	
SC09-13F	2	2	.536	2	1.000	1.246	4	.000	45.176	-11.180	.113	
5GN3510-E	3	3	.424	2	.984	1.718	1	.016	11.311	-.803	-1.661	
CD09-3D	3	3	.797	2	.992	.453	4	.008	9.698	-2.027	-1.586	
CD09-3E	3	3	.659	2	.876	.834	4	.124	4.300	-2.801	-.886	
CD09-3H	3	3	.969	2	.974	.063	4	.025	6.905	-2.129	-.852	
SC09-1A	3	3	.813	2	.961	.414	4	.039	6.389	-2.471	-1.202	

SC09-1B	3	3	.816	2	.928	.407	4	.072	5.072	-2.396	-.541
SC09-1D	3	3	.901	2	.995	.208	4	.004	10.875	-1.433	-.947
SC09-1F	3	3	.861	2	.973	.300	4	.027	7.006	-2.344	-1.232
SC09-5spot1	3	3	.748	2	.997	.580	4	.002	12.295	-1.562	-1.615
SC09-6A	3	3	.640	2	.853	.893	4	.147	3.957	-2.578	-.280
SC09-6C	3	3	.730	2	.996	.629	1	.002	13.927	-1.193	-1.308
SC09-6G	3	3	.238	2	.850	2.873	1	.148	7.687	-.197	-.828
SC09-6H	3	3	.842	2	.938	.344	4	.062	5.329	-2.341	-.553
SC09-7A	3	3	.778	2	.911	.501	4	.089	4.713	-2.495	-.561
SC09-18spot1	3	3	.534	2	.978	1.256	4	.021	8.457	-1.563	.145
5GN850-1I	4	4	.498	2	1.000	1.394	5	.000	24.748	3.527	-1.928
5GN850-2B	4	4	.494	2	1.000	1.412	5	.000	24.788	3.536	-1.928
5GN850-4H	4	4	.380	2	.955	1.937	5	.045	7.107	2.330	.095
5GN2269-A	4	4	.830	2	1.000	.372	5	.000	21.721	2.678	-1.876
5GN3510-F/ BF09-3F	4	4	.333	2	1.000	2.197	5	.000	26.345	3.862	-1.948
BF09-4G	4	4	.507	2	1.000	1.357	5	.000	24.669	3.509	-1.927
BP09-8D	4	4	.316	2	.937	2.304	5	.063	6.763	2.546	.236
CD09-3A	4	4	.593	2	1.000	1.047	5	.000	23.962	3.341	-1.916
CD09-3B	4	4	.201	2	.955	3.207	2	.045	7.996	.813	-1.761
CD09-3C	4	4	.418	2	.995	1.742	2	.005	11.054	1.321	-1.792
CD09-3G	4	4	.996	2	1.000	.009	5	.000	16.780	2.470	-1.344
CD09-3I	4	4	.192	2	.949	3.300	2	.051	7.847	.786	-1.759
CD09-4A	4	4	.407	2	.967	1.798	5	.033	7.625	1.940	-.082
CD09-4D	4	4	.460	2	1.000	1.554	5	.000	25.085	3.602	-1.932
SC09-6B	4	4	.759	2	1.000	.552	5	.000	20.525	3.222	-1.571
SC09-6D	4	4	.209	2	.959	3.128	2	.041	8.125	.837	-1.762
SC09-6E	4	4	.333	2	1.000	2.197	5	.000	26.345	3.862	-1.948

SC09-6I	4	4	.269	2	.979	2.625	2	.021	9.027	.994	-1.772
SC09-7B	4	4	.964	2	1.000	.074	5	.000	18.631	2.655	-1.527
SC09-10spot3	4	4	.243	2	.958	2.831	5	.024	9.218	1.142	-.343
SC09-10spot5	4	4	.834	2	1.000	.363	5	.000	21.640	2.648	-1.874
SC09-11C	4	4	.719	2	1.000	.660	5	.000	19.776	3.336	-1.435
SC09-12B	4	4	.560	2	1.000	1.161	5	.000	17.814	3.593	-1.062
SC09-13D	4	4	.769	2	1.000	.525	5	.000	15.417	3.176	-.938
SC09-18spot3	4	4	.409	2	.989	1.787	2	.010	9.664	1.202	-1.259
SC09-23A	4	4	.305	2	.931	2.377	5	.069	6.618	2.530	.260
SC09-23F	4	4	.318	2	.984	2.294	5	.016	9.531	3.255	.053
SC09-26C	4	4	.837	2	1.000	.356	2	.000	19.098	2.381	-1.857
MP09-1H	4	4	.597	2	.991	1.032	5	.009	9.406	2.525	-.265
5GN840-F	5	5	.680	2	.996	.770	1	.004	12.738	1.059	1.967
5GN850-3B	5	5	.496	2	.989	1.402	1	.011	11.369	2.637	2.089
5GN852-1D	5	5	.137	2	1.000	3.974	1	.000	35.445	1.865	4.634
5GN1982-G	5	5	.699	2	1.000	.716	1	.000	18.926	2.342	3.064
BP09-2C	5	5	.718	2	1.000	.663	1	.000	22.329	1.927	3.404
BP09-4G	5	5	.846	2	.999	.335	1	.001	15.067	2.173	2.583
SC09-3B	5	5	.073	2	1.000	5.229	1	.000	39.275	1.773	4.938
SC09-3I	5	5	.647	2	1.000	.872	1	.000	21.167	2.267	3.311
SC09-6J	5	4**	.101	2	.802	4.585	5	.150	6.989	.908	.107
SC09-8I	5	5	.581	2	1.000	1.086	1	.000	25.831	1.204	3.623
SC09-10 T3B	5	5	.654	2	.985	.849	1	.015	10.113	2.065	1.863
SC09-10 T3D	5	5	.342	2	.954	2.148	1	.046	9.182	2.743	1.742
SC09-13A	5	5	.542	2	.998	1.225	1	.002	14.796	.659	2.074
SC09-18B	5	5	.073	2	.661	5.242	1	.190	8.683	.378	.722
SC09-22A	5	5	.700	2	1.000	.715	1	.000	18.892	2.343	3.061
SC09-23B	5	5	.438	2	.981	1.653	1	.019	10.512	2.677	1.958